The Analysis of ^{108m}Ag, ^{166m}Ho and ^{94}Nb in Decommissioning Waste

by

Andrew Robert King

A Doctoral Thesis submitted in partial fulfilment of the requirements for the award of

Doctor of Philosophy

of Loughborough University

November 2003

Research Supervisor: Prof. P. Warwick

Abstract

Contaminated waste consisting of various materials results from the decommissioning of nuclear power plants. Disposal of Decommissioning Waste requires as much measurement data for the radionuclides contained within the waste as possible. Data that are obtained is then used to create an inventory of the radionuclides in the various types of wastes. This research investigates a route to obtaining additional measurement data for such inventories. The importance of these inventories is to provide as much information as possible so that a reliable risk assessment can be performed on the waste samples and the proposed method of disposal.

The principal isotopes of interest are those with long half-lives which could impact on the ability to demolish reactor components in the long term (after short-lived radionuclides have decayed), or have implications for consignment of waste to NIREX (Nuclear Industries Radioactive Waste Executive). Decommissioning data and inventories for long-lived radionuclides are generally based on a few analytical measurements in conjunction with a considerable input from nuclear data calculations and estimations. Currently there are no adequate methods for the analysis of a number of potentially significant radionuclides, particularly ^{108m}Ag, ^{94}Nb and ^{166m}Ho in Decommissioning Waste. The provision of such methods and their application to samples taken from facilities currently being decommissioned would help to remove conservative estimates and uncertainties from the inventories.

Acknowledgements

I would like to thank my supervisor, Prof. Peter Warwick at Loughborough University for the opportunity to be involved in this interesting Environmental Radiochemistry research project. I would like to thank Karen Verrall and Colin Harvey at BNFL Nuclear Sciences & Technology Services and Bill Westall at BNFL Environmental Services, Berkeley Centre for their supervision, advice and providing financial support to fund the research.

Thanks to the Environmental Radiochemistry Group at Loughborough University for their guidance and help throughout. In particular Prof. P. Warwick, Dr. A. Hall and Linda Sands for their advice and support.

I would like to acknowledge the Civil Engineering Department at Loughborough University for the use of their ICP-AES instrument.

Thanks also to my family and friends for their encouragement and friendship. Finally a special thanks to my gorgeous girlfriend Katherine for all her love and understanding which gave me motivation when things were not going to plan.....I love you more than words can express.

Contents

List of figures

List of tables

Page

Abbreviations

NIREX = Nuclear Industries Radioactive Waste Executive
ICP = Inductively Coupled Plasma
ICP-MS = Inductively Coupled Plasma Mass Spectrometry
ICP-AES = Inductively Coupled Plasma Atomic Emission Spectrometry
HF = Hydrofluoric acid
JCHESS = Java CHemical Equilibrium with Species and Surfaces
PHREEQC = pH, REdox, Equilibrium written in computer programme C
ET-AAS = Electrothermal Atomic Emission Spectrometry
v/v = volume to volume
Ksp = Solubility product
d^x = x electrons in d orbitals
MIBK = Methyl isobutyl ketone
rpm = revolutions per minute
R = Alkyl group
M = Metal
X = Halide
A = Anion
EDTA = Ethylenediame tetra-acetic acid
K_{MY} = Metal-EDTA formation constant
$K`_{MY}$ = Metal-EDTA conditional constant
w/v = weight to volume
TnOA = Tri-n-octylamine
HDEHP = di(2-ethylhexyl) orthophosphoric acid
TRU = Transuranic
Ln = Lanthanide resin
cps = counts per second
HPLC = High Performance Liquid Chromatography
BNFL = British Nuclear Fuels Limited
O/F = Overflow
sd = Standard deviation
MDA = Minimum Detectable Amount
K = Volume correction factor
N_0 = Number of counts
E_c = Counting efficiency
V_s = Sample volume
D = Decay factor
$t_{1/2}$ = Half-life
L = ligand

Chapter 1

Introduction

1.0 Introduction

1.1 Decommissioning issues

Decommissioning is the set of actions taken at the end of a facility's economic life to take it permanently out of service and subsequently make the site available for other purposes[1,2]. Once a nuclear power plant is at the end of its useful life it needs to be decommissioned. The process of decommissioning nuclear power plants involves transforming the buildings that have contained radioactive materials into a safe state ready for demolition. The primary concern in decommissioning is to make sure the site and ultimately the environment remain safe. This often involves following Government policies which state that the process of decommissioning nuclear plants should be undertaken as soon as practically possible, taking into account relevant factors[1]. The relevant factors are dealt with in decommissioning strategies which include the justification of timetables proposed and demonstrate adequate financial provision to implement the strategies[1]. The radioactivity present during decommissioning arises from several sources.

1 Neutron activation of the structural materials over the operational life of the plant[3].

2 Contamination from activated corrosion products deposited around the reactor and in the gas circuits[3].

3 Fission products outside of the reactor released from fuels (e.g. in the pond water treatment plant)[3].

The most important source of radioactivity in Decommissioning Waste is neutron activation of the reactor structure. Neutrons are produced inside the reactor core by reactions such as $^{235}U + n \rightarrow {}^{236}U$. The resulting uranium radioisotope is unstable and spontaneously decays producing two fission products, γ photons, heat, neutrinos and several neutrons. Isotopes that are already present in the waste material are then

bombarded with neutrons producing contamination radioisotopes which emit α and β induced radiation and characteristic γ ray energies[4].

1.1.1 Stages of decommissioning

Decommissioning a nuclear power plant involves three stages.

Initial decommissioning takes the plant permanently out of service. The plant is therefore defuelled and hence a large percentage of the radioactivity present on the site is removed. Further initial decommissioning tasks include large projects such as demolition of the ponds, waste retrieval, lowering of boilers, building intermediate level waste stores etc.

The second stage is a period of structural protection and monitoring allowing radioactivity levels to reduce while ensuring the structural integrity of the buildings to prevent any of the radioactivity remaining on-site from entering the environment, e.g. weather proofing the building.

The third stage is dismantling which could happen immediately after the second stage or the plant may be left for a period of time to allow further radioactive decay thus reducing the radioactive wastes naturally. The waste other than operational waste produced at this stage is either intermediate-level, low-level or free release waste. Intermediate-level waste consists largely of concrete and steel containing long-lived radionuclides which primarily consist of activated Co and Fe from the steel structure of the reinforced concrete and also ion exchange resin from water treatment ponds consisting of various radionuclides such as ^{3}H and ^{137}Cs. Low-level waste is of high volume and low specific activity consisting of paper and packaging containing relatively short-lived radionuclides. Both classifications of waste typically contain 4 GBq t^{-1} alpha activity and 12 GBq t^{-1} for beta and gamma activity. Free-release waste contains radionuclides at levels lower than 0.4 Bq g^{-1} total activity and is therefore safe to release into the environment.

1.1.2 Decommissioning of Magnox nuclear power stations

Five Magnox (named after the magnesium non-oxidising fuel cladding used to contain the fuel) power stations are currently being decommissioned, Berkeley, Trawsfynydd, Hunterston A, Bradwell and Hinkley Point A. The strategy known as 'Safestore' is used which is based on the principle that the longer the radioactivity is left to decay naturally, the simpler and more economic it becomes to clean up[3]. Under this strategy decommissioning will take up to 80 years to achieve. This is done over three phases.

1 Defuelling is the first phase and takes two to three years. Over this period 99.9% of all radioactivity is removed from the site. This is achieved by removing the fuel from the closed station for reprocessing[5].

2 Phase two is "Care and Maintenance" and involves securing and monitoring any buildings that contain traces of radioactivity by storing the contents of the buildings in sealed structures[5].

3 The final dismantling phase allows workers to enter the plant with standard radiological protective clothing and technology to completely clear the site. This occurs when the remaining radioactivity has decayed to very low levels[5] but also depends on various factors including the site involved, financial costs, advances in technology and pressure from the Nuclear Installations Inspectorate.

1.1.3 Decommissioning radioactive inventories

A radioactive inventory is essential for deciding the strategy for decommissioning, the strategy for waste management and for making a safety assessment of the waste material. The aim is therefore to produce an inventory of all the radionuclides of significance (usually only radionuclides with a half-life of greater than a year are considered significant)[6].

The accuracy of the inventory is dependent on the quality of input data such as the activating neutron flux, the elemental composition of the waste material, accuracy of modelling and the reliability of nuclear data[3]. All but the nuclear data can be verified and certain measurements can be directly compared to calculated values. It is generally assumed that the nuclear data are known with adequate certainty and so will not contribute significantly to uncertainties in the inventory[3]. This nuclear data is also outside of the scope of decommissioning studies. Re-assessments are often required of long-term dose rates in Decommissioning Waste when additional measurement data is obtained for radionuclide inventories[7].

1.1.4 Significance of determining ^{108m}Ag, ^{166m}Ho and ^{94}Nb in decommissioning waste for radioactive inventories

Once the Magnox reactors have been defuelled the gamma dose rate in the concrete surrounding the reactor vessel (the bioshield) is almost completely due to ^{60}Co which decays with a half-life of 5.27 years. The decay scheme for ^{60}Co is shown below.

Figure 1 ^{60}Co decay scheme[8,9]

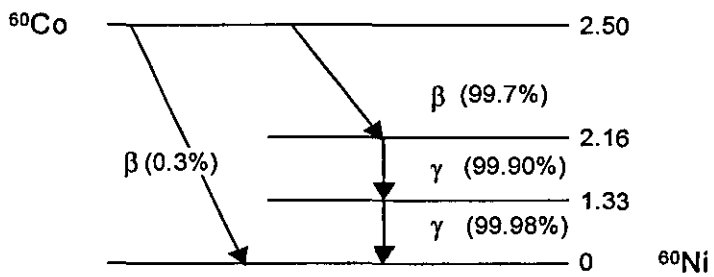

The energy levels are quoted in MeV. If the β decay results in a ^{60}Ni nuclear excited state, each ^{60}Co decay gives rise to two γ-rays of energy 1.17 and 1.33 MeV. At approximately 70 to 100 years after final shutdown, radionuclides with longer half-lives become dominant gamma emitters and the reduction in gamma dose rate with time becomes more gradual. The most important of the long-lived gamma emitting radionuclides are ^{108m}Ag, ^{166m}Ho and ^{94}Nb which are focused on throughout this research. The neutron activation routes to these radionuclides and ^{60}Co are shown below.

Figure 2 Neutron activation routes to radionuclides of interest[10,4]

$^{93}Nb\ (n,\gamma)\ ^{94}Nb$

$^{107}Ag\ (n,\gamma)\ ^{108m}Ag$

$^{165}Ho\ (n,\gamma)\ ^{166m}Ho$ and $^{164}Dy\ (n)\ ^{165}Dy\ (n)\ ^{166}Dy\ (\beta^-)\ ^{166m}Ho$

$^{59}Co\ (n,\gamma)\ ^{60}Co$

Consequently, the levels of ^{166m}Ho formed in the waste depends on initial concentrations of holmium and dysprosium. Dysprosium is sometimes found inside the reactor core and increases the chance of ^{166m}Ho contamination via the second ^{166m}Ho production route. Although ^{108m}Ag, ^{166m}Ho and ^{94}Nb are more important gamma emitters at times close to final shutdown, they are present at much lower levels than ^{60}Co. They cannot be measured directly using gamma spectrometry until many decades after final shutdown when ^{60}Co has decayed. However it is necessary to assess their radiological consequences as soon as possible to support the decommissioning strategy developed around the time of final shutdown. Therefore specific methods are required to measure the radionuclides of importance in the presence of much higher levels of ^{60}Co. The experimental work in chapter 2 contains method development work that has been performed to achieve this requirement and to ultimately provide additional measurement data for the radionuclide inventories.

1.1.5 Importance of sampling in the radioactive inventory

Outside of the reactor core the radioactive inventory cannot be calculated and must be measured because the radioactivity is mostly due to contamination radioactivity caused by neutron activation. Sampling is not always possible especially if the station is still operational. An alternative approach is *in situ* gamma spectrometry, which is non-invasive and uses portable detectors[6]. However only about half of the radionuclides of interest in fission power reactors emit useful gamma rays and therefore some supporting measurements are needed. The contamination is often

sampled by wiping a piece of swab material or filter paper (55mm diameter 540-542 hardened grade) over the contaminated material to transfer any radioisotopes onto the surface of the swab or filter for measurement[6]. Swabbing is the term used when this technique is performed using tacky swab material which is a cotton based material with an adhesive surface. The technique is not quantitative because the removal fraction depends on the surface, contamination matrix and the operator. Therefore the activation product isotopes (e.g. ^{108m}Ag, ^{94}Nb and ^{166m}Ho) are ratioed to the principal, easily measured ^{60}Co radionuclide which can then be multiplied by the inventory of that radionuclide measured from the *in situ* gamma spectrometry[6]. The ratios measured from the swab samples must therefore be quantitative to allow calculation of the total radioactive inventory from the inventory of the principal radionuclide. Similarly fission product and actinide activity are ratioed to ^{137}Cs and calculated in a similar manner[6].

1.2 Sample pre-treatment

Radiochemical analysis often consists of the following steps[11]:

(i) Sample pre-treatment and extraction (e.g. dissolution, digestion etc.).

(ii) Sample pre-concentration (e.g. evaporation, precipitation etc.).

(iii) Separation of analytes from the matrix and each other (e.g. solvent extraction, ion exchange etc.).

(iv) Transformation of the separated fraction into a source suitable for measurement and determination of the analytes.

The required combination of sub-procedures is determined by the analytes under investigation, the amounts involved, matrix composition and performance required[11].

1.2.1 Extraction using dissolution and digestion

Dissolution and digestion procedures transfer the analytes of a sample from a solid matrix (e.g. concrete, steel, swab material etc.) into solution so that it becomes simpler to carry out pre-concentration and separation steps on the analytes. The sample matrix determines the reagent required for dissolution. Many samples are soluble in acids such as HCl, HNO_3 and HF[12,13]. Heating may also be required to dissolve many samples[12]. Microwave acid assisted digestions using HNO_3 / H_2O_2 and HNO_3 / HF have been used for samples such as soil sediment and steel[14,15,16]. The samples are broken down at accelerated rates due to the high temperatures and pressures involved. Ashing and peroxide fusion are often used as additional steps in a dissolution process[15,17]. Ashing procedures involve heating to high temperatures ($\approx$ 500°C) to remove organic molecules present in the sample that may interfere with chemical analysis. Ashing is only suitable for non-volatile species such as transition metals. Na_2O_2 fusion is a very powerful oxidising technique and is used to complete dissolution procedures by mobilising metal ions that remain unaffected by acid attack. By heating to high temperatures (> 500°C), a molten liquid forms which ensures the sample matrix breakdown.

1.2.2 Sample pre-concentration

Pre-concentration can be defined as transferring the analyte from a phase of large volume to one of small volume and hence increasing the concentration of the analyte[18]. This step may be necessary if the analytical technique is not sensitive enough to measure very low concentrations. The precipitation of analytes is often used as a pre-concentration step[19]. Another common example of sample pre-concentration is the use of ion exchange to pre-concentrate the analytes of interest by adsorption onto a resin[20,21]. Samples that involve no pre-treatment or pre-concentration[22] are preferred because the number of sources of contamination and hence interferences in the analysis are reduced.

1.2.3 Separation of analytes from their matrix and each other

There are many different types of radioanalytical separation techniques available such as extraction chromatography and co-precipitation[23,24]. These often include the use of hold-back carriers prior to extraction or precipitation so that one or more of the analytes remain in solution[19,25]. The technique applied depends on other elements or radioisotopes in the sample and the sample matrix. Extraction chromatography is applicable to a wide range of trace metals and is suitable for multi-element analysis by sequentially eluting the trace metals with increasing strengths of an appropriate eluant[20,21]. However it maybe more appropriate to use a specific complexing reagent for an analyte[26] or even a combination of complexation with extraction chromatography[27]. There are therefore many possibilities for the analysis of trace metals and the analytical procedures mentioned are investigated in chapter 2.

1.2.4 Transformation of sample solution for analysis

The separated fraction containing an analyte is sometimes not in an appropriate form for measurement and determination by the preferred detector. Therefore the solution has to be treated or diluted for it to be successfully analysed on the appropriate detector. For example the determination of trace metals is often performed using ICP-MS / AES (inductively coupled plasma mass spectrometry / atomic emission spectrometry) analysis and sample solutions often contain high acid concentrations especially if the pre-concentration stage involves dissolution with strong acids. Therefore dilution of the sample solutions is required to obtain a solution with an acid concentration of below 5% (a suitable acid concentration for ICP analysis). However this may result in a reduction in analyte concentration and it maybe the case that an alternative method of detection is required if the concentration falls below the detection limits of the detector.

1.3 Waste sample matrices and reactor design

The analysis methods for Decommissioning Waste depend on the sample matrix. The sample matrix is determined by the reactor component being analysed. Figure 3 shows the design of a Magnox reactor.

Figure 3 Magnox reactor design[28]

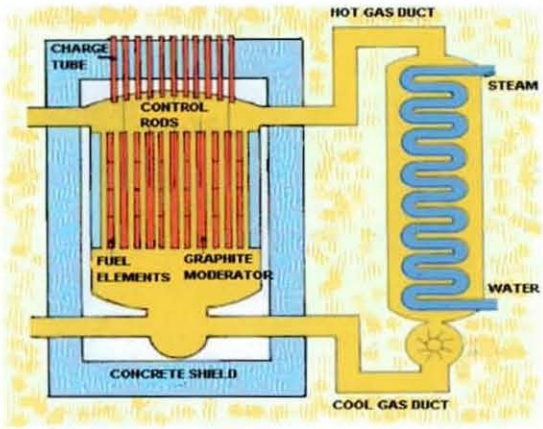

Fuel rods inside the reactor vessel of a Magnox reactor are composed of natural uranium contained within a magnesium alloy can. The graphite moderator provides an array of channels which assists steel rods in slowing down neutrons so that an efficient chain reaction occurs and the speed of the fission reactions are controlled. A thick steel containing concrete bio-shield surrounds the reactor, adsorbing neutrons escaping the reactor core. Heat created from the controlled nuclear reaction inside the reactor core is transferred by CO_2 gas via gas circuits to the pressurised boilers which produces steam used to generate electricity. Decommissioning Waste primarily consists of building materials and plant components. The most important waste matrices are therefore steel, graphite and concrete.

When decommissioning nuclear reactors, it is essential to be able to determine the radioactivity contained in the structural materials of the reactor plant. Radionuclides of Ag, Ho and Nb are produced by neutron activation and are relatively long lived. The necessary analytical methods should be relatively simple and safe and be able to be used routinely. The aim of this work was therefore to develop a method or methods for the measurement of these radionuclides in a number of different materials.

Chapter 2

Experimental

2.0 Experimental

2.1 Reagents and instrumentation

Throughout the method development for dissolution and separation ICP-AES measurements were obtained using a Sci-Tek Jarrell Ash AtomScan 16 spectrometer by Thermo Elemental with a pump rate of 100 rpm. ICP-MS measurements were also obtained in two experiments using a VG PQ Excell instrument manufactured by Thermo Elemental.

The ICP-AES instrument used for radioactive samples was an IRIS Advantage HR enhanced resolution spectrometer equipped with radial plasma and used with a pump rate of 100 rpm manufactured by Thermo Elemental. Gamma spectrometry was also used to measure the radioactive samples using a High Purity Germanium Detector manufactured by EG&G ORTEC using the software EG&G Gamma Vision I. The instrument was calibrated using a mixed radionuclide standard containing ^{241}Am, ^{109}Cd, ^{57}Co, ^{139}Ce, ^{203}Hg, ^{113}Sn, ^{85}Sr, ^{137}Cs, ^{60}Co and ^{88}Y from High Technology Sources Limited.

All experiments were performed using analytical grade reagents. Cellulose nitrate filter paper was used throughout for filtration steps unless otherwise stated.

2.2 Dissolution method development for tacky swab / filter paper samples

Tacky swab and filter paper samples are widely used to support radionuclide inventory data by sampling radioisotopes from decommissioning waste. As stated in chapter 1, the principal radioisotopes of interest in the waste are ^{108m}Ag, ^{166m}Ho, and ^{94}Nb, these radioisotopes are products of neutron activation which then decay over long periods of time. The radioisotopes of interest are difficult to measure quantitatively because the peaks corresponding to their gamma emission signals are swamped by the Compton edge scattering caused by the ^{60}Co radioisotope which is present at much higher concentrations. The Compton effect is the predominating mode of gamma photon interaction resulting in the appearance of Compton electrons and scattered photons in addition to photoelectrons in the detector[29]. The cascade of

Compton scattering from the large excess of ^{60}Co swamps the smaller signals of the radioisotopes of interest when measured by gamma spectrometry. Removing the ^{60}Co interference from samples allows the smaller signals to be measured because of the removal of the interfering Compton scattering. The removal of the ^{60}Co radioisotope requires the analytes to be present in solution, this is achieved by dissolving the solid sample. The method development for the dissolution of tacky swab and filter paper samples involved doping unused samples with inactive Ag, Co, Ho and Nb. These elements of interest were measured in solution by ICP analysis and techniques for the separation of Co from solution were then investigated. All analytical techniques used in conventional chemistry may be used for the separation and isolation of radioactive elements in trace concentrations[30]. This provides plenty of chemical methods to consider for investigation. Once successful dissolution and separation methods have been developed they will be applied to radioactive samples that are either known or predicted to contain the radioanalytes.

2.2.1 Speciation in dissolution samples

Speciation is important when analysing trace elements because analytical difficulties are related to the choice of relevant techniques for measurement of the individual species[31]. For suitable chemical methods to be applied to samples it is important to know the species of the analytes so that their behaviour can then be predicted. Pre-treatment of samples can cause the species of analytes to change. A change in analyte species does not always affect the detection of the analyte. This is the case for ICP analysis used throughout the experimental work although speciation has to be considered in the method development prior to detection for an understanding of why the detection of analytes in a solution was either successful or not. The following experimental work involves doping samples with Ag, Co, Ho and Nb from 1000 mg dm^{-3} stock solutions. The stock solutions were either produced by dissolving the solid nitrates $AgNO_3$, $Ho(NO_3)_3.5H_2O$ and $Co(NO_3)_2.6H_2O$ in water or obtained as readily made ICP standard solutions. The Nb stock solution was obtained as an ICP standard solution which contained trace amounts of HF to prevent Nb from precipitating. It is known that Nb dissolves in aqueous solutions of HF to give the anionic fluoro complex $[Nb^{(v)}OF_5]^{2-}$[32] and therefore this species was predicted to be present in solution after dissolution. The other elements of interest were predicted to be present

as soluble nitrate complexes containing the cations Ag^{+}, Ho^{3+} and Co^{2+}. In addition to the literature there were speciation programmes available such as JCHESS[33] and PHREEQC[34] to help understand speciation in solutions of varying concentrations and components.

2.2.2 ICP standard solutions

Trace metal concentrations are commonly determined in different media by the analytical methods of inductively coupled plasma mass spectrometry (ICP-MS)[35,36], inductively coupled plasma atomic emission spectrometry (ICP-AES)[37,38] and electrothermal atomic absorption spectrometry (ET-AAS)[39]. Only ICP-AES and to a lesser extent ICP-MS were available at Loughborough University for the analysis of trace levels of Ag, Co, Ho and Nb. A series of standard solutions ranging from 0.1 to 3 mg dm^{-3} Ag, Co, Ho and Nb were produced for ICP analysis of the trace metals in dissolution samples. The solutions were produced by pipetting appropriate volumes of the 1000 mg dm^{-3} stock solutions into volumetric flasks, addition of concentrated HNO_3 (5 cm^3) and dilution to 100 cm^3 with distilled water. Nitric acid was added to the standards for two reasons. The first being to match the acidity of the dissolution sample matrix and the second, to satisfy the ICP requirement of sample acidity (solutions should ideally contain up to 5% acid concentration).

Of the ICP techniques mentioned previously, ICP-MS has the lowest detection limits for trace metals, however the detection limits of ICP-AES were shown to be suitable for the analysis of Ag, Co, Ho and Nb in dissolution samples. Table 1 shows ICP-AES lower detection limits for the analytes of concentrations 10 mg dm^{-3} at specific wavelengths.

Table 1 ICP-AES detection limits[40]

Element	Ag	Co	Ho	Nb
Emission line wavelength (nm)	328.068	228.616	345.600	316.340
Minimum detectable concentration (mg dm^{-3})	0.007	0.007	0.0057	0.004

A multiplication factor of three is usually applied to these detection limits to account for varying instrument performances.

2.2.3 Dissolution using HNO_3

A method was provided by Berkeley Centre which used HNO_3 and HCl for the dissolution of tacky swab and filter paper samples[17]. The following method was based on this method and was performed on unused tacky swab samples. The method was adapted for investigation by using a closed system to prevent acid vapours escaping into the fume cupboard (apparatus are shown in figure 4) although the original method was commonly performed at Berkeley Centre using an open neck conical flask.

A swab sample (2 g) was weighed and placed in a 3-necked round-bottomed flask. Concentrated nitric acid (20 cm^3) was added to the flask and left overnight. Fe carrier solution (2 cm^3 of 3.7 g Fe (III) nitrate in water with 5 cm^3 6 mol dm^{-3} nitric acid made to 100 cm^3 with water) and a magnetic stirrer were added to the flask which was then heated to between 80 and 90°C for 1 hour using a water bath. Concentrated HCl (10 cm^3) was added dropwise via a dropping funnel and the mixture simmered for 30 minutes. The mixture was allowed to cool and diluted with distilled water (150 cm^3). The solution was filtered through a 47 mm diameter 0.8 μm pore filter paper to remove the insoluble glue providing a transparent yellow filtrate. The filtered material was transferred to a zirconium crucible, placed in a muffle furnace, heated to 500°C and maintained at this temperature for 30 minutes. Na_2O_2 (1.0 g) was added to the black residue to oxidise the remaining carbonaceous material and to make soluble any remaining metals[15,17,41]. The residue was heated to 600°C for 30 minutes. The resulting black residue was cooled and suspended in water (70 cm^3) and 6 mol dm^{-3} HNO_3 (10 cm^3). This was filtered and added to the previous yellow filtrate. The combined filtrate was diluted to 500 cm^3 with distilled water.

Figure 4 Dissolution apparatus

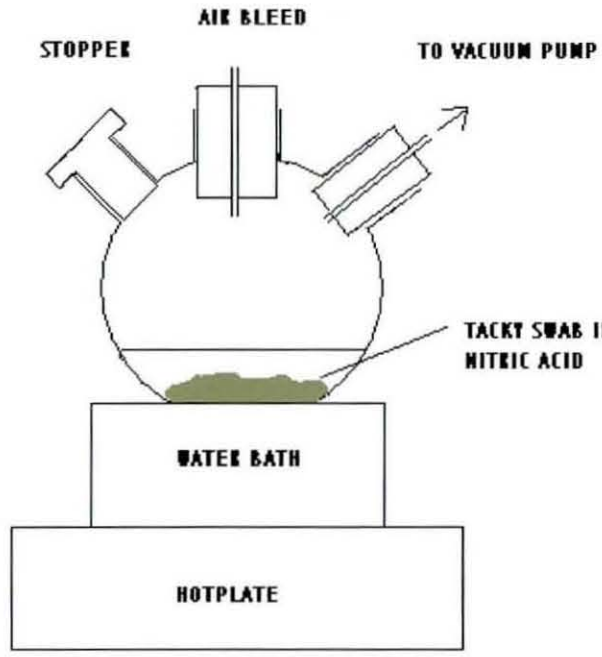

The experiment was performed twice on tacky swab samples that were doped with Ag, Co, Ho and Nb (1 cm^3 of 500 mg dm^{-3} stock solutions). The first dissolution experiment performed on a tacky swab sample was measured by ICP-MS. The second dissolution experiment was measured by ICP-AES for comparison.

2.2.4 Dissolution using fuming HNO_3

Fuming HNO_3 is nitric acid that has been saturated with NO_2 and this is achieved by passing nitrogen dioxide through the nitric acid[42]. The oxidising action of the acid is increased and NO_2 fumes are observed.

Aqua-regia (HNO_3 / HCl) is commonly used for dissolution because of the oxidising power of HNO_3 combined with the strong acidity and complexing properties of HCl[43]. However Ag and Ho were found to precipitate as chloride complexes. This was a problem in developing a dissolution method using ICP measurement and would also be a problem measuring inactive tracer elements in radioactive samples. The replacement of HCl (10 cm^3) with fuming HNO_3 in the dissolution method was chosen for this reason and because of the high solubility of Ag, Co, Ho and Nb in HNO_3 together with the rapid oxidising action of the acid. The initial addition of 20

cm^3 concentrated HNO_3 was also replaced with fuming HNO_3 (15 cm^3) to reduce the volume of acid used. The modified experiment was performed six times and analysed by ICP-AES.

To confirm that none of the analytes were present in the swab material prior to doping, the experiment was performed a further three times without the addition of Ag, Co, Ho and Nb.

After successful dissolution using fuming HNO_3, attempts were made to dissolve tacky swab samples using a lower volume of fuming HNO_3. This was desirable to avoid handling unnecessarily large volumes of this highly corrosive acid.

The dissolution method was therefore repeated using only 15 cm^3 fuming HNO_3. The further 10 cm^3 that was previously added in place of HCl was not added because the swab sample was observed to dissolve in the initial 15 cm^3. A 0.1 μm pore filter was used for the filtration steps because of its availability and it was thought that this would have no significant affect on the recoveries of the analytes. The amount of acid and water used to suspend the residue in the final step of the method was 6 mol dm^{-3} HNO_3 (5 cm^3) and H_2O (45 cm^3). The combined filtrate was analysed by ICP-AES.

2.2.5 Nb stabilisation in ICP standard solutions

A control solution containing 1 mg dm^{-3} Ag, Co, Ho and Nb was produced from the respective stock solutions and measured against the standard solutions that were used to measure Ag, Co, Ho and Nb concentrations in the previous experiments. The standard solutions contained the expected concentrations of Ag, Co, Ho and Nb. However another control solution was produced in the same way and measured against the same set of standard solutions several days later and the Nb concentration detected was unexpectedly high.

The unexpectedly high Nb concentration was investigated by analysing the 1 mg dm^{-3} standard solution using ICP-MS to eliminate the unexpected result being a detector

error. This was compared to the freshly diluted 1 mg dm^{-3} control solution and analysed by ICP-MS.

It is known that Nb can be made soluble by the addition of HF[44] to form stable anionic complexes[45]. A combination of HNO_3 with trace HF is also used to stabilise Nb in the 1000 mg dm^{-3} stock solution therefore it was questioned whether or not HNO_3 was suitable for stabilisation of Nb in lower Nb concentration solutions without any additional HF. The stabilisation of Nb by HNO_3 alone was investigated by preparing five separate 4 mg dm^{-3} Nb solutions containing 1%, 2%, 3%, 4% and 5% (v/v) HNO_3 (using 1, 2, 3, 4 and 5 cm^3 of concentrated HNO_3 respectively). These solutions were left for 24 hours and measured by ICP-AES.

The Nb standard solutions used for the following experiments were freshly produced for each series of samples to avoid Nb precipitation over time.

2.2.6 Recoveries of analytes at higher concentrations

The following dissolutions involve doping swab samples with higher concentrations of Ag, Co, Ho and Nb stock solutions to determine whether or not the successful recoveries of the analytes were dependent on initial concentrations.

Eight dissolution experiments were performed using the successful dissolution method (described in the previous section). The samples were doped with 1000 mg dm^{-3} Ag, Co, Ho and Nb solutions (2 cm^3 of each). The filtrates were analysed by ICP-AES.

Five similar experiments were then performed with the addition of 1000 mg dm^{-3} Ag, Co, Ho and Nb solutions (4 cm^3 of each) and the solutions were analysed by ICP-AES. A further three experiments were performed with the addition of the same concentrations of Ag, Co and Ho but excluding the addition of Nb. This was to investigate whether or not the HF in the Nb stock solution had an affect on the recovery of Ag because it was considered that AgF may have formed when a higher volume of Nb stock solution was added due to the increased concentration of HF. The filtrates for these experiments were also analysed by ICP-AES.

2.2.7 Solubility of AgF and AgCl

The low recovery of Ag at these higher concentrations led to the investigation of the solubility of possible AgF or AgCl species. The solubility products (Ksp) of AgCl and AgF are shown in equations 1 and 2.

$Ag^+(aq) + Cl^-(aq) \rightarrow AgCl(s)$ $\quad Ksp = 1.8 \times 10^{-10}\ mol\ dm^{-3}$ Equation 1[46]

$Ag^+(aq) + F^-(aq) \rightarrow AgF(s)$ $\quad Ksp = 205\ mol\ dm^{-3}$ Equation 2[46]

The solubility product comparison shows that AgF has a relatively high solubility product compared to AgCl and was not likely to precipitate from solution[46]. However a AgCl precipitate may have formed.

The following experimental section investigates washing the filter of dissolution experiments to ensure that Ag was soluble and present in the filtrate.

2.2.8 Filter washing

Typical Ag complexes are shown below. The series shows the order of decreasing stability of these dissolved Ag complexes.

$$[Ag(CN)_2]^- > [Ag(S_2O_3)_2]^{3-} > [Ag(NH_3)_2]^+ \qquad \text{Equation 3[47]}$$

Ag can be made soluble with cyanide, thiosulphate and amine ligands. AgCl precipitates are known to readily dissolve in ammonia solution forming the complex ion $[Ag(NH_3)_2]^+$[41,47]. The following experiments investigate the use of HNO_3 and ammonia solution to wash the filters of dissolution experiments.

Two dissolutions were performed to contain final concentrations of 1 mg dm^{-3} of the elements of interest. The filter paper from one dissolution sample was washed twice with concentrated HNO_3 (15 cm^3) / H_2O (75 cm^3). The washings were then combined, diluted to 500 cm^3 with distilled water and analysed separately to the initial filtrate by ICP-AES. The filter paper from the second dissolution sample was washed twice with

concentrated ammonia solution (15 cm^3) / H_2O (75 cm^3). The washings were combined, diluted to 500 cm^3 with distilled water and analysed by ICP-AES.

Following the successful transfer of Ag, Co, Ho and Nb from tacky swab sample to solution, the investigation focussed on methods of separating the analytes (Ag, Ho and Nb) from Co.

2.3 Separation methods by complexation

Methods of selectively extracting Co from solution using complexing agents were investigated in an attempt to achieve a one step Co separation from the analytes Ag, Ho and Nb.

Cobalt has a small cation size, comparatively large nuclear charge and appropriate electronic arrangement which are ideal properties for complex formation[48]. In the divalent state only comparatively unstable ionic complexes form whereas in the trivalent state stable covalent species form[48].

2.3.1 Oxidation of Co in complex formation

The dissolution samples contain Co^{2+} ions which are very stable in solution. However many complexes containing Co^{2+} ions are readily oxidised to Co^{3+} complexes[49]. A common reaction illustrating this is shown below.

$$[Co^{II}(NH_3)_6]^{2+} \rightarrow [Co^{III}(NH_3)_6]^{3+} \qquad \text{Equation 4[49]}$$

This reaction occurs because the crystal field stabilisation energy of Co^{3+} with a d^6 electron configuration is higher than that of the Co^{2+} which has a d^7 arrangement of electrons[47]. This creates a more stable octahedral Co complex where all the electrons are paired in the preferred d^6 configuration.

2.3.2 Co complexation with 1-nitroso-2-naphthol

α-Nitroso-β-naphthol is known to precipitate various transition metals including cobalt from slightly acidic solutions[50,51]. Its structure is shown below.

Figure 5 α-Nitroso-β-naphthol[50]

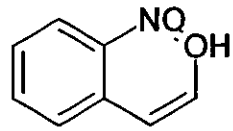

This reagent oxidises Co to the trivalent state and is then precipitated as the complex shown below.

Figure 6 Co nitroso naphthol complex[50]

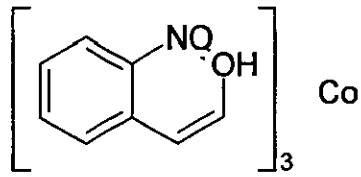

The attempted Co extraction experiment described below involved the formation of this cobalt complex and was based on a method provided by Berkeley Centre[52].

The 1-nitroso-2-naphthol reagent was prepared by dissolving 1-nitroso-2-naphthol (4 g) in glacial acetic acid (100 cm^3). Once the solid had dissolved, distilled water at 80°C (100 cm^3) was added and the solution stored in the dark. A solution containing 1 mg dm^{-3} Ag, Co, Ho and Nb (5 cm^3) was pipetted into a 250 cm^3 beaker. The solution was diluted to 50 cm^3 with distilled water and cobalt chloride (0.1 g) was added. 1-nitroso-2-naphthol reagent (75 cm^3) was filtered through Whatman 542 filter paper and added to the beaker. The solution was stirred and heated gently to boiling. The solution was left to stand for 2.5 hours before being filtered through 542 filter paper. The filtered material was washed with 80°C 1 mol dm^{-3} HCl (10 cm^3). The

filtrate was filtered a second time. The filtrate was evaporated down to approximately 80 cm^3 and transferred (after cooling) to a 100 cm^3 volumetric flask and diluted with distilled water. A sample of this solution (50 cm^3) was then taken and diluted to 100 cm^3 with distilled water. The solution was filtered several times until the solution was clear before ICP-AES analysis.

2.3.3 Solvent extraction of Co complexes

Metal ions, even when hydrated do not extract well into an organic phase. However complexed metals are commonly extracted by various organic solvents[53]. The complexation of Co with 1-nitroso-2-naphthol has been extracted with various solvents such as methyl isobutyl ketone (MIBK)[54] and chloroform[55]. The solvent extraction of Ho in certain matrices is also known[56,57]. However such methods were not fully investigated because of the high level of solvent waste produced in the methods which would be undesirable for routine methods that may be used in decommissioning waste analysis.

The following inorganic ligand was suggested for the attempted separation of Co from Ag, Ho and Nb. It was known that the ligand was Co specific in some solutions, however its behaviour in the presence of the other analytes was not known.

2.3.4 Diphenyl sulfimide ligand

The diphenyl sulfimide ligand $Ph_2S{=}NH$ is known to react with transition metals[58,59] and has a strong tendency to react with Co. An experiment was performed to confirm the ligands strong tendency to react with Co.

$Ph_2S{=}NH$ (0.01 g) was added to a 1000 mg dm^{-3} Co solution (1 cm^3) and shaken. The solution was then filtered through a 0.1 μm pore filter and the filtrate diluted to 250 cm^3 with distilled water for ICP-AES analysis. The experiment was repeated with excess ligand (0.05 g) and analysed by ICP-AES.

The following set of experiments investigate the behaviour of Co with the inorganic ligand in the presence of the two analytes Ag and Ho in an attempt to achieve a separation of Co from these analytes. 0.025 g of ligand were chosen for the following experiment because this was the amount calculated to give a 100% reaction with Co. The experiment was performed to determine the selectivity of the ligand towards Co.

1000 mg dm^{-3} Ag, Co and Ho solutions (1 cm^3 of each) were pipetted into a small glass vial and 0.025 g of the ligand added. This was filtered without shaking. The ligand turned blue and began to dissolve but did not dissolve completely. Therefore shaking did not induce dissolution. The filtrate was diluted to 250 cm^3 with distilled water. The experiment was performed three times and analysed by ICP-AES.

The following experiment was performed to prevent the partial dissolution of the ligand observed in the last three experiments. An excess of the ligand (0.05g) was added to a solution containing 1000 mg dm^{-3} Ag, Co and Ho solutions (0.1 cm^3 of each) in distilled water (5 cm^3) and the sample was filtered. By using a lower concentration of Ag, Co and Ho a lower volume of stock solutions was used resulting in a decrease of HNO_3 concentration preventing the dissolution of the ligand. After filtration, the filtrate was diluted to 50 cm^3 with distilled water for ICP-AES analysis.

.

A chelation method avoiding the problem of Co oxidation by using acetylacetone as a chelating reagent has been reported[60]. Co^{2+} was separated from Co^{3+} by chelation and solvent extraction using benzene however as mentioned previously a method involving solvent extraction was undesirable for the dissolution samples, therefore the investigation was focussed on different methods of separation.

2.3.5 Co precipitation as Co nitrite

When a solution of Co^{2+} ions is treated with NO_2^- ions, Co^{2+} is again oxidised to Co^{3+} and then the soluble $[Co(NO_2)_6]^{3-}$ complex is formed[49]. The addition of a metal cation such as Cs^+ results in the formation of a caesium cobaltinitrite $Cs_3[Co(NO_2)_6]$ precipitate[49].

The following method provided by Berkeley Centre[61], involves the precipitation of a cobalt nitrite complex by the addition of sodium nitrite. The caesium solution was made from caesium chloride instead of caesium nitrate due to availability of reagents.

Cobalt solution (100 cm^3) was produced by dissolving cobalt nitrate (2.47 g) in distilled water and 6 mol dm^{-3} HNO_3 (1.7 cm^3). Caesium solution (100 cm^3) was produced by dissolving caesium chloride (1.5 g) in distilled water and 6 mol dm^{-3} HNO_3 (1.6 cm^3). A solution containing 10 mg dm^{-3} Ag, Co, Ho and Nb (5 cm^3) was added to a 50 cm^3 beaker. Glacial acetic acid (2 cm^3) was added to the beaker and the pH adjusted to pH 4 with 50% (w/v) NaOH solution (5 drops). After the solution had cooled, sodium nitrite (2 g) was added and the solution was stirred to dissolve. Caesium solution (1 cm^3) and cobalt solution (1 cm^3) were added. The solution was cooled in an ice bath then placed in a fridge overnight. The resulting observation was a yellow solution containing a yellow precipitate. The solution was centrifuged at 20,000 rpm for 30 minutes. The yellow solution was filtered and diluted to 100 cm^3 with distilled water for ICP-AES analysis.

Many complexing agents are known to complex with Co such as dithizone and nitroso-naphthol[62]. However similar metals are often also complexed with these reagents such as Ag with dithizone[63] and Ho with nitroso-naphthol (shown in previous experiments). The similarity in behaviour of Co and Ho in all the complexation methods investigated led to the investigation of ion exchange methods of separation.

2.4 Co and Nb separation from solution by ion exchange

Separation methods for transition metals often involve ion exchange because their strength of adsorption to the ion exchange resin depends on the charge and size of the ion involved which means the eluant and eluant strength can be adjusted to desorb various different metals. Table 2 shows various types of ion exchange resins and some of their properties

Table 2 Selected exchange resins and their properties[64]

Name	Type	Effective operating pH range	Functional group	Ionic form
Amberlite IR-120 Dowex 50	Strogly acidic cation exchanger	0-14	$—SO_3^-H^+$;polystyrene	H or Na
Amberlite IRA-400 Dowex-1	Strongly basic anion exchanger	0-14	Quaternary amine $—CH_2—N^+(CH_3)_3$;polystyrene	Cl
Amberlite IR-4B Dowex 3	Weakly or medium basic	0-7	—NHR or NR_2;phenol or polyamine condensation	OH
Amberlite IRC 50	Weakly acidic	7-14	Polyacrylic or polymethacrylic acid	H

Cation exchange resins contain acidic functional groups. Weakly acidic cation exchangers contain carboxylic acid functional groups whereas strongly acidic cation exchangers contain sulphonic acid functional groups[65].

$$n\mathrm{R}_h\mathrm{SO}_3^-\mathrm{H}^+ + \mathrm{M}^{n+} \leftrightarrow (\mathrm{R}_h\mathrm{SO}_3^-)_n\mathrm{M}^{n+} + n\mathrm{H}^+ \qquad \text{Equation 5[65]}$$

Anionic exchangers contain basic groups. Weakly basic anion exchangers contain amine functional groups whereas strongly basic anion exchangers contain quaternary ammonium functional groups[65].

$$n\mathrm{R}_h\mathrm{NR}_3^+\mathrm{X}^- + \mathrm{A}^{n-} \leftrightarrow (\mathrm{R}_h\mathrm{NR}_3^+)_n\mathrm{A}^{n-} + n\mathrm{X}^- \qquad \text{Equation 6[65]}$$

^{60}Co has been separated from low-level liquid radioactive waste samples using a combination of an inorganic ion exchange resin with an organic ion exchange resin[66]. The strongly acidic Amberlite IR-120 cation exchange resin was chosen for investigation because the elements of interest were present in the dissolution samples as Co^{2+}, Ho^{3+} and Ag^+ and once adsorbed could be eluted by an appropriate eluant. Nb was expected not to adsorb because it was predicted to be present as $[NbOF_5]^{2-}$ [32] (discussed in section 2.2.1) and hence pass straight through the cation exchange resin. Nb is known to adsorb to anion exchange resins in dissolution samples which

supports the anionic complex prediction[32,67,68]. Furthermore, investigations into the retention of metal cations on cation exchange resin in different strength hydrofluoric acid eluants show that Nb was one element that showed no significant retention[69] whilst trivalent cations such as Ho and Co were strongly adsorbed[70].

The role of the exchange ion in the eluant of ion exchange separations is to compete with analyte ions for the fixed ions on the stationary phase and to separate the mixture of analyte ions into well-defined bands[71]. The important eluant characteristics are shown below[71].

(i) Compatibility with the detection mode
(ii) Nature of the competing ion
(iii) Concentration of the competing ion
(iv) Eluant pH
(v) Buffering capacity
(vi) Complexing ability
(vii) Organic modifier content

The first section of experimental work involving ion exchange investigates the fourth and sixth characteristics listed above.

2.4.1 Cation exchange resin with EDTA and HCl eluants

Different transition metal ions can be selectively determined by complexation with the hexadentate chelate complex EDTA which consists of two nitrogen atoms containing lone pairs of electrons and four carboxylic acid groups. By adjusting the concentration of EDTA and the pH one ion can be complexed while another ion remains uncomplexed[72]. The ligand is however less selective to ions of similar charge[72]. Co is known to complex with EDTA forming $[Co(EDTA)]^-$[72]. A method using polyurethane foam as the solid phase to pre-concentrate Co^{3+} through the oxidation of Co^{2+} followed by elution with 2 mol dm^{-3} HCl has been reported[73] whilst the retention of Nb in HCl was reported to be very high[74]. Cobalt is believed to produce the mono-valent anion $[CoCl_3]^-$ in strong HCl solutions[27]. Therefore by

passing these eluants through a cation exchange resin it was expected that Co would be eluted.

For practical purposes, the disodium salt Na_2H_2EDTA was preferred as a reagent[75]. The salt has a higher solubility than the parent acid. The four electron rich COOH groups together with the two nitrogen lone pairs constitute a ligand which will form complexes with octahedral geometry[75].

2.4.1.1 pH effect on EDTA solutions

EDTA is a tetrabasic acid and dissociates in solution to give four different ionic species, H_3EDTA^-, H_2EDTA^{2-}, $HEDTA^{3-}$, $EDTA^{4-}$ (shown in figure 7), the relative amounts of which depend upon the pH of solution[75].

Figure 7 EDTA ionic species[76]

(a)

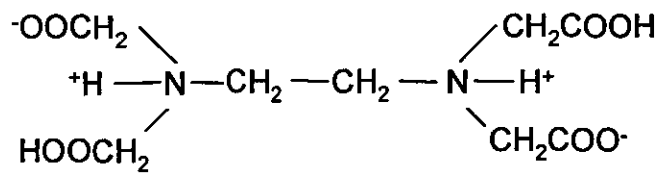

H_4EDTA

(b)

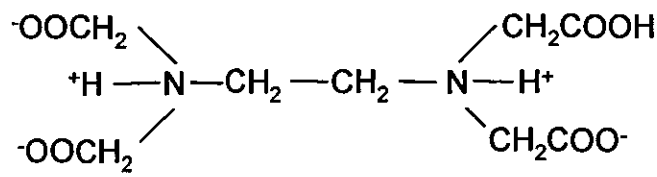

H_3EDTA^-

(c)

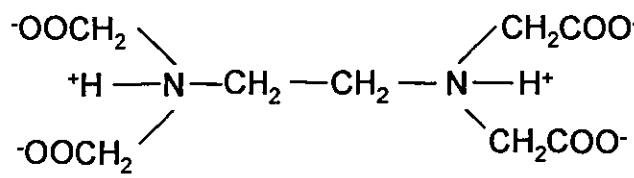

H_2EDTA^{2-}

(d)

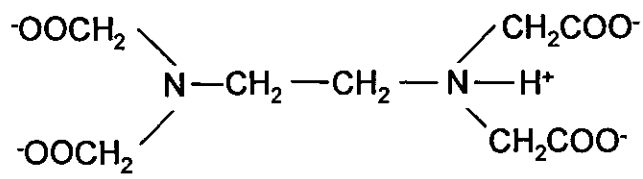

HEDTA^{3-}

(e)

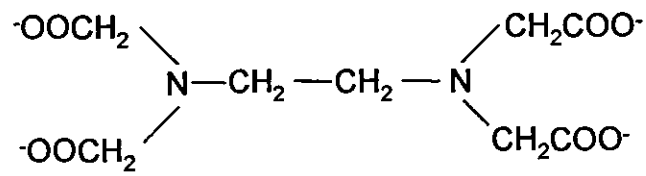

EDTA^{4-}

The proportion of the species present are represented by α-values and α_4 corresponds to the species EDTA^{4-}. Table 3 shows the fraction of this species present at various pH values.

Table 3 Fraction of EDTA^{4-} at pH 2 to 12[75]

pH	α_4
2	3.7×10^{-14}
3	2.5×10^{-11}
4	3.6×10^{-9}
5	3.5×10^{-7}
6	2.2×10^{-5}
7	4.8×10^{-4}
8	5.4×10^{-3}
9	5.2×10^{-2}
10	3.5×10^{-1}
11	8.5×10^{-1}
12	9.8×10^{-1}

The higher the pH of solution the more $EDTA^{4-}$ species are formed. Selected metal-EDTA formation constants (K_{MY}) are also shown in table 4.

Table 4 Selected metal-EDTA formation constants[75]

Cation	K_{MY}
Ag^{+}	2×10^{7}
Fe^{2+}	2.1×10^{14}
Co^{2+}	2×10^{16}
Ni^{2+}	4.2×10^{18}
Fe^{3+}	1×10^{25}
V^{3+}	8×10^{25}

From the data given in tables 3 and 4, a conditional constant ($K`_{MY}$) can be calculated that predicts whether or not the metal-EDTA complex will form at a certain pH from equation 7.

$$K`_{MY} = K_{MY}\alpha_4 \qquad \text{Equation 7[75]}$$

For example the stoiciometric reaction of a Mg^{2+} ion requires $K`_{MY} \geq 10^{6}$. For $Co^{2+}$ at pH 2 $K`_{MY} = (3.7 \times 10^{-14})(2 \times 10^{16}) = 7.4 \times 10^{2}$ this value is much lower than that required for Mg^{2+}. Therefore at pH 2 it would be unlikely that Co^{2+} would form a complex with EDTA. However it is known that the presence of octahedral complexes causes oxidation of Co^{2+} to Co^{3+}[75,77] and table 4 shows that 3+ charged ions have much higher formation constants than 2+ charged ions. Therefore the conditional constant of Co^{3+} calculated using EDTA at pH 2 was thought to be suitable for complex formation of Co with EDTA.

2.4.1.2 Elution with EDTA and HCl eluants

The following experiments investigate the effect on Ag, Co, Ho and Nb of using 0.01 mol dm^{-3} disodium EDTA and 5 mol dm^{-3} HCl eluants with a cation exchange resin.

A small column was prepared by placing 5 g of Amberlite IR-120 cation exchange resin (Na form) in a small glass burette. The column was washed with 5 mol dm^{-3} HCl (60 cm^3) converting the resin to H form. This was performed to ensure that the EDTA solution remained at a low pH as it passed through the column. The column was washed with distilled water (10 cm^3).

Two experiments were performed with a solution initially containing Co. The first experiment involved the sample being loaded onto the resin, followed by elution with EDTA solution and HCl. The second experiment involved a Co in EDTA solution being passed through the resin followed by elution of the resin with HCl. The two experiments were then compared to investigate the reaction of Co with EDTA at pH 2. A high concentration of Co was used for these experiments and the behaviour of Co was observed. The solutions were initially a pink colour because of the high Co^{2+} concentration.

In the first experiment 1000 mg dm^{-3} of Co solution (2 cm^3) was loaded onto the previously prepared resin. This was eluted with 0.01 mol dm^{-3} disodium EDTA solution (50 cm^3) at pH 2. The resin was then eluted with 5 mol dm^{-3} HCl (50 cm^3).

In the second experiment another column was prepared as described previously but this time the Co solution was passed through the column in a 0.01 mol dm^{-3} EDTA solution (50 cm^3) at pH 2. The resin was then washed with 5 mol dm^{-3} HCl (50 cm^3). A further 5 mol dm^{-3} HCl eluant (150 cm^3) was passed through the resin.

The eluates of these experiments were not measured by ICP because the concentrations of Co were too high, however the observations are discussed in section 3.3, chapter 3.

2.4.1.3 Reduced Co concentration

A lower concentration of Co was used in the next experiment for detection by ICP to give quantitative results. Another resin column was prepared in the same way as before and a 10 mg dm^{-3} Co solution (5 cm^3) in 0.01 mol dm^{-3} EDTA solution (pH 2) was passed through the column. The final volume was produced by passing water through the resin and diluting the eluate to 50 cm^3 for ICP-AES analysis. 5 mol dm^{-3} HCl (50 cm^3) was then passed through the resin in an attempt to remove the lower concentration of Co^{3+} adsorbed to the resin. The HCl solution was diluted for ICP-AES analysis.

The experiment was then repeated with 10 mg dm^{-3} Ag, Ho and Nb solutions (5 cm^3 of each) on the same resin to investigate the behaviour of these analytes compared to Co.

The experiment was repeated twice but the solution was added to a freshly made column as a mixture containing 10 mg dm^{-3} Ag, Co, Ho and Nb in EDTA solution (5 cm^3) instead of adding each element separately. The solutions were analysed by ICP-AES analysis.

A stronger concentration of EDTA solution was then used to elute a solution of Ag, Co and Ho from a cation exchange resin after the analytes were pre-loaded onto the resin.

2.4.1.4 Elution with higher concentration EDTA solution at pH 8

In this experiment the EDTA solution was adjusted to a higher pH of 8 with ammonium hydroxide solution so that a higher proportion of $EDTA^{4-}$ existed in solution providing a higher probability of Co-EDTA formation (a higher conditional constant would be obtained using the information in section 2.4.1.1). The resin was used in the Na form to prevent a decrease in pH as the solution was passed through the resin. The experiment was performed with 0.1 mol dm^{-3} EDTA solution. Nb was

not included in this experiment because it was found to be separated from the other elements instantly by elution with water.

5 g of Amberlite IR-120 cation exchange resin (Na form) was placed into a glass column and washed with water. 100 mg dm^{-3} Ag, Co and Ho (1 cm^3) were loaded onto the resin and washed with 0.1 mol dm^{-3} EDTA solution (50 cm^3) at pH 8. This was repeated and the solutions were analysed by ICP-AES.

The following experimental section investigates the nature and concentration of the competing ion of eluants (the second and third characteristics of eluants listed in section 2.4) for the sequential separation of Ag, Co, Ho and Nb from each other. The investigation of eluants that cause octahedral complexes and therefore were non selective towards Co were avoided for the remaining separation method development.

2.4.2 Attempted sequential elution of Ag, Co, Ho and Nb on cation resin

The nature of competing ions is related to the selectivity coefficient for the ion exchange reaction between the analyte ion and the eluant ion[71]. An elutropic series showing the order of selectivity coefficients of selected cations is shown below.

Figure 8 Order of selectivity coefficients for selected cations[78]

$$Pu^{4+} >> Ho^{3+} > Al^{3+} >> Pb^{2+} > Ca^{2+} > Ni^{2+} > Cu^{2+} > Co^{2+} > Mg^{2+} >> Ag^{+} > Cs^{+} > K^{+} > NH_4^{+} > Na^{+} > H^{+} > Li^{+}$$

Figure 8 shows that higher charged cations are more strongly adsorbed to the cation exchange resin than lower charged cations. At equal ionic charge, the elution strength sequence depends primarily on the size of the ion and its polarisability but it also depends on the properties of the ion exchanger itself[79].

The following experiments investigate the elution behaviour of Ag, Co, Ho and Nb by increasing the strength of various eluants in attempts to sequentially elute these

elements. The experiments were performed using Amberlite IR-120 cation exchange resin.

2.4.2.1 Elution with NH_4OH

Ammonium hydroxide is formed in ammonia solution via the equilibrium shown below.

$$NH_3 + H_2O \leftrightarrow NH_4OH \leftrightarrow [NH_4]^+ + [OH^-] \qquad \text{Equation 8[80]}$$

As the strength of ammonium hydroxide increases the equilibrium shifts to the right increasing the amount of NH_4^+ and OH^- ions in solution. This therefore increases the chance of eluting the adsorbed cations by the exchange of NH_4^+ ions with the adsorbed cations. Increasing strengths of ammonium hydroxide solutions were used in an attempt to elute Ag^+, Co^{2+} and Ho^{3+} from a cation exchange resin. Nb was not included in the experiment because it was known from previous experiments to pass through the resin as an anionic fluoro complex.

2 g of Amberlite IR-120 cation exchange resin were placed in a small column. 100 mg dm^{-3} Ag, Co and Ho solution (4 cm^3) was loaded onto the resin. The column was then washed with 0.1 mol dm^{-3} ammonia solution producing a 50 cm^3 eluate. 0.5, 1, 2, 3, 4 and 5 mol dm^{-3} ammonia solutions were then passed through the resin (50 cm^3 of each). Each eluate was diluted by pipetting 12.5 cm^3 and diluting to 50 cm^3 with distilled water for ICP-AES analysis.

Despite ammonium hydroxide possessing strong complexation properties through amine complex formation, the elutropic series in figure 9 shows that the hydroxide ion has the lowest selectivity coefficient of the ions shown in the series.

Figure 9 Order of selectivity coefficients for selected anions[78]

$$C_6H_5O_7^{3-} > ClO_4^- > SCN^- > I^- > S_2O_3^{2-} > CrO_4^{2-} > SO_3^{2-} > HPO_4^{2-} > NO_3^- > Br^- > NO_2^- > CN^- > HCO_3^- > CH_3COO^- > HCOO^- > ClO_3^- > F^- > OH^-$$

The low selectivity coefficient of the hydroxide ion does not favour the separation of the analytes from each other by selective de-adsorption. Experiments were therefore performed using an eluant containing an anion that was higher in the elutropic series than OH^- and therefore possessed a higher selectivity coefficient.

2.4.2.2 Elution with HNO_3

Increasing strengths of HNO_3 solutions were investigated. The following experiments were batch experiments rather than column experiments for simplification. Nb was included in this experiment and used as a control. It was known that Nb passed through the resin as a fluoro complex therefore the elution of the other analytes were compared to the 100% elution of Nb.

The batch experiments involved placing Amberlite IR-120 cation exchange resin (1.5 g) into twelve small glass vials. 1000 mg dm^{-3} Co, Ag, Ho and Nb solutions (0.1 cm^3 of each) were pipetted into each of the first nine vials and 0.2 cm^3 into the other three vials. The increased concentration was to enable the detection of the analytes after dilution of the eluates. The vials were covered with cling film and left standing for 2 hours to ensure complete adsorption of the cations to the resin. 0.1 mol dm^{-3} HNO_3 (10 cm^3) was added to each of the first three vials. 0.2 mol dm^{-3} HNO_3 (10 cm^3) was added to each of the next three vials. 0.5 mol dm^{-3} HNO_3 (10 cm^3) was added to a further three vials and 1 mol dm^{-3} HNO_3 (10 cm^3) was added to the last three vials. Each vial was shaken and left to stand for 12 minutes. The acid was then poured carefully into volumetric flasks taking care not to transfer any resin from the vials. The procedure was repeated several times until a final volume of 100 cm^3 was collected in each volumetric flask. The solution collected from the last three vials was diluted by measuring 50 cm^3 and diluting to 100 cm^3 with distilled water for ICP-AES analysis. The dilution was necessary to lower the acid concentration before analysis.

A method which separates Co from Ag, Ho and Nb was ideal. However the attempted methods so far did not achieve this which led to the investigation into the separation of individual analytes from Co. The next section investigates methods of separating Ag from Co.

2.5 Separation of Ag from Co

Thiocyanate is known to complex with Ag forming the Ag cyanide complexes $[Ag(CN)_2]^-$, $[Ag(CN)_3]^{2-}$ and $[Ag(CN)_4]^{3-}$[81]. These complexes occupy a relatively large amount of sites on an exchange resin and it was therefore possible to pre-concentrate Ag on an anion exchange resin[82]. Ammonium thiocyanate was not suitable for the determination of Ag in samples containing Fe (e.g. steel samples) where it was desirable to separate Ag from Fe because of the formation of complexes containing $Fe(CN)_6$[83]. It has also been reported that Ag was pre-concentrated in matrices containing other metals such as Fe, Cu, Ni etc. on Amberlite XAD-16 cation exchange resin in an acidic medium using a potassium thiocyanate eluate[84]. After careful consideration it was decided not to attempt a method of separation for Ag from Co using a thiocyanate eluant because of the eluants ability to react with many different metals including Cu, Zn, Ni and Fe[83,84]. Eluants containing the SCN^- ion are also shown to be higher in the elutropic series (Figure 9, section 2.4.2.1, chapter 2) than eluants containing the NO_3^- ion. This information together with results from HNO_3 elution of the analytes suggest that because of the strength of the eluant, Co would be eluted with Ag.

The focus of the investigation was then turned away from ion exchange and towards a different method of Ag separation.

2.5.1 Ag precipitation

AgCl precipitation was a problem in the original dissolution method where HCl was added to the dissolving solution. However the next set of experiments investigates the precipitation of AgCl as a possible separation method for separating Ag from Co after the successful transfer of these elements from solid waste samples to solution. NaCl was chosen instead of HCl to precipitate AgCl to avoid altering the acidity of solution.

2.5.1.1 Precipitation using NaCl

A solution containing 100 mg dm^{-3} Ag, Co, Ho and Nb (1 cm^3) was added to a 50 cm^3 volumetric flask. This was diluted to 50 cm^3 with 0.1 mol dm^{-3} NaCl solution. The solution was filtered through a 0.1 μm pore filter paper. The procedure was carried out twice and analysed by ICP-AES.

The concentration of NaCl was then increased in an attempt to fully precipitate Ag. A solution containing 100 mg dm^{-3} Ag, Co and Ho (1 cm^3) was added to a 100 cm^3 volumetric flask. This was diluted to 100 cm^3 with 0.2 mol dm^{-3} NaCl solution. The solution was filtered through a 0.1 μm pore filter paper and analysed by ICP-AES.

The following experiments were performed to determine the type of species of the remaining Ag which did not precipitate.

2.5.1.2 Precipitation using NaCl followed by cation exchange

A solution containing 100 mg dm^{-3} Ag, Co, Ho and Nb (1 cm^3) was added to a 100 cm^3 volumetric flask. This was diluted to 100 cm^3 with 0.2 mol dm^{-3} NaCl solution. The solution was filtered through a 0.1 μm pore filter paper. The solution was passed through 5 g Amberlite IR-120 cation exchange resin. The method was performed twice and the solutions were analysed by ICP-AES.

The next experiment was performed to confirm the nature of the remaining Ag species.

2.5.1.3 Precipitation using NaCl followed by anion exchange

A solution containing 100 mg dm^{-3} Ag, Co, Ho and Nb (1 cm^3) was added to a 100 cm^3 volumetric flask. This was diluted to 100 cm^3 with 0.2 mol dm^{-3} NaCl solution. The solution was filtered through a 0.1 μm membrane filter paper. The solution was then passed through 5 g of Dowex IX8-50 (chloride form) resin. The experiment was performed twice and the solutions analysed by ICP-AES.

A precipitating reagent that forms a Ag complex with a much lower solubility product than AgCl was investigated.

2.5.1.4 Precipitation using KI

The solubility of AgI and AgCl are compared below.

Figure 10 Solubility products for AgCl and AgI[85]

AgCl $K_{sp} = 1.8 \times 10^{-10}$ mol dm^{-3}

AgI $K_{sp} = 1.08 \times 10^{-16}$ mol dm^{-3}

Figure 10 shows that AgI is less soluble than AgCl and therefore KI was used in an attempt to precipitate 100% Ag as AgI.

A solution containing 100 mg dm^{-3} Ag, Co, Ho and Nb (1 cm^3) was added to a 50 cm^3 volumetric flask. This was diluted to 50 cm^3 with 0.1 mol dm^{-3} KI solution. The solution was filtered through a 0.1 μm pore filter paper. The experiment was performed twice and the solutions analysed by ICP-AES.

Ag and Co have been known to co-precipitate as metal dithizonates with precipitation of phenolphthalein in water samples[86]. However the following zirconium hydrogen phosphate method was chosen for investigation because it involves specific co-precipitation of AgI in the presence of similar elements to the analytes under investigation. This method reported quantitative levels of Ag below ppb levels[87].

2.5.2 Attempted AgI co-precipitation with $Zr(HPO_4)_2$

Phosphoric acid reacts with zirconium nitrate producing $Zr(HPO_4)_2$[88,87]. The crystalline phases of zirconium phosphate ($Zr(HPO_4)_2$) consist of layer structures similar to 2:1 clay minerals[89]. The formation of these crystals have been reported to co-precipitate Ag as AgI by adsorption to its surface[87].

The following method was attempted to achieve co-precipitation of AgI with $Zr(HPO_4)_2$ by the addition of KI. The method was originally reported to have been performed on mineral samples of Galena to determine Ag in the presence of various different elements including Pb[87]. The method involved a similar HNO_3 dissolution stage to that investigated for tacky swab samples. The method was therefore applied to solutions containing Ag, and Co as described below.

1000 mg dm^{-3} Ag and Co solutions (0.1 cm^3) were added to a 100 cm^3 volumetric flask. Concentrated HNO_3 (0.96 cm^3) was added to the flask to obtain a similar matrix composition to that of dissolved tacky swab samples. The solution was diluted to 97 cm^3 with distilled water. KI (1.6 g) was added to the solution and dissolved. 0.01 mol dm^{-3} zirconium nitrate solution (1 cm^3) was added to the flask. Concentrated phosphoric acid (1 cm^3) was added dropwise and the solution was diluted to 100 cm^3 with distilled water. The solution was left to stand for 30 minutes before it was filtered through a 0.1 μm pore filter paper and analysed by ICP-AES.

To promote the co-precipitation reaction, the experiment was repeated three times using excess Ag and $ZrO(NO_3)_2$. 1000 mg dm^{-3} Ag and Co stock solutions (0.2 cm^3) and 0.05 g of $ZrO(NO_3)_2$ solid were used. $ZrO(NO_3)_2$ was initially dissolved using an ultrasonic bath. The solution was left overnight before filtration. The filtrate was analysed by ICP-AES.

Although Ag precipitation experiments using NaCl were successful at separating 80% Ag from Co, a method was preferred that achieved a separation with Ag remaining in solution rather than as a solid precipitate. This was preferred to avoid a different

counting geometry than the solution at the dissolution stage of the method when applied to radioactive samples analysed for ^{108m}Ag.

It was shown in previous method development work that it was difficult to separate Co from Ag, Ho and Nb in one step using cation exchange methods. The next method of Ag separation from Co involved the elution of a cation exchange resin with a Ag selective eluant.

2.5.3 Elution of cation exchange resin with $NaNO_2$ eluant

Previous experiments showed that the elution of cation exchange resins loaded with Ag and Co using ammonium hydroxide and hydrochloric acid were unsuccessful at eluting either Ag or Co. The use of a nitric acid eluant showed elution of both Ag and Co. The NO_3^- ion reacted with Ag and Co but favoured reaction with Ag. The NO_2^- ion which was shown to possess similar elution characteristics to NO_3^- (Figure 9, section 2.4.2.1) was therefore considered.

Ag was reported to be quantitatively separated from Co on Amberlite IR-120 cation exchange resin (Na form) by using a 2% (w/v) $NaNO_2$ eluant[90,91]. The Ag nitrite complex formation is shown below.

$$Ag^+ + 2NaNO_2 \rightarrow [Ag(NO_2)_2]^- + 2Na^+ \qquad \text{Equation 9[90]}$$

The following experiments were performed in a fume cupboard because the acidic solution containing Co and Ag that passed through the resin caused evolution of the brown nitrogen dioxide gas.

10 g of Amberlite IR-120 cation exchange resin (Na form) were placed into a small plastic column and washed with 100 cm^3 distilled water. 1000 mg dm^{-3} Ag and Co stock solutions (0.1 cm^3) and concentrated HNO_3 (0.96 cm^3) were diluted to 100 cm^3, passed through the resin and analysed by ICP-AES. The solution was slightly acidic to match the matrix of dissolved tacky swab samples. 2% $NaNO_2$ solution (200 cm^3) was passed through the resin and collected in 10 cm^3 fractions for ICP-AES analysis. The concentration of $NaNO_2$ was then increased in an attempt to elute the remaining

Co from the resin. A 5% $NaNO_2$ solution (200 cm^3) was then passed through the resin and collected in 50 cm^3 fractions for ICP-AES analysis.

2.5.3.1 Increased contact time of $NaNO_2$ on the resin

The last experiment was repeated with the first 10 cm^3 2% $NaNO_2$ left in contact with the resin for 30 minutes before elution. The contact time was increased to prevent elution of the small amount of Co observed in the second 10 cm^3 fraction that was believed to be a result of the formation of nitrogen dioxide gas bubbles that produced a channel through the resin through which Co escaped adsorption to the resin. After 30 minutes most of the gas bubbles had escaped from the resin and the elution with $NaNO_2$ was performed. The 200 cm^3 2% $NaNO_2$ eluate was collected in 20 cm^3 fractions for ICP-AES analysis. The resin was then eluted with a further 100 cm^3 2% $NaNO_2$ solution and also collected in 20 cm^3 fractions. This was performed in an attempt to elute a higher yield of Ag and hence increase its separation from Co. The resin was then eluted with 5% $NaNO_2$ solution (400 cm^3) to remove Co from the resin. The resin was finally eluted with 8% $NaNO_2$ solution (200 cm^3) to elute any remaining Co on the resin. The solutions were collected as 100 cm^3 for ICP-AES analysis.

The experiment was repeated four times with 200 cm^3 2% $NaNO_2$ eluent because this was found to be sufficient for the Ag separation from Co in previous experiments. The solutions were analysed by ICP-AES.

2.6 Separation of Ho from Co

The similarity of the behaviour of Ho and Co towards EDTA led to the investigation being focussed on the separation of Ho from Co using different eluants on a cation exchange resin.

2.6.1 Ammonium citrate eluant

Ion exchange methods have been developed for the separation of rare earth elements using Amberlite cation exchange resin[92]. The rare earth elements adsorbed to the

resin and were then eluted with citric acid-ammonium citrate solutions[92]. The method has also been applied to radioactive isotope separations[92].

The citrate anion $C_6H_5O_7^{3-}$ elutes the rare earth 3+ charged cations[93,94]. Therefore experiments were performed to investigate separating Ho^{3+} from Co^{2+} on a cation exchange resin by eluting the resin with ammonium citrate solution. It was shown previously in figure 9 (section 2.4.2.1, Chapter 2) that the citrate ion occupied the highest position in the elutropic series and therefore was the most likely of the anions shown in the figure to elute the strongly bound Ho cation from the resin.

5 g of Amberlite IR-120 cation exchange resin were placed into a small glass burette. 100 mg dm^{-3} Ag, Co and Ho solution (1 cm^3) was loaded onto the resin and washed with 0.1 mol dm^{-3} ammonium citrate solution (50 cm^3) at pH 8. The experiment was performed twice and the solutions analysed by ICP-AES.

It was noticed that the use of a cation exchange resin in the hydrogen form reduced the pH of the ammonium citrate solution as it passed through the resin therefore the experiment was repeated a further two times using the sodium form of the cation exchange resin and the solutions were analysed by ICP-AES.

Two eluants were then chosen for investigation that were expected to selectively elute Co from a cation exchange resin leaving Ho adsorbed.

2.6.2 Ammonium oxalate eluant

Ammonium oxalate contains the oxalate anion $C_2O_4^{2-}$[76] and was used as a complexing reagent to elute Co from cation exchange resin.

5 g of Amberlite IR-120 cation exchange resin (Na form) were placed into a small glass burette. 100 mg dm^{-3} Ag, Co and Ho solution (1 cm^3) was loaded onto the resin and washed with 0.1 mol dm^{-3} ammonium oxalate solution (50 cm^3) at pH 8. The experiment was performed twice and the solutions analysed by ICP-AES.

2.6.3 Nitroso-R salt eluant

The nitroso-R salt reagent (sodium 1-nitroso-2-hydroxynaphthalene-3,6-disulphonate) is a common complexing reagent for Co[95,94,97]. Experiments were performed to investigate the complexing behaviour of the salt towards Co and Ho in attempts to separate Co from Ho by the elution of a Co nitroso complex from cation exchange resin.

100 mg dm^{-3} Co and Ho solution (1 cm^3) were loaded onto 5 g of Amberlite IR-120 cation exchange resin. The resin was washed with 0.01 mol dm^{-3} nitroso-R salt solution (50 cm^3). The resin was washed with a further 50 cm^3 0.01 mol dm^{-3} nitroso-R salt solution and the solutions were analysed by ICP-AES.

None of the eluants investigated were found to be successful at separating Ho from Co after they were loaded onto cation exchange resin. It was however reported that Co was successfully extracted from solution and separated from similar metals such as Fe and Ni using a chromatographic column coated with tri-n-octylamine(TnOA)[98]. After careful consideration the method involving the Co specific TnOA reagent was not investigated further because the separated metals were present as anionic chloro complexes from a HCl medium. The method was therefore not suitable for the separation of Co in a solution containing the Ag analyte because of AgCl precipitation. An anion exchange method was also reported for the separation of Ho from similar rare earth elements using HEDTA solution[99]. However a Ho specific resin was instead chosen for investigation, provided by Eichrom Europe[100].

2.6.4 Lanthanide resin

Table 5 shows selected extraction chromatography resins and their applications.

Table 5 Applications of selected extraction chromatography resins[100]

Resin	Selectivity
TRU resin	Actinides(III, IV, VI), Ln(III)
UTEVA resin	U(VI)
Ln resin	Ln(III)
Actinide resin	Actinides

Ln resin is the abbreviation for lanthanide resin, this material is used in extraction chromatography[100] for the separation of rare earth elements and was therefore suitable for the pre-concentration of Ho. The use of the resin for pre-concentration combines the selectivity of liquid extraction with column chromatography[100,101]. The lanthanide resin consists of an inert support of porous silica with the stationary phase being a dialkyl phosphoric acid such as HDEHP[100,98]. Selectivity is achieved through electrostatic and steric effects[100].

2.6.4.1 Extraction of Ho using lanthanide resin

The following experiments investigate the adsorption of Ho onto lanthanide resin in the presence of Co. The procedure was adapted from a Pm / Sm separation method provided by Berkeley Centre[102].

1.65 g of lanthanide resin were mixed with 0.15 mol dm^{-3} HNO_3, placed in a 10 cm^3 plastic column and left to settle. 0.15 mol dm^{-3} HNO_3 (5 cm^3) was then passed through the column. 1000 mg dm^{-3} Co and Ho solutions (0.5 cm^3) in 0.15 mol dm^{-3} HNO_3 (4 cm^3) were loaded onto the resin. The resin was then eluted with 0.15 mol dm^{-3} HNO_3 (150 cm^3). The eluate was diluted to 250 cm^3 with distilled water. The elution was repeated with further 0.25 mol dm^{-3} HNO_3 (2 × 150 cm^3) and 1 mol dm^{-3}

HNO_3 (150 cm^3) and the same dilutions made with distilled water. The eluates were analysed by ICP-AES.

The experiment was repeated without elution of the resin with 1 mol dm^{-3} HNO_3. The eluates were analysed by ICP-AES.

Experiments were performed to investigate the behaviour of Ho towards the lanthanide resin with the analytes Nb and Ag also in solution.

2.6.4.2 Extraction of Ho and Nb using lanthanide resin

1000 mg dm^{-3} Co, Ho and Nb solutions (0.5 cm^3 of each) in 0.15 mol dm^{-3} HNO_3 (3.5 cm^3) was pipetted onto 1.65 g lanthanide resin and washed with 0.15 mol dm^{-3} HNO_3 (150 cm^3). The sample was diluted to 250 cm^3 with distilled water. The experiment was repeated three times and the solutions analysed by ICP-AES

1000 mg dm^{-3} Ag, Co, Ho and Nb stock solutions (0.25 cm^3 of each) were added to 1.65 g lanthanide resin and washed with 0.15 mol dm^{-3} HNO_3 (150 cm^3). The sample was diluted to 250 cm^3 with distilled water. The experiment was performed three times and the solutions analysed by ICP-AES.

The successful separation of Ho and Nb from Ag and Co using lanthanide resin was then applied to dissolved tacky swab samples.

2.6.4.3 Application of Ln resin separation to dissolution samples

The dissolution samples prepared in previous experiments contained a HNO_3 concentration similar to that used for the successful separations of Ho and Nb from Ag and Co. Therefore these dissolved tacky swab samples were passed through lanthanide resin columns for comparison.

A dissolution sample containing 4 mg dm^{-3} Ag, Co, Ho and Nb was diluted by pipetting 12.5 cm^3 of the 500 cm^3 solution into a 50 cm^3 flask and diluting to 50 cm^3 with distilled water to produce a solution with a sufficiently low acid concentration

for the separation using lanthanide resin. This was analysed by ICP-AES. Another dilution was made from the same sample in the same way and passed through 1.65 g of lanthanide resin and analysed by ICP-AES. The experiment was repeated several times using different dissolution samples.

Dissolution samples containing higher concentrations of Ag, Co, Ho and Nb (8 mg dm^{-3}) were then diluted in the same way as in the last experiment and passed through lanthanide resin columns and analysed by ICP-AES.

The dissolution samples were passed through the lanthanide resin at a very slow rate of less than one drop per second and the method of separation was very time consuming. The following experiment investigates the effect of increasing the flow rate of solution through the resin on the adsorption of Ho and Nb in an attempt to reduce the time of separation.

2.6.4.4 Flow rate of solution through lanthanide resin

Solutions containing 1000 mg dm^{-3} Ag, Co, Ho and Nb (4 cm^3 of each) were diluted to 2000 cm^3. 500 cm^3 of this solution was then pumped through 1.65 g of lanthanide resin at approximately 40 cm^3 min^{-1} using a peristaltic pump and stored for analysis. Another 500 cm^3 of the same solution was pumped through the resin at approximately 70 cm^3 min^{-1} and stored for analysis. This was repeated at a faster flow rate of approximately 100 cm^3 min^{-1} using another 500 cm^3 of solution. Each of the solutions were analysed by ICP-AES.

Following the successful separation of Ag, Ho and Nb from Co, the analysis of radioactive tacky swab and filter paper samples was investigated.

2.7 Radioactive tacky swab / filter paper samples

The easily measured principal long-lived radionuclide ^{60}Co is known to be present in excess on radioactive tacky swab and filter paper samples. The long-lived radionuclides ^{108m}Ag, ^{94}Nb and ^{166m}Ho are estimated to be present in Decommissioning Waste at much lower concentrations and may therefore be present in tacky swab and filter paper samples. Some properties of the radionuclides of interest are listed in table 6.

Table 6 Isotope properties[103]

Radionuclide	Half-life (y)	Energies of gamma emissions (keV)	Intensity of energies (%)
^{108m}Ag	418	720	90
		620	90
		430	90
^{94}Nb	20,000	890	100
		703	100
^{166m}Ho	1,200	80	100
		185	100
		706	80
		817	80
^{60}Co	5.27	1332	99
		1172	99

Each isotope has a long half-life and emits gamma emissions of various energies which give rise to peaks when measured by gamma spectrometry. The two ^{60}Co signals produce Compton edge scattering which swamps any peaks that arise from the analyte radionuclides because ^{60}Co is present in excess. Therefore the detection of the analytes by gamma spectrometry is difficult and requires the removal of ^{60}Co from these analytes.

2.7.1 Application of dissolution and separation methods

The flow chart in figure 11 shows the combined dissolution and separation methods performed on two duplicate radioactive tacky swab samples and two duplicate radioactive filter paper samples at Berkeley Centres Low Level Active Facility. The samples were used to transfer dust consisting of various radionuclides carried via the gas circuits that collect in the boilers outside of the reactor core of the Berkeley Magnox reactor.

Figure 11 Summary of combined methods for swab / filter samples

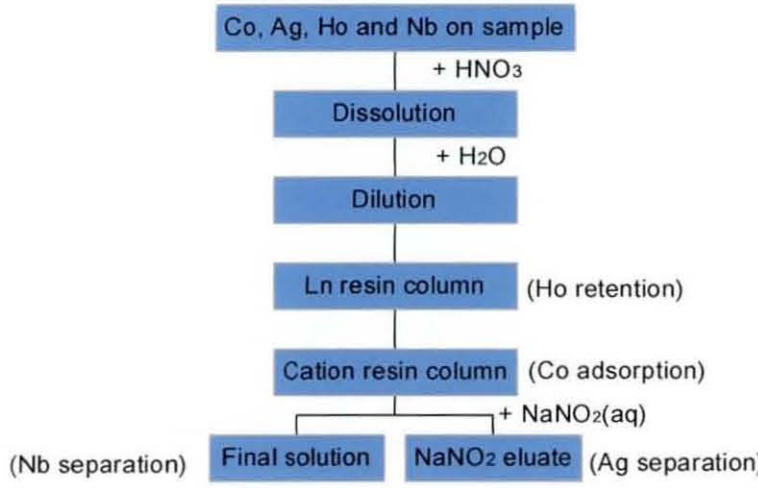

The radioactive samples were doped with inactive Ag, Co, Ho and Nb tracers for two reasons.

(i) To compare the behaviour of those tracer elements with method development experiments.

(ii) To correct activity measurements for the yield of the particular element of interest.

Once the radioactive samples were dissolved, the lanthanide resin, cation resin and $NaNO_2$ separation methods were applied to separate and determine the radioanalytes and inactive tracer elements. The following experimental procedure details these combined methods performed on radioactive samples. The step by step procedure is

also shown in the Work Instruction (MSTLU002, Appendix A) produced for BNFL for the analysis of radioactive samples.

2.0 g of radioactive sample were placed into a 250 cm^3 conical flask. The sample was doped with 1000 mg dm^{-3} Ag, Ho and Nb stock solutions (2 cm^3 of each) and 10,000 mg dm^{-3} Co stock solution (0.2 cm^3). Fuming HNO_3 (15 cm^3) was added to the flask, covered with a watch glass and left overnight. 5 mg dm^{-3} iron carrier solution (2 cm^3) and a magnetic stirrer were added to the flask and heated between 80 and 90°C for 1 hour using a hot plate. The solution was cooled to room temperature and diluted with distilled water (150 cm^3). The solution was filtered through a 0.45 μm pore filter. The filter was heated to 500°C for 30 minutes in a zirconium crucible. After cooling, Na_2O_2 (1.0 g) was added and the residue was heated to 600°C for 30 minutes. The black residue was cooled, suspended in distilled water (40 cm^3) / 6 mol dm^{-3} HNO_3 (10 cm^3) and filtered through a 0.45 μm pore filter. The two filtrates were combined and diluted to 2000 cm^3 with distilled water obtaining a solution with a sufficiently low acid concentration for the following separation stages. The solution was pumped through 1.65 g of lanthanide resin at approximately 10 cm^3 min^{-1} using a peristaltic pump. The solution was passed through 10 g of pre-washed Amberlite IR-120 cation exchange resin (Na form) and collected for analysis. 2% $NaNO_2$ solution (10 cm^3) was added to the cation resin and left in contact with the resin for 30 minutes. The resin was eluted with 2% $NaNO_2$ solution producing a 200 cm^3 eluate. The solution was analysed at each stage of the method by ICP-AES analysis to trace the behaviour of Ag, Co, Ho and Nb. The solutions and resins were analysed by gamma spectrometry.

2.7.2 ICP-AES analysis

10,000 mg dm^{-3} Co, 1000 mg dm^{-3} Ag and Ho and 1011 mg dm^{-3} Nb stock solutions were used to produce the following ICP-AES standards. A 50 mg dm^{-3} Ag, Co, Ho and Nb solution was produced by pipetting 10,000 mg dm^{-3} Co solution (0.5 cm^3), 1000 mg dm^{-3} Ag and Ho solutions (5 cm^3 of each) and 1011 mg dm^{-3} (4.9 cm^3) into a flask and diluting to 100 cm^3 with distilled water. A series of standards were then produced containing Ag, Co, Ho and Nb at 0.5, 1.5, 3 and 6 mg dm^{-3} by pipetting 1, 0.75, 6 and 12 cm^3 of the 50 mg dm^{-3} solution respectively into separate flasks and

diluting to 100 cm^3 with distilled water and concentrated HNO_3 (5 cm^3). HNO_3 was added to match the dissolution sample matrices.

The wavelengths used for detection were 328.0 nm for Ag, 228.6 nm for Co, 345.6 nm for Ho and 309.4 nm for Nb.

2.7.3 Blank swab / filter samples

2 g of inactive tacky swab and filter paper samples were doped with inactive tracer elements and the combined dissolution and separation methods detailed in section 2.6.2 were performed on these samples at Berkeley Centre. The inactive method development experiments performed at Loughborough University showed different behaviour of the Nb analyte to the radioactive samples and it was therefore necessary to perform these blank sample experiments at Berkeley Centre using the Nb stock solution provided for doping the radioactive samples.

2.7.4 Gamma spectrometry analysis

The radioactive swab and filter samples were analysed by gamma spectrometry in 100 cm^3 top pots at each stage of the method. Total counting time was not less than 20,000 seconds. Long counting times were chosen for analysis to improve the sensitivity of detection. The counting efficiency for each sample was calculated using equation 10.

$$\mathbf{E_c\ (\%) = \frac{cps}{dps} \times 100} \qquad \text{Equation 10}$$

cps = counts per second, dps = disintegrations per second

The resins were measured as slurries and the counting geometry was accounted for by measuring the slurries as 'filter' geometries with the resin beads evenly spread out across the bottom of the pots.

Following the successful development and application of dissolution and separation methods for tacky swab and filter paper samples, the project focused on developing dissolution and separation methods that can be applied to directly measure radioanalytes in steel waste samples.

2.8 Steel samples

The type of steel used in nuclear power stations varies depending on which components are used in each specific part of the building. Boron containing steel is common in Decommissioning Waste because throughout the life of the reactor, the fission process is controlled by "control rods", containing boron. When these rods are lowered into the reactor, they adsorb neutrons and the fission process slows down. The reactor vessel itself consists of eight inch thick steel and the concrete shield around the reactor vessel is lined with stainless steel. Therefore it is important to analyse the various types of steel and to assess the impact of neutron activation on the varying elements contained in those steels. Waste metal includes structural components, valves, pumps and tools made of stainless steel, mild steel or nonferrous metals, used during maintenance or decommissioning of nuclear facilities. Table 7 shows the typical elemental composition of common steel samples in Decommissioning Waste.

Table 7 Selected steel compositions[104]

Type of Steel	Typical Elemental Composition
Stainless Steel	Mostly Fe, 18% Cr, 9% Ni, 1%Ti, < 1% C, P, S, Mn, Si, Al
Mild Steel	99% Fe, 0.007-0.2% Ni, < 1% C, P, S, Mn, Si, Al
Boron Steel	Mostly Fe, 8% Ni, 3-4% B, < 1% C, P, S, Mn, Si, Al
Low alloy Steel	Mostly Fe, 1% Ni, < 1% C, P, S, Mn, Si

^{108m}Ag and ^{94}Nb are the dominant radionuclides in steel waste[3]. Radioactive steel samples often require direct gamma measurement of ^{108m}Ag, ^{94}Nb and to a lesser extent ^{166m}Ho radionuclides in the presence of excess ^{60}Co and ^{55}Fe[7]. The determination of ^{108m}Ag and ^{94}Nb by separation from excess ^{60}Co is required because of the Compton edge scattering in gamma spectrometry similar to the radioactive swabs and filters. The determination of Ag and Nb by separation from Fe is also required because high concentrations of Fe interfere with ICP emission spectra of Ag, Nb and Ho tracer elements added to radioactive samples.

Traces of ^{60}Co have been successfully determined in steel samples without pre-concentration and pre-separation by HPLC[105]. However the following investigations into Co separation from Ag and Nb involve relatively simple ion exchange techniques and ICP-AES is a standard measurement technique for measuring Co in steel samples[106].

Steel samples have been digested by microwave digestion methods[16]. Methods have also been reported that involve analysis of specific radioisotopes such as ^{3}H in steel and ^{36}Cl and ^{129}I in concrete which use acid dissolution as a pre-concentration step[107,108]. The following experimental work investigates dissolution and separation methods for the analysis of the four common types of steel in decommissioning waste shown in table 7. Like previous tacky swab method development work, the method development for steel samples involved using samples that were not radioactive. The determination of Ag, Co, Ho and Nb in the following dissolution and separation experimental work for steel samples was performed by ICP-AES analysis. The dissolution method development for steel samples was based on a method provided by Berkeley Centre[109]. The method involved dissolving the steel samples in HCl, HNO_3 and HF.

2.8.1 Stainless steel dissolution

A stainless steel control sample (0.5 g) was added to a 250 cm^3 polypropylene conical flask. Concentrated HNO_3 (3.5 cm^3), concentrated HCl (5 cm^3) and concentrated HF (1.5 cm^3) were added to the sample and left overnight. The sample had not fully dissolved therefore it was heated at 90°C for 20 minutes. The sample was diluted to 500 cm^3 with distilled water for ICP-AES analysis.

The experiment was then repeated but the dissolved sample was doped with 1000 mg dm^{-3} Ag, Co, Ho and Nb solutions (1 cm^3 of each). HCl was not added to the sample to prevent precipitation of AgCl observed in previous tacky swab and filter paper samples. HCl was replaced by the addition of a further 5 cm^3 concentrated HNO_3 (8.5 cm^3 concentrated HNO_3 in total). The sample was much more difficult to dissolve without HCl and was therefore heated for 1 hour at 90°C, left overnight and then heated for a further 3 hours at 90°C. Most but not the entire sample dissolved. The sample was diluted to 500 cm^3 with distilled water for ICP-AES analysis.

The last experiment was repeated with 3 hours of heating at 90°C, left overnight and a further 3 hours of heating at 90°C to further dissolve the sample. The sample was diluted to 500 cm^3 with distilled water for ICP-AES analysis.

Stainless steel was found to be too difficult to fully dissolve without using HCl and therefore methods of separation for Fe and Co were investigated on the partially dissolved steel sample.

Fe and Cr are known to be removed from steel samples with zinc oxide allowing determination of Co[110]. This method appears suitable for the removal of Fe from stainless steel samples which also contain Cr. It has also been reported that Fe, Co and Ni were separated from each other on an ion exchange resin with varying concentrations of HCl[111]. However both these methods of Fe and Co removal were not suitable for the analysis of Ag because they involved the use of HCl which would produce a AgCl precipitate.

2.8.2 Separation of Nb from Co in stainless steel

The determination of trace amounts of ^{94}Nb in steel and stainless steel have been reported[112,113,114]. The separation of Nb in steel samples has also been investigated by the removal of the iron matrix[115]. However the method uses a solvent extraction technique which is undesirable for large scale radionuclide separations because of the large amount of organic solvent waste produced.

It was thought that Nb may be separated from Co and Fe using a similar method to that used for tacky swab samples. Most of the trace metals in stainless steel dissolutions are present as cations (e.g. Co^{2+} and Fe^{3+}) in soluble nitrates whereas Nb was thought to be present as the anionic fluoro complex $[NbOF_5]^{2-}$ and would therefore pass through a cation exchange resin. The theory was supported by reports of Nb retention on anion exchange resin in the presence of 2 mol dm^{-3} HF whilst the Fe matrix was not retained[116,117]. The method reported, used a flow injection technique which is widely applied to the separation and pre-concentration of trace and ultra trace concentrations of metals to improve the sensitivity of determination and to eliminate interferences from the sample matrix[118,119,120]. The instrumentation available was limited and therefore the principals of this method were investigated using a relatively simple ion exchange experiment. Instead of eluting Nb from anion exchange resin with a mixture of HNO_3 and HCl reported in the method[116], the interfering elements Fe and Co were retained on a cation exchange resin whilst Nb passed through the resin in solution. This avoided using an unnecessary elution step.

The partially dissolved stainless steel samples from the last two experiments were therefore passed through two separate columns containing 10 g of Amberlite IR-120 cation exchange resin and the solutions were analysed by ICP-AES.

2.8.3 Separation of Ag from Co in stainless steel

Ag has been determined in alloy steel by elution from a cation exchange resin with potassium thiocyanate[84]. However this was achieved in the presence of high concentrations of Fe, Ni and other metals. Therefore this method was not suitable for the steel samples being investigated because Ag requires separation from excess Fe and Co. Ammonium thiosulphate has been reported to separate Ag from Fe after loading a strong cation exchange resin with the $Ag[SC/NH_2/_2]_2^+$ thiourea cation complex[121]. The Ag was then eluted as the $AgS_2O_3^-$ complex[121]. After careful consideration it was chosen not to investigate this method further because steel samples contain many different metal cations and resins generally exhibit non-selective adsorption characteristics. This would complicate Ag desorption with the high loading of metal ions on the resin[121]. This reason also applies to the considered investigation of the $NaNO_2$ eluate for the elution of Ag from a cation exchange resin. However as the method was successful at separating Ag from Co in tacky swab samples, the relatively simple method was attempted on dissolved stainless steel samples.

The two cation exchange resins that the previous two partially dissolved stainless steel samples passed through were both eluted with 200 cm^3 $NaNO_2$ solution (2% w/v). The eluates were diluted to 500 cm^3 and analysed by ICP-AES.

Mild steel does not contain any Cr or Ti and the samples were therefore easily dissolved in HNO_3.

2.8.4 Mild steel dissolution

A piece of mild steel (0.5 g) was added to a 250 cm^3 polypropylene conical flask. The sample began to react with HNO_3 as it was being added and therefore 5 cm^3 concentrated HNO_3 was added to the sample. The sample fully dissolved in HNO_3 after 1 hour of heating at 90°C. The sample was diluted to 500 cm^3 with distilled water for ICP-AES analysis. The dissolution was performed twice and the solutions analysed by ICP-AES.

The mild steel dissolution was then repeated, doping the sample with 1000 mg dm^{-3} Ag, Co, Ho and Nb solutions (0.2 cm^3 of each). The sample was diluted to 100 cm^3 with distilled water and analysed by ICP-AES. The experiment was repeated.

2.8.5 Separation of Nb from Co in mild steel

A mild steel sample was doped with 1000 mg dm^{-3} Ag, Co, Ho and Nb solutions (0.5 cm^3 of each) and dissolved in 5 cm^3 concentrated HNO_3. After dissolution concentrated HF (1 cm^3) was added to the solution and diluted to 100 cm^3 with distilled water. HF was added to promote the formation of the anionic fluoro Nb complex for separation. The solution was then passed through 25g of Amberlite IR-120 cation exchange resin. A larger amount of resin was used compared with stainless steel samples in an attempt to avoid the small amount of Co shown to have passed through the resin. The sample was diluted to 500 cm^3 with distilled water for ICP-AES analysis. The experiment was performed on four samples.

The Nb separation experiment was repeated twice more on mild steel samples with an increased HF concentration added. These were performed to investigate the affect on Ag retention because a small amount of Ag passed through cation exchange resin in the last four samples after the addition of 1 cm^3 concentrated HF. Therefore concentrated HF (2 cm^3) was added to a dissolved mild steel sample before it was passed through 25 g of the cation exchange resin. Concentrated HF (3 cm^3) was added to another dissolved mild steel sample before it was passed through 25 g of cation exchange resin. Both samples were initially doped with 1000 cm^3 Ag, Co, Ho and Nb (0.2 cm^3 each) and diluted to 100 cm^3 with distilled water before ICP-AES analysis.

2.8.5.1 Use of NaF for the separation of Nb from Co

An experiment was then performed involving the use of NaF instead of HF for the separation of Nb from Co. Successful separation using NaF would lower the risks associated with handling HF (NaF is initially present as a solid and therefore handling is not as dangerous as handling HF liquid). Although HF will be used throughout the remaining steel method development, it would provide an alternative for Nb separation.

A mild steel sample was doped with 1000 mg dm^{-3} Ag, Co, Ho and Nb solutions (0.2 cm^3 of each) and dissolved as before in concentrated HNO_3 (5 cm^3). After dissolution, 1 g of NaF was dissolved in 1 cm^3 water and added to the sample. The sample was diluted to 100 cm^3 and passed through 25 g cation exchange resin and analysed. The experiment was repeated and the solutions analysed by ICP-AES.

2.8.6 Separation of Ag from Co in mild steel

The separation of Ag and Nb from Co for mild steel samples in a single step was not achieved and the following experimental work focuses on separating Ag from Co. The use of the $NaNO_2$ eluant on a cation exchange resin was investigated for stainless steel samples but was not appropriate for the separation in mild steel because it was found to elute a mixture of Ag and Co nitrite complexes. The method was therefore not selective towards either Ag or Co.

2.8.6.1 Separation using co-precipitation

When a precipitate separates from a solution it is not always pure, it may contain varying amounts of impurities depending on the nature of the precipitate and the conditions of precipitation[122]. Surface adsorption is a common form of co-precipitation and involves adsorption at the surface of the particles which are exposed to solution[122]. Ag has been determined by co-precipitation from water with a thionalide solution at various pH values[123]. This co-precipitation method was however not successful at separating Ag from Co and Fe because these elements were also removed from solution. A different Ag co-precipitation method was then investigated.

Palladium is known to be reduced from Pd^{2+} to Pd metal and precipitated by the addition of ascorbic acid[124,125,126]. Ascorbic acid ($C_6H_6O_6$) is commonly represented as H_2A and is a common reducing agent for some platinum group metals. The redox reaction and potential of H_2A and Pd are shown in equations 11 and 12.

$$A + 2H^+ + 2e \leftrightarrow H_2A \qquad +0.40 \text{ (potential, V)}$$ Equation 11[126]

$$Pd^{2+} + H_2A \leftrightarrow Pd(s) + A + 2H^+ \qquad +0.55 \text{ (potential, V)}$$ Equation 12[126]

From the redox reactions it is shown that Pd precipitates as a solid via its reduction. The precipitation and co-precipitation of trace elements such as Co and Fe in copper salt matrices and analysis by ICP has been investigated[127]. However a more appropriate separation method involving the co-precipitation of Ag by reduction and precipitation of Pd in high purity iron and steel has been achieved[127,128]. The method separates Ag from many other metals such as Co, Fe and Ni[129]. However increasing the components (elements present) of a solution requires a higher ascorbic acid concentration for the same yield of Pd[126]. This is because the ascorbic acid has a reducing affect on other elements present such as Fe.

$$2Fe^{3+} + H_2A \leftrightarrow 2Fe^{2+} + A + 2H^+$$ Equation 13[126]

2 g of ascorbic acid were reported to be necessary for precipitation of 3 mg Pd and 0.5 g ascorbic acid necessary for quantitative recovery of 0.2 μg Ag in a high purity iron sample containing 10 components[129].

The precipitation of Pd has been performed on highly radioactive waste samples[107,108] and would therefore be a suitable method of Ag separation assuming the applied method is successful.

The following experimental procedure was performed on further mild steel samples.

0.5 g of mild steel was doped with 1000 mg dm^{-3} Ag, Co, Ho and Nb solutions (0.2 cm^3 of each). Higher concentrations of the elements of interest than the concentration of Ag added in the original method[129] were added to the sample because the analysis was performed using ICP-AES rather than ET-AAS. The sample was dissolved in concentrated HNO_3 (5 cm^3) and heated for 1 hour at 90°C. 1000 mg dm^{-3} Pd solution (3 cm^3) was added. Concentrated H_2SO_4 (10 cm^3) and concentrated H_3PO_4 (10 cm^3) were then added to solution and heated until the solution began to

turn to gas. This step was necessary because HNO_3 impedes the reduction of Pd by ascorbic acid. The orange solution was cooled to room temperature and diluted to 80 cm^3 with distilled water. Ascorbic acid (3 g) was then added to the flask and the solution turned black which then turned clear after 5 to10 minutes. The solution was left to stand for 3 hours and the solution remained clear with no visible precipitate, therefore a further 3 g of ascorbic acid was added forming a black solution which remained black after standing for 30 minutes before turning clear again. There was no precipitate to re-dissolve therefore ICP-AES analysis was not performed in this experiment, the observations however are discussed in section 3.12.1, Chapter 3.

To simplify the experiment and reduce the possibility of Pd oxidation by HNO_3, the experiment was performed with the addition of a lower concentration of Ag and lower concentration of acid.

2.8.6.1.1 Steel doped with Ag and dissolved with lower HNO_3 concentration

The precipitation of Pd was attempted again by repeating the experiment using a 0.5 g mild steel sample doped with 1000 mg dm^3 Ag solution (0.1 cm^3). 7 mol dm^{-3} HNO_3 (10 cm^3) and 6 mol dm^{-3} HCl were added instead of concentrated HNO_3 for dissolution. The lower concentration of HNO_3 was added to prevent HNO_3 oxidising Pd to Pd^{2+}. HCl was then required to achieve dissolution of the sample. Furthermore the flask was left standing with a stopper after the addition of ascorbic acid to prevent excess oxygen entering the flask. After the addition of ascorbic acid the solution was left to stand for 30 minutes. The solution turned colourless but was however filtered through a 1.0 μm pore polycarbonate filter paper. A small amount of white / brown precipitate was collected and dissolved in concentrated HNO_3 (5 cm^3), diluted to 100 cm^3 with distilled water and analysed by ICP-AES. The results are discussed in section 3.12.6.1.1, Chapter 3.

A higher concentration of ascorbic acid was then added to a repeat experiment to prevent the re-oxidation of Pd.

2.8.6.1.2 Addition of more ascorbic acid

The last experiment was repeated using a 0.5 g mild steel sample with the addition of a further 3 g of ascorbic acid after the solution had turned clear to overcome the oxidation of Pd. The solution remained black and was then filtered through a 1.0 μm pore polycarbonate filter paper. The small amount of brown precipitate was dissolved in HNO_3 as in the last experiment. The ICP-AES analysis is discussed in section 3.12.6.1.2, chapter 3.

An experiment was performed to trace the behaviour of Pd because it was thought that Pd was not successfully precipitated in previous experiments.

2.8.6.1.3 Determination of Pd

The last experiment was repeated with the addition of 9 g of ascorbic acid. The black solution was filtered, diluted to 500 cm^3 and analysed for Pd by ICP-AES. The filter paper was dissolved in 5 cm^3 concentrated HNO_3, diluted with distilled water and analysed for Pd by ICP-AES.

3, 6, 9 and 12 mg dm^{-3} Pd standard solutions were produced for calibration of the ICP-AES instrument because the maximum concentration of Pd in solution after dilution assuming that Pd was not precipitated was 6 mg dm^{-3}.

2.8.6.2 Precipitation in mild steel samples

Ag was separated from some of the initial concentration of Co added in stainless steel samples by the elution of a cation exchange resin with $NaNO_2$. However Ag remained in the presence of a large amount of Fe which may interfere with the detection of Ag in radioactive samples. Ideally a method that removes Fe as well as Co from Ag in steel samples was preferred. The investigation into the separation of Fe, Co and Ag in steel samples was performed on mild steel samples because of the simple dissolution method developed. It would have been far more problematic to develop a method such as this on the more difficult to dissolve steel samples.

It was reported that Fe was removed from stainless steel liquor containing a HNO_3 / HF medium by solvent extraction[130] and ^{60}Co has been determined in steels and alloy steels by extraction of iron chloride with an organic solvent followed by precipitation of the potassium cobaltinitrite complex[131]. However organic solvent separations are not desirable as large scale radioisotope separation methods because of the large volume of organic waste produced. Furthermore a method that separates Fe and Co from Ag was preferred. The precipitation of Ag as Ag_2S using H_2S is known and has a very low solubility in water (Ksp $\approx 10^{-50}$ mol dm^{-3})[132], however Co was also expected to precipitate with this reagent. The precipitation of Ag in the presence of Fe has been reported[133]. In this method EDTA was used to mask large concentrations of Fe, Ni, Cu, Zn, Co, Al and Pb most of which are present in steel samples. The drawback with this method was that the dissolution of the precipitate involved the use of the hazardous potassium cyanide reagent. It was therefore decided to concentrate the investigation on the precipitation of Fe from Ag rather than Ag from Fe so that Ag could easily be measured in solution by ICP analysis.

Iron is known to precipitate from solution as a red / brown $Fe(OH)_3$ compound[134]. In the previously mentioned extraction method (section 2.3.3) using TnOA, Fe was stripped from a column and determined by the precipitation of $Fe(OH)_3$[98]. Precipitation of Fe in solution with Ag, Co, Ho and Nb was therefore investigated. It is known that Fe precipitates between pH 2 and 3 but it was not certain how the analytes (Ag, Ho and Nb) would behave at varying pH values in a mixed component solution. There was concern about Co remaining in solution with this method once Fe was precipitated. Co, the other interfering isotope in radioactive samples would swamp the detection of Ag and Nb radioisotopes. There was also concern that the analytes would precipitate with Fe because it was reported that various metal radioisotopes were scavenged through iron hydroxide precipitation[135]. However the separation technique appeared promising from a prediction made by the speciation programme JCHESS[33]. The programme predicted that Ag would remain in solution after the precipitation of Fe. The following graph was the result of inputting the concentrations of elements in solution over a pH range of 2 to 14. The programme then calculated the species of analytes, Co and Fe expected to be present over this pH range using various data including stability constants.

Figure 12 JCHESS predicted precipitation of analytes

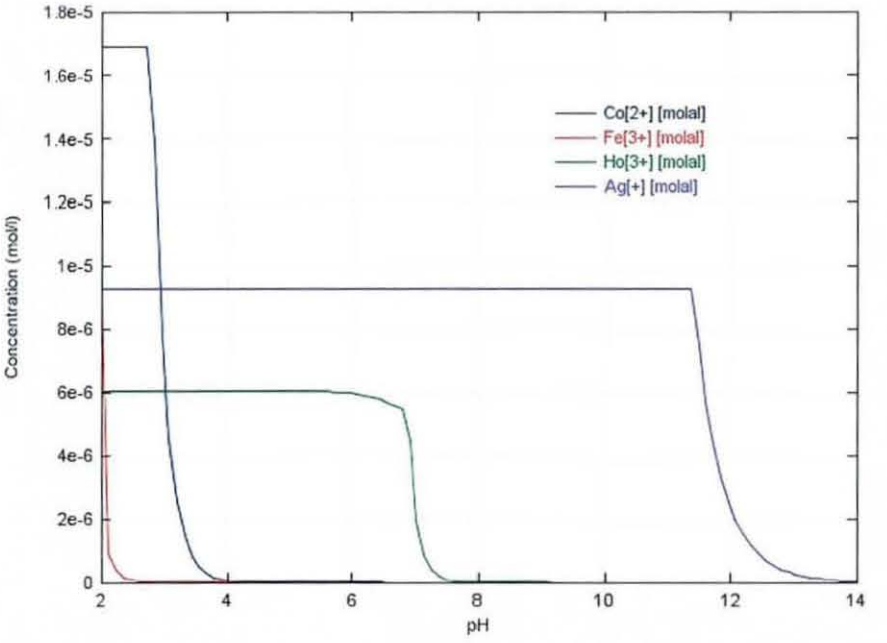

The graph shows the concentration of each element in mol dm^{-3} plotted against pH. The programme predicted that Fe would precipitate between pH 2 and 3. Co was predicted to precipitate between pH 3 and 4, Ho between pH 6 and 8 leaving Ag in solution up to pH 11 where Ag was finally predicted to precipitate. The programme output was therefore promising for the separation of Ho and more importantly Ag from Fe and Co. The predicted behaviour of Nb was not available because the stability constants for this analyte were not present in the programme database.

2.8.6.2.1 Precipitation of Fe using NaOH

A mild steel sample (0.5 g) was doped with 1000 mg dm^{-3} of Ag, Co, Ho and Nb solutions (0.2 cm^3 of each) and dissolved in concentrated HNO_3 (5 cm^3). After dissolution the sample was diluted to 50 cm^3 with distilled water. NaOH solution (1 mol dm^{-3}) was added and the solution stirred until pH 2 was achieved (0.1 mol dm^{-3} NaOH solution was added to fine tune the pH). The volume of NaOH added was recorded and the expected concentration of the analytes was calculated using this value. The solution was filtered through a 0.1 μm pore filter paper. The procedure was

performed on a further ten mild steel samples adjusting the pH of each sample so that a range of results between pH 2 and 12 were obtained. The high pH solutions were acidified after filtration for ICP-AES analysis (1.5 cm^3 HNO_3 added).

The set of experiments over the pH range 2 to 12 were repeated and analysed by ICP-AES.

The analytes were found to behave differently to the predicted analyte behaviour and the theory of co-precipitation of the analytes with Fe was confirmed by repeating the set of experiments without any steel present. Therefore the same dissolution and separation method was applied to solutions containing the same initial concentrations of analytes and the solutions analysed by ICP-AES.

Ammonia solution was then used to precipitate Fe and to avoid co-precipitation of Ag with Fe.

2.8.6.2.2 Precipitation of Fe using NH_4OH solution

Ag forms an ammine complex which is very soluble[47]. Ammonia solution was therefore considered for the precipitation of Fe and separation of Ag from Fe and Co. The JCHESS speciation programme[33] was run a second time with 1 mol dm^{-3} NH_4OH inputted with the analytes and interferences (Ag, Ho, Nb, Co and Fe). The output graph produced was the same as the one shown in figure 12, section 2.8.6.2. However the accompanying analysis data provided additional information about the behaviour of Ag over the pH range. At between pH 5 and 7, Ag^+ was predicted to begin precipitating. However the Ag diammine complex $[Ag(NH_3)_2]^+$ also began to form between pH 5 and 7 preventing the precipitation of Ag. The speciation prediction was promising because of the high solubility of the strong Ag diammine complex formation.

A set of experiments were performed in the same way as the NaOH precipitation experiments in section 2.8.6.2.1 using the same concentrations of analytes and adjusting the pH of solution with 1 mol dm^{-3} NH_4OH over a range of pH 2 to pH 10 (fine tuning of pH was performed using 0.1 mol dm^{-3} NH_4OH). The solutions were

analysed by ICP-AES analysis. The set of experiments that involved using NH_4OH were repeated.

Following the successful methods of separating Nb and Ag from mild steel samples, the dissolution of inactive steel containing boron similar to that used in the control rods of nuclear reactors was investigated.

2.8.7 Dissolution of boron containing steel

A boron containing steel sample (0.5 g) was added to a 250 cm^3 polypropylene conical flask. Concentrated HNO_3 (5 cm^3) and concentrated HF (1 cm^3) were added to the sample and heated to 90°C. The sample was more difficult to dissolve than mild steel. The sample fully dissolved after 1 hour of heating and was therefore not as difficult to dissolve as stainless steel. The sample was diluted to 100 cm^3 with distilled water for ICP-AES analysis.

The experiment was then performed a further two times after doping the steel with 1000 mg dm^{-3} of Ag, Co, Ho and Nb solutions (0.2 cm^3 of each) and analysed by ICP-AES.

2.8.8 Separation of Nb from Co in boron containing steel

The two doped sample experiments were repeated and passed through separate columns of cation exchange resin (25 g). The solutions were analysed by ICP-AES. It was expected that the HF added would promote the formation of anionic Nb fluoro complexes which would pass through the resin similar to results obtained for stainless and mild steel samples.

The successful Ag separation method for mild steel samples was then performed on boron containing steel samples.

2.8.9 Separation of Ag from Co in boron containing steel

A further two doped samples were dissolved. The solutions were diluted to 50 cm^3 with distilled water, adjusted to pH 9 with 1 mol dm^{-3} NH_4OH and filtered through a 0.1 μm pore filter paper. The samples were acidified with 1.5 cm^3 concentrated HNO_3 before ICP-AES analysis.

The fourth commonly found type of steel in Decommissioning Waste was then investigated using the successful dissolution, Nb separation and Ag separation methods applied to inactive samples.

2.8.10 Dissolution of low alloy steel

A sample of low alloy steel (0.5 g) was added to a 250 cm^3 polypropylene conical flask. Concentrated HNO_3 (5 cm^3) and concentrated HF (1 cm^3) were added to the sample and heated at 90°C. The sample fully dissolved after 1 hour of heating. The sample was diluted to 100 cm^3 with distilled water for ICP-AES analysis. The experiment was repeated and the solutions were analysed by ICP-AES.

The experiment was then performed a further two times after doping of the steel with 1000 mg dm^{-3} of Ag, Co, Ho and Nb solutions (0.2 cm^3 of each). The solutions were analysed by ICP-AES.

2.8.11 Separation of Nb from Co in low alloy steel

The two doped sample experiments were repeated and passed through separate columns of cation exchange resin (25 g). The solutions were then analysed by ICP-AES.

2.8.12 Separation of Ag from Co in low alloy steel

A further two doped samples were dissolved. The solutions were diluted to 50 cm^3 with distilled water, adjusted to pH 9 with 1 mol dm^{-3} NH_4OH and filtered through 0.1 μm pore filter paper. The samples were acidified with 1.5 cm^3 concentrated HNO_3 before ICP-AES analysis.

It was necessary to create an overall method of analysis for the steel samples through the combination of the individual dissolution and separation methods. This was performed on mild steel samples because of the simplicity of dissolution for these samples and because radioactive mild steel samples were available for analysis once an overall method was successful.

2.8.13 Combination of successful dissolution and separation methods for mild steel samples

An experiment was performed that involved the separation of Ag and Nb in successive steps after the dissolution of a mild steel sample. A summary of the overall process and the detailed experimental method are shown below.

Figure 13 Combined method for mild steel

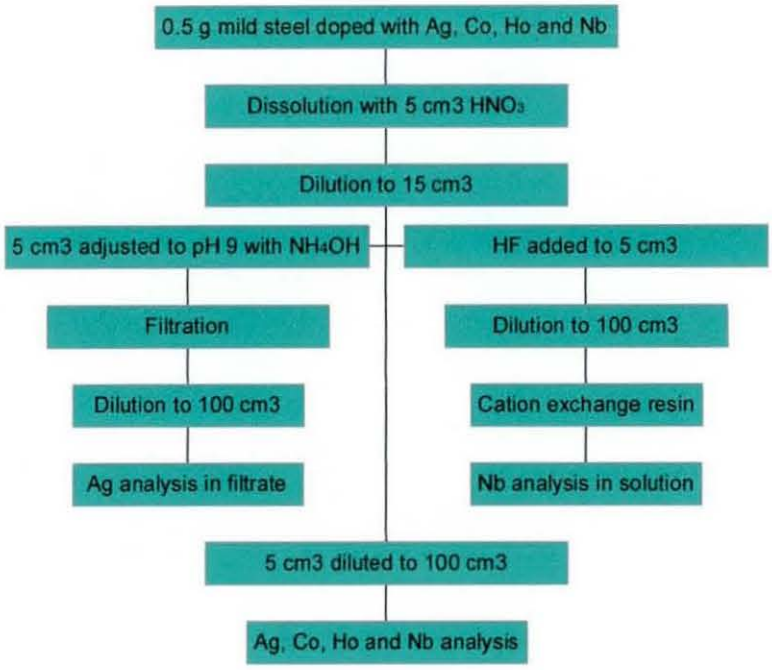

Dissolution:

Mild steel (0.5 g) was added to a 250 cm^3 conical flask and doped with 1000 mg dm^{-3} of Ag, Co, Ho and Nb solutions (0.2 cm^3 of each). Concentrated HNO_3 was then added to the sample (5 cm^3) and heated for 1 hour at 90°C. After dissolution the sample was pipetted into a small plastic vial and the volume pipetted was recorded. Distilled water was then added to the flask, swirled and pipetted to the same plastic vial until a total of 15 cm^3 of solution was in the vial. This was to ensure the transfer of all the dissolved steel sample from the flask to the vial.

Nb separation:

5 cm^3 of solution from the vial was then pipetted into a 100 cm^3 volumetric flask with concentrated HF (1 cm^3) and diluted to 100 cm^3 with distilled water. This was then passed through 25 g of pre-washed Amberlite IR-120 cation exchange resin (washed with 100 cm^3 distilled water) and stored for ICP-AES analysis.

Ag separation:

Another 5 cm^3 sample solution was pipetted from the vial and adjusted to pH 9 with 1 mol dm^{-3} ammonia solution in a beaker with a stirrer. The brown precipitate was then filtered through a 0.1 μm pore filter paper. The filtrate was diluted to 100 cm^3 with distilled water. 20 cm^3 of the diluted filtrate was then transferred to another plastic vial, concentrated acid (1.5 cm^3) was added to acidify the sample for ICP-AES analysis.

The final 5 cm^3 sample solution was diluted to 100 cm^3 with distilled water and analysed by ICP-AES for conformation of successful transfer of the analytes from the steel sample to solution. The experiment was repeated and the solutions analysed by ICP-AES.

2.8.14 Radioactive mild steel analysis

The successful dissolution and separation method combination detailed in the previous section was applied to six radioactive mild steel samples of mass 0.34 g to 0.95 g provided by Berkeley Centre. The samples were taken from pressurised heat exchanger vaults of a typical magnox reactor. The step by step procedure used is also shown in the Work Instruction (MSTLU003, Appendix A) produced for BNFL for the analysis of radioactive samples. The initial ^{60}Co, ^{55}Fe and ^{63}Ni activity was estimated in the six solid steel samples prior to the experimental procedure. Two of the samples had relatively large masses (0.79 g and 0.95 g) and therefore did not fully dissolve when the dissolution method was applied to them. An additional 1cm^3 concentrated HF was then added to these steel samples and further heating was applied until dissolution was complete (between 3 and 5 hours heating at 90°C). This additional step for these two samples provided a third of the amount of HF required for the Nb separation stage and therefore only 0.75 cm^3 concentrated HF was added before the first 5 cm^3 of sample solution was passed through the cation exchange resin.

2.8.14.1 ICP-AES analysis

The inactive tracer elements Ag, Co, Ho and Nb were measured in solution at the three stages (dissolution, Nb separation and Ag separation) for each of the six radioactive samples after they were measured by gamma spectrometry analysis. The ICP-AES calibration was performed using Ag, Co, Ho and Nb standard solutions produced from 1000 mg dm^{-3} stock solutions. 2000 mg dm^{-3} Fe was added to the standard solutions for the analysis of sample solutions where Fe was present (after the dissolution and Nb separation stages of the method).

The wavelengths used for detection were 328.0 nm for Ag, 228.6 nm for Co, 345.6 nm for Ho and 309.4 nm for Nb.

2.8.14.2 Gamma spectrometry analysis

The cation exchange resin and filter paper from the two separation stages of each steel sample were transferred to top-pots and each solution was transferred to 100 cm^3 beakers for gamma spectrometry analysis. The counting time varied between 5000 to 20000 seconds. The counting efficiency was calculated similarly to the previous tacky swab and filter paper samples using equation 10, section 2.7.4. The resins were measured as slurries and the counting geometry was accounted for by measuring the slurries as 'filter' geometries with the resin beads evenly spread out across the bottom of the pots.

Chapter 3

Results and Discussion

3.0 Results and discussion

3.1 Dissolution method development for tacky swab / filter paper samples

Table 8 shows the ICP results for the dissolution of two tacky swab samples doped with inactive Ag, Co, Ho and Nb using HNO_3 / HCl in a dissolution method provided by Berkeley Centre[17].

Table 8 Analysis of tacky swab dissolution samples

ICP-MS			ICP-AES		
	Conc. (mg dm^{-3})	% Recovery		Conc. (mg dm^{-3})	% Recovery
Ag	0.15	15	Ag	0.23	23
Co	0.77	77	Co	1.04	100
Ho	0.39	39	Ho	0.58	58
Nb	0.71	71	Nb	0.49	49

The maximum concentration of analytes in solution assuming that the analytes were completely transferred from the swab samples to solution was 1 mg dm^{-3}. The first dissolution sample was measured by ICP-MS and shows similar recoveries to the second dissolution sample that was measured by ICP-AES. Both samples show a significant loss of Ag, Ho and Nb. The loss of these analytes was thought to be because of precipitation of chloride complexes formed from the use of HCl in the dissolution procedure. Co was not observed to precipitate and a good recovery was shown by both instruments. ICP-AES was chosen for analysis throughout the method development because the availability of the ICP-MS instrument at Loughborough University was limited.

The following section shows results of the dissolution procedure performed without the addition of HCl to avoid precipitation of the analytes.

3.1.1 Dissolution using fuming HNO_3

Figure 14 summarises the percentage recoveries of Ag, Co, Ho and Nb calculated from ICP-AES results when the dissolution was performed with fuming HNO_3 instead of concentrated HNO_3 and concentrated HCl.

Figure 14 Dissolution using fuming HNO_3

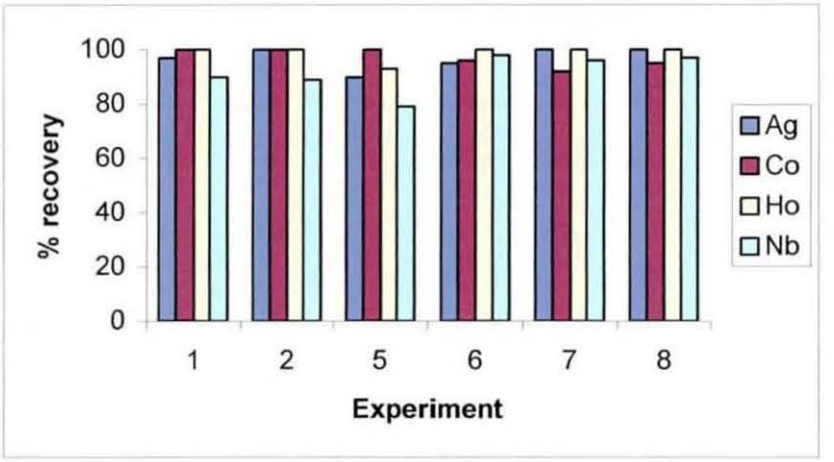

The maximum concentration from ICP-AES results of each analyte in solution assuming that the analytes were completely transferred from the swab samples to solution was 1 mg dm^{-3}. This concentration was equivalent to 100% recovery shown in figure 14. The results show that > 80% recovery of each analyte was achieved. The use of fuming HNO_3 resulted in the successful transfer of the analytes to solution confirming that the use of HCl in the dissolution procedure was the cause for the loss of analytes.

The ICP-AES results of a dissolution using a lower volume of fuming HNO_3 to investigate the effect of reduced acid concentration on analyte recoveries are shown in table 9.

Table 9 Dissolution with 15 cm^3 fuming HNO_3

	Ag	Co	Ho	Nb
Conc. (mg dm^{-3})	1.17	0.94	0.93	0.88

The maximum concentration of each element in solution assuming the complete transfer of these elements from the swab sample to solution was 1 mg dm^{-3}. The results show that 15 cm^3 fuming HNO_3 was sufficient to dissolve the swab sample and transfer the analytes to solution. 15 cm^3 will therefore be used for future dissolutions and the use of unnecessarily high concentrations of fuming HNO_3 was avoided.

The use of 0.1 μm instead of 0.45 μm pore filter paper for filtration did not affect the recoveries and were therefore also used in future dissolution experiments.

3.1.2 Nb stabilisation in ICP standard solutions

Table 10 shows the comparison of a freshly produced control solution with the previously used Nb standard solution. Both of these solutions were diluted from the original 1000 mg dm^{-3} Nb stock solution to concentrations of 1 mg dm^{-3}.

Table 10 ICP-MS analysis of Nb standard solution

Sample	Counts per second
Nb control solution	1.2×10^7
Nb standard	4.7×10^6

These results show that the Nb standard solution was approximately three times less concentrated than expected indicating a loss of Nb from solution. The loss was thought to be precipitation of Nb from solution over time because the standards had not been used for several days. The precipitation theory was confirmed by the observation of a cloudy precipitate at the bottom of the standard solution flask. Nb therefore requires trace HF to remain in solution as the Nb fluoro complex. The trace HF from the original stock solution was diluted in the process of producing the

standard solutions and was therefore not a sufficient concentration to prevent Nb precipitating over time.

Table 11 shows the ICP-AES results of five solutions containing varying concentrations of HNO_3 for the investigation into the effect of HNO_3 concentration on the stabilisation of solutions containing Nb.

Table 11 Stabilisation of Nb solutions with HNO_3

HNO_3 acid content (v/v)	Nb (mg dm^{-3})
1 %	4.16
2 %	3.97
3 %	4.12
4 %	4.04
5 %	3.87

The maximum concentration of Nb in each solution assuming that Nb remained soluble was 4 mg dm^{-3}. Niobium was shown to be stable for 24 hours in solutions with a HNO_3 content between 1 and 5%. Therefore an acid content between 1 and 5% HNO_3 was suitable for Nb standard solutions that were freshly produced for the analysis of a set of samples. It was realised that HNO_3 had no affect on the stabilisation of Nb and that Nb remained in solution up to several days because of a trace amount of HF from the dilution of the stock solution. This was confirmed by reports that no soluble Nb nitrates are available for analytical work[44]. After several days, Nb undergoes hydrolytic decomposition[44]. Such balanced reactions which do not readily proceed to completion, give rise to colloidal suspensions of hydrated oxides[44] explaining the cloudiness of Nb solutions containing no HF. This phenomena is related to the 'use by' date on the Nb stock solution and Nb becomes less stable in solution over time. Additional HF would be required to prevent the precipitation of Nb in the standard solutions if they were not freshly prepared prior to analysis.

The conclusions of Nb stabilisation from this section of the report were taken into consideration when measuring future samples against ICP standard solutions.

The following section shows the results of further dissolutions involving the addition of higher concentrations of Ag, Co, Ho and Nb.

3.1.3 Recoveries of analytes at higher concentrations

Figure 15 shows percentage recoveries of Ag, Co, Ho and Nb calculated from ICP-AES results for swab samples that were doped with higher concentrations of the elements of interest.

Figure 15 Recoveries of analytes at higher concentration of 4 mg dm^{-3}

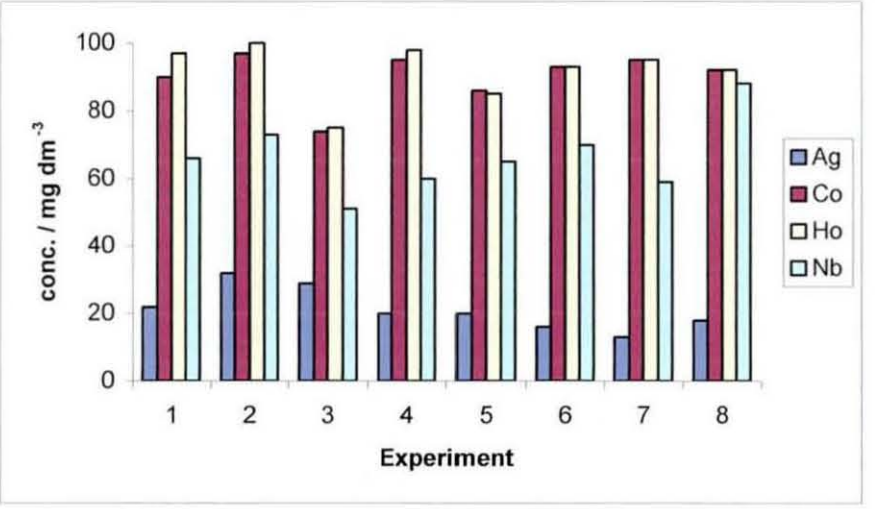

The maximum concentration from ICP-AES results of each analyte in solution assuming that the analytes were completely transferred from the swab samples to solution was 4 mg dm^{-3}. Therefore 100% recovery shown in figure 15 was equivalent to 4 mg dm^{-3}. The results show that an average of 88% Co, 89% Ho and 67% Nb were detected. Only 25% Ag was detected however the average concentration of Ag measured was 0.8 mg dm^{-3} which was similar to the concentrations measured in previous experiments where samples were doped with lower concentrations of Ag. This result indicates that 0.8 mg dm^{-3} was the maximum soluble amount of Ag.

Figure 16 shows percentage recoveries of the elements of interest calculated from ICP-AES results for five swab samples that were doped with higher concentrations of Ag, Co, Ho and Nb and three swab samples that were doped with higher concentrations of Ag, Co and Ho.

Figure 16 Recovery of analytes at higher concentrations of 8 mg dm^{-3}

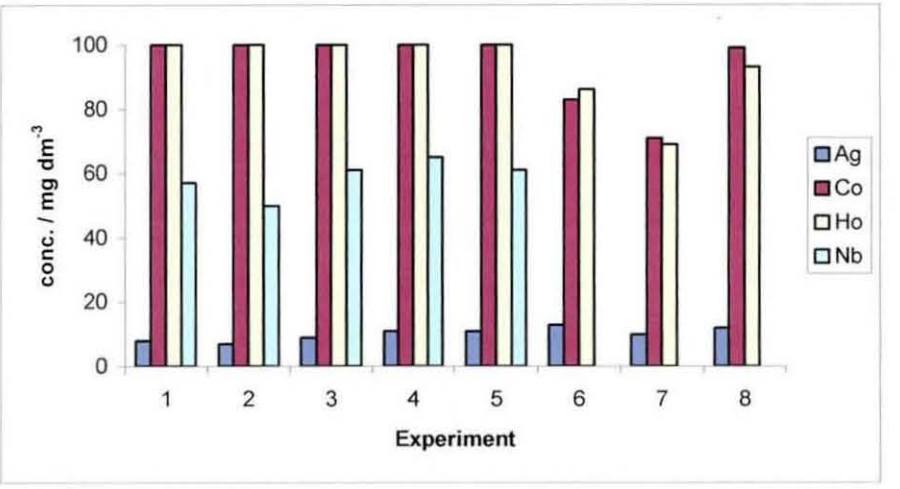

The maximum concentration from ICP-AES results of each analyte in solution assuming that the analytes were completely transferred from the swab samples to solution was 8 mg dm^{-3}. Therefore 100% recovery shown in figure 16 was equivalent to 8 mg dm^{-3}. The results show good recoveries for Co and Ho and an average of 59% Nb in the samples where Nb was added.

An average concentration of 0.8 mg dm^{-3} Ag was again detected and the same results were observed in the three experiments without the addition of Nb. This suggests that the low recovery of Ag was not related to the increased HF content of solution, which occurs because of the higher concentration of Nb stock solution added. The theory was supported by the relatively high solubility product of AgF shown in equation 2, section 2.2.7, chapter 2.

Generally the dissolution of doped swab samples producing solutions containing higher concentrations than 1 mg dm^{-3} of the elements of interest were not successful for the recovery of 100% Ag. It was thought that a possibility for this observation was

that Cl^- may be present in the tacky swab material or from contaminated glass wear causing the formation of AgCl. The maximum soluble amount of Ag in the dissolution samples was calculated to be approximately 0.8 mg dm^{-3} using the solubility product shown in equation 1, section 2.2.7, chapter 2. This explains why no more than 0.8 mg dm^{-3} of Ag was being detected in any of the dissolution samples. The concentration of Nb in the swab samples decreases slightly with increased initial Nb concentration suggesting that Nb was becoming less stable in solution at higher concentrations.

3.1.4 Filter washing

The ICP-AES results of another dissolution resulting in a solution containing expected concentrations of 1 mg dm^{-3} Ag, Co, Ho and Nb is shown in table 12. The table also shows ICP-AES results of the acid / water solution used to wash the filter of this experiment.

Table 12 Filter washed with HNO_3 / H_2O

	Ag (mg dm^{-3})	Co (mg dm^{-3})	Ho (mg dm^{-3})	Nb (mg dm^{-3})
Dissolution filtrate	0.81	1.06	1.04	0.93
HNO_3 / H_2O washing	0.02	0.00	0.00	0.00

The maximum concentration of each element in the filtrate assuming the complete transfer of each element from the swab sample to solution was 1 mg dm^{-3}. The dissolution filtrate shows similar results to those obtained in previous experiments and the successful transfer of the elements of interest to solution. However it was not certain whether or not the 20 to 30% of initial concentration of Ag that was not detected after dissolution precipitated as AgCl. At these relatively low concentrations it was believed that the slightly lower than expected concentrations of Ag may be due to experimental error. The results of the filter washing analysis strengthen this theory because no significant amount of Ag was detected. HNO_3 may not have been

appropriate for re-dissolving AgCl and therefore table 13 shows the ICP-AES results of another dissolution sample filter washed with ammonia solution.

Table 13 Filter washed with ammonia solution

	Ag (mg dm^{-3})	Co (mg dm^{-3})	Ho (mg dm^{-3})	Nb (mg dm^{-3})
Dissolution filtrate	0.70	1.07	1.09	0.87
NH_4OH washing	0.06	0.00	0.00	0.05

The maximum concentration of each element in the filtrate assuming the complete transfer of each element from the swab sample to solution was 1 mg dm^{-3}. AgCl is very soluble in ammonia solution[47] therefore these results suggest that AgCl was not present on the filter and that all of the Ag was transferred to solution .The slightly lower than expected concentration of Ag detected in the dissolution sample was believed to be experimental error.

Ag recovery for samples doped with higher concentrations of Ag was not investigated because the last set of experiments confirm that the transfer of Ag to solution was successful for solutions containing a final expected concentration of 1 mg dm^{-3} which is sufficient for the analysis of radioactive samples using Ag tracers.

Filter paper samples were found to dissolve more easily than tacky swab samples and the dissolution process was therefore also suitable for filter paper samples.

3.2 Separation of Co by complexation

Following the successful method of dissolution, the separation of Co from Ag, Ho and Nb was investigated using Co specific complexing reagents.

3.2.1 Co complexation with 1-nitroso-2-naphthol

The observations of experiments performed using 1-nitroso-2-naphthol as a complexing reagent for Co are discussed. The experiment was performed four times, however ICP-AES results showed no recovery of the analytes. Therefore the complexing reagent was successful at oxidising Co^{2+} to Co^{3+} as expected. This was because 1-nitroso-naphthol is an octahedral complexing agent, however it was not selective at separating Co from the other analytes.

The following section shows results of a different Co specific reagent for the attempted separation of Co from Ag, Ho and Nb in one step.

3.2.2 Diphenyl sulfimide ligand

Table 14 shows ICP-AES results for the filtrates of two solutions initially containing Co.

Table 14 Co reaction with diphenyl sulfimide ligand

Amount of ligand (g)	Co in filtrate (mg dm^{-3})
0.01	2.19
0.05	0.02

The maximum concentration of Co in solution after filtration and dilution assuming that Co did not complex with the ligand was 4 mg dm^{-3}. The results show that when 0.01 g of diphenyl sulfimide ligand was added to a solution containing Co, 45% of the initial concentration of Co complexed with the ligand and was therefore filtered from solution. When the amount of ligand added was increased to 0.05 g, 100% Co

complexed with the ligand. The results therefore show that approximately 0.025 g of diphenyl sulfimide ligand was required to completely remove Co from solution. The Co complex that formed in the experiments was octahedral and required six ligands to complex with each Co cation[59].

The ICP-AES results for the filtrates of repeat experiments using 0.025 g of the ligand with the inclusion of the analytes Ag and Ho in solution are shown in table 15.

Table 15 0.025 g diphenyl sulfimide ligand added to a solution of Co, Ag and Ho

Experiment	Ag (mg dm^{-3})	Co (mg dm^{-3})	Ho (mg dm^{-3})
1	3.43	3.30	3.28
2	2.95	2.81	2.80
3	2.86	2.89	2.66

The maximum concentration of Ag, Co and Ho in solution after filtration and dilution assuming that these elements did not complex with the ligand was 4 mg dm^{-3}. The results show that an average of 25% of the initial concentration of each element reacted with the ligand and therefore the ligand was not selective towards Co in the presence of Ag and Ho. The ligand partially dissolved when the stock solutions of Ag, Co and Ho were added. This was explained by the fact that the ligand was soluble in HNO_3 which was present in the Ag, Co and Ho stock solutions.

Table 16 shows the ICP-AES results of a filtrate for an experiment which used lower volumes of analyte stock solutions to decrease the concentration of HNO_3 preventing ligand dissolution.

Table 16 0.05 g diphenyl sulfimide ligand added to lower concentrations of Co, Ag and Ho

	Ag	Co	Ho
Filtrate (mg dm^{-3})	1.46	0.95	0.00

The maximum concentration of Ag, Co and Ho in solution after filtration and dilution assuming that these elements did not complex with the ligand was 2 mg dm^{-3}. The results show that 50% Co, 100% Ho and 25% Ag were removed from solution. These results therefore confirm that the ligand was not selective for the removal of Co from solution. It was also shown that because an excess amount of the ligand was added, Ho was preferred to react with the ligand shown by 100% removal of Ho. The similar behaviour of the ligand towards Ho and Co can be explained by their ionic charges. The ligand was known to have a strong tendency towards Co because of the oxidation of Co^{2+} to Co^{3+}. Therefore it was not surprising that the ligand was found to also have a strong tendency towards Ho. This together with the knowledge that the inorganic ligand dissolves in HNO_3 made the method unsuitable for the separation of Co in dissolution samples.

The following section shows results of the investigation into another Co complexation experiment involving the precipitation of a cobaltinitrite complex.

3.2.3 Co precipitation as cobalt nitrite

The ICP-AES results of a filtrate after the attempted precipitation of a cobaltinitrite complex are shown in table 17.

Table 17 Co precipitation as cobalt nitrite

	Ag	Co	Ho	Nb
Conc. (mg dm^{-3})	0.13	O / F	0.07	0.38

The maximum concentration of Ag, Ho and Nb in solution after filtration assuming that these elements did not complex with the ligand was 0.5 mg dm^{-3}. O / F is an abbreviation for over-flow and was recorded because the amount of Co detected was above the highest detection limit of the detector. This was because of the excess amount of Co added as the Co reagent. All the Co was expected to precipitate as the complex $Cs_3[Co(NO_2)_6]$[49]. However the loss of Ho and Nb from solution indicate that these analytes competed with Co for the reaction with $NaNO_2$. This explains the result that some of the Co reagent remained in solution causing the final concentration of Co to be detected above the detection limits of the spectrometer. A loss of Ag from solution was also observed, this was believed the result of AgCl precipitation from the caesium chloride reagent added. This could have been avoided with the use of a caesium nitrate reagent. The experiment was not however repeated using this reagent because the method was similar to the other three Co complexation methods investigated and was not selective towards Co in the presence of Ho.

The following results show the analysis of various eluants used to elute and separate Co from Ag, Ho and Nb on a cation exchange resin.

3.3 Cation exchange resin with EDTA and HCl eluants

The following discussion is a comparison of observations from experiments involving samples containing Co in EDTA solution that were passed through a cation exchange resin and, the elution of Co pre-adsorbed to a cation exchange resin.

A pink solution was observed in the first experiment when the resin containing pre-adsorbed Co was eluted with 0.01 mol dm^{-3} EDTA solution. A colourless solution was observed when the resin was eluted with 5 mol dm^{-3} HCl. These observations indicate that Co was eluted from the resin with the EDTA solution and the strong pink colour suggests that Co was present in solution. The reaction taking place was thought to be first the oxidation of Co^{2+} to Co^{3+} followed by the reaction shown in equation 14.

$$Co^{3+} + [H_2EDTA]^{2-} \leftrightarrow [CoEDTA]^{-} + 2H^{+}$$ Equation 14[71]

The colourless 5 mol dm^{-3} HCl solution indicates that all or most of the initial amount of Co was eluted in the previous EDTA eluate. This experiment strengthens the theory that Co^{3+} forms a complex with EDTA from the calculation using metal-EDTA formation constants (section 2.4.1.1, Chapter 2).

In contrast, a colourless solution was observed in the second experiment after the Co in EDTA solution had passed through the resin suggesting that the protons on the resin reacted with the $[Co(EDTA)]^{-}$ complex as it passed through the resin displacing Co and allowing Co to adsorb to the resin. The following 5 mol dm^{-3} HCl eluate was a pale pink colour and the solution was also eluted pink after the addition of a further 5 mol dm^{-3} HCl solution. This observation indicates that 5 mol dm^{-3} was not a high enough concentration of HCl to elute the total concentration of Co.

The difference in the two experiments was explained by the charge on the Co ion. When Co was pre-adsorbed to the resin, it was in the form of Co^{2+} and was easily removed from the resin with a low concentration EDTA solution via oxidation and the reaction shown in equation 14. However when Co adsorbed to the resin from EDTA solution it was in the form of Co^{3+}. It was more difficult to remove Co^{3+} from the resin than it would have been to remove Co^{2+} from the resin because higher charged cations are generally adsorbed more strongly. This explains why further HCl solution was not eluting all of the Co.

The following section shows results for an experiment that involved a lower initial concentration of Co and the elution of the cation exchange resin with HCl in an attempt to elute Co.

3.3.1 Reduced Co concentration

Table 18 shows ICP-AES results of separate solutions containing Co, Ag, Ho and Nb in EDTA solution after they were passed through cation exchange resin.

Table 18 Lower Co concentration and comparison with Ag, Ho and Nb solutions

Eluate	Co (mg dm^{-3})	Ag (mg dm^{-3})	Ho (mg dm^{-3})	Nb (mg dm^{-3})
EDTA / H_2O	0.00	0.00	0.00	0.84
HCl	0.00	0.00	0.00	0.00

The maximum concentration of each element in the H_2O eluate assuming there was no adsorption of the elements was 1 mg dm^{-3}. The results show that Nb passed straight through the resin and suggests that EDTA did not complex with Nb allowing Nb to remain in solution as an anionic fluoro complex. Co, Ag and Ho were not detected in the EDTA / H_2O eluate and were therefore adsorbed to the resin. The maximum concentration of each element in the HCl eluate assuming that they were fully eluted from the resin was 0.05 mg dm^{-3}. This relatively low concentration was because of the dilution of the acid solutions for ICP-AES analysis. The results show that no trace of Co, Ag and Ho were detected in the HCl eluate.

The ICP-AES results for a repeat experiment involving a solution containing a mixture of Ag, Co, Ho and Nb in EDTA solution after it was passed through cation exchange resin are shown in table 19.

Table 19 Ag, Co, Ho and Nb solution mixture in EDTA passed through cation exchange resin

Eluate	Sample	Ag (mg dm^{-3})	Co (mg dm^{-3})	Ho (mg dm^{-3})	Nb (mg dm^{-3})
H_2O	1	0.00	0.00	0.00	0.85
	2	0.00	0.00	0.00	0.78
5 mol dm^{-3} HCl	1	0.00	0.00	0.00	0.00
	2	0.00	0.00	0.00	0.00

The maximum concentration of each element assuming that they were completely eluted from the resin was 1 mg dm^{-3} for the H_2O eluate and 0.05 mg dm^{-3} for the HCl eluate. The results were similar to previous results. Nb was shown to pass through the resin with water and was therefore separated from Co in the H_2O eluate. The elution of Co at the concentration added using HCl was not possible because the use of a higher concentration of HCl to remove the Co from the resin would require dilution to an extent whereby Co would be below the lower detection limit of the ICP-AES instrument.

The following section shows results for experiments involving an increased EDTA concentration and pH to elute low concentrations of Co pre-loaded onto a cation exchange resin.

3.3.2 Elution with higher concentration EDTA solution at pH 8

The ICP-AES results of the eluates for two separate experiments after being passed through cation resin pre-loaded with Ag, Co and Ho are shown in table 20.

Table 20 Elution of cation exchange resin with 0.1 mol dm^{-3} disodium EDTA at pH 8

Experiment	Ag (mg dm^{-3})	Co (mg dm^{-3})	Ho (mg dm^{-3})
1	1.14	1.56	1.49
2	1.42	1.37	1.14

The maximum concentration of Ag, Co and Ho assuming that these elements were completely eluted from the resin was 2 mg dm^{-3}. The results for the EDTA elution show partial elution of each element. It was believed that the high pH provided more available sites on the EDTA molecules for reaction with the elements of interest and therefore proved non-selective for Co at this high pH.

The similar behaviour of Ho and Co towards EDTA was explained by the fact that they both complex as trivalent ions and the same behaviour as with previous complexation experiments was observed. Ho is a lanthanide element and complexes with EDTA to form hydrated complexes such as $Ln(EDTA)(H_2O)_\chi$[136] which explains the same observed behaviour of Ho and Co.

The following experiments do not involve eluants that form octahedral complexes with transition metals to avoid the problem of Co and Ho behaving similarly by the oxidation of Co^{2+} to Co^{3+}.

3.4 Attempted sequential elution of cation resin with NH_4OH

Table 21 shows ICP-AES results of an ammonia solution eluate after it was passed through a cation exchange resin pre-loaded with Ag, Co and Ho.

Table 21 Ammonium hydroxide elution

NH_4OH solution (mol dm^{-3})	Ag (mg dm^{-3})	Co (mg dm^{-3})	Ho (mg dm^{-3})
0.1	0.00	0.00	0.00
0.5	0.00	0.00	0.00
1	0.00	0.00	0.00
2	0.00	0.00	0.00
3	0.03	0.00	0.00
4	0.00	0.00	0.00
5	0.00	0.00	0.00

The maximum concentration of Ag, Co and Ho in solution after dilution of the eluates assuming that these elements were eluted was 2 mg dm^{-3}. The results show that up to 5 mol dm^{-3} ammonia solution was not successful at eluting Ag, Co or Ho from the cation exchange resin. Therefore the results suggest that ammine complexes were not formed with the adsorbed cations and a contribution to this affect could be that the OH^- ion possessed a low selectivity coefficient (shown in figure 9, section 2.4.2.1, chapter 2) and the cations remained strongly adsorbed to the resin.

The following section shows the results of an eluant containing an anion displaying higher selectivity properties in the elutropic series (shown in figure 9, section 2.4.2.1, chapter 2).

3.5 Attempted sequential elution of cation resin with HNO_3

The average percentage recoveries of Ag, Co, Ho and Nb calculated from ICP-AES results for three experiments performed using HNO_3 eluant concentrations of 0.1, 0.2, 0.5 and 1 mol dm^{-3} are shown in figure 17.

Figure 17 HNO_3 elution of cation exchange resin

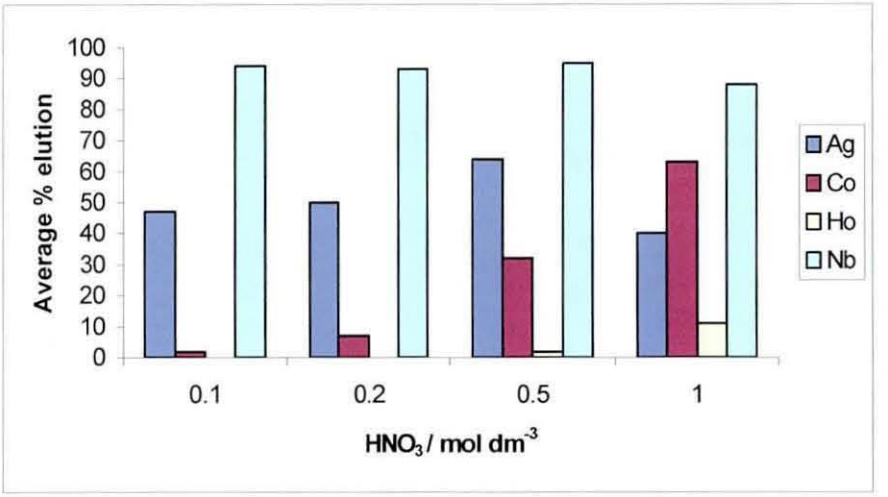

The results show that Nb was not adsorbed to the resin because of the formation of a niobium fluoro complex as expected. Ag was partially eluted at low concentrations of HNO_3. This was explained by the knowledge that Ag possesses the lowest charge of the four elements of interest and was eluted as $AgNO_3$. However no more than 65% of Ag initially added was recovered at these low concentrations of HNO_3 and only a partial separation of Ag from Co was achieved. Cobalt was gradually eluted as $Co(NO_3)_2$ over the range of HNO_3 concentrations because it was more strongly bound as the Co^{2+} cation. Co was expected to be eluted with a 1 mol dm^{-3} HNO_3 because it had been reported to have been eluted from a Amberlite XAD-16 cation exchange resin with 1 mol dm^{-3} HNO_3 in acetone eluant[137]. The most strongly bound cation of the analytes was Ho^{3+} and therefore only began to be eluted between 0.5 and 1 mol dm^{-3} HNO_3. To summarise these experiments, the only separation observed was > 90% Nb and between 40 and 50% Ag from Co using 0.1 mol dm^{-3} HNO_3 because the elution bands of the analytes overlapped. Further experiments determined that Co and Ho were fully eluted at concentrations of HNO_3 higher than 5 mol dm^{-3}.

The investigated methods of separating Co from Ag, Ho and Nb in one separation step were unsuccessful and only Nb was successfully separated from Co using cation exchange resin. The following results show Ag separation from Co by precipitation methods.

3.6 Ag precipitation using NaCl

The ICP-AES results of filtrates for two experiments involving the addition of 0.1 mol dm^{-3} NaCl and precipitation of AgCl are shown in table 22.

Table 22 Ag precipitation with 0.1 mol dm^{-3} NaCl solution

Experiment	Ag (mg dm^{-3})	Co (mg dm^{-3})	Ho (mg dm^{-3})
1	0.37	2.02	1.95
2	0.44	2.03	1.98

The maximum concentration of each element in the filtrates assuming that each element remained soluble was 2 mg dm^{-3}. The results show that 100% Co, 100% Ho and 20% Ag were detected in solution after filtration. Therefore 80% of the initial concentration of Ag precipitated.

The ICP-AES results of a repeat experiment using a higher concentration NaCl solution of 0.2 mol dm^{-3} are shown in table 23.

Table 23 Ag precipitation with 0.2 mol dm^{-3} NaCl solution

	Ag	Co	Ho	Nb
Conc. (mg dm^{-3})	0.20	1.00	0.91	0.90

The maximum concentration of each element in the filtrate assuming that each element remained soluble was 1 mg dm^{-3}. The analyte, Nb was included in this experiment and was also shown to remain in solution with Co and Ho. Similar results to the previous experiment were observed.

The following results determine the nature of the Ag species that was observed not to precipitate with NaCl.

3.6.1 Precipitation using NaCl followed by cation exchange

The ICP-AES results of filtrates for two experiments after the addition of NaCl and the precipitation of AgCl followed by passage through a cation exchange resin are shown in table 24.

Table 24 Ag precipitation followed by cation exchange

Experiment	Ag (mg dm^{-3})	Co (mg dm^{-3})	Ho (mg dm^{-3})	Nb (mg dm^{-3})
1	0.16	0.11	0.08	1.82
2	0.34	0.31	0.30	1.83

The maximum concentration of each element in the filtrates assuming that each element remained soluble and were not retained by the resin was 1 mg dm^{-3}. The results show that the remaining Ag in solution after precipitation of AgCl was present as an anionic species believed to be a soluble chloro complex. Anionic species of Ho and Co were also shown to have formed. The following results confirm that the remaining Ag species was anionic.

3.6.2 Ag precipitation using NaCl followed by anion exchange

The ICP-AES results of filtrates for two experiments after the addition of NaCl and the precipitation of AgCl followed by passage through an anion exchange resin are shown in table 25.

Table 25 Ag precipitation followed by anion exchange

Experiment	Ag (mg dm^{-3})	Co (mg dm^{-3})	Ho (mg dm^{-3})	Nb (mg dm^{-3})
1	0.01	0.91	0.71	0.40
2	0.06	0.89	0.66	0.28

The maximum concentration of each element in the filtrates assuming that each element remained soluble and were not retained by the resin was 1 mg dm^{-3}. The results show that the Ag remaining in solution which did not precipitate as AgCl was removed from solution by the resin confirming that the soluble Ag was present as an anionic species.

The precipitation results have shown that 80% of the initial concentration of Ag was precipitated as AgCl. The remaining 20% was soluble and this result can be related to the AgCl solubility product shown in figure 10, section 2.5.1.4, chapter 2 and equation 1, section 2.2.7, chapter 2.

The results of experiments using a reagent that was known to form a Ag complex with a much lower solubility product are shown in the following section.

3.6.3 Precipitation using KI

The ICP-AES results of filtrates for two experiments after the addition of KI and the precipitation of AgI are shown in table 26.

Table 26 Ag precipitation with 0.1 mol dm^{-3} KI solution

Experiment	Ag (mg dm^{-3})	Co (mg dm^{-3})	Ho (mg dm^{-3})	Nb (mg dm^{-3})
1	1.00	2.41	0.67	2.13
2	1.19	2.31	0.67	2.10

The maximum concentration of each element in the filtrate assuming that each element remained soluble was 2 mg dm^{-3}. The precipitation of Ag using KI was shown to be less successful than the precipitation with NaCl despite the solubility product of AgI being much lower than AgCl.

3.7 Attempted AgI co-precipitation with $Zr(HPO_4)_2$

The ICP-AES results of an experiment involving the attempted co-precipitation of AgI from a solution containing Ag and Co are shown in table 27.

Table 27 AgI co-precipitation with $Zr(HPO_4)_2$

	Ag	Co
Conc. (mg dm^{-3})	0.85	0.91

The maximum concentration of Ag and Co in solution assuming that Ag and Co remain in solution was 1 mg dm^{-3}. The results show that 85% of the initial concentration of Ag added remained in solution and AgI was therefore not successfully precipitated. The concentration of KI provided excess I^- ions for the formation of AgI which indicates that there was either not a high enough concentration of Zr or not a high enough concentration of phosphoric acid to form the $Zr(HPO_4)_2$ complex required for co-precipitation of AgI.

The ICP-AES results below show three repeat experiments using excess zirconium.

Table 28 AgI co-precipitation using excess zirconium

Experiment	Ag (mg dm^{-3})	Co (mg dm^{-3})
1	1.82	1.77
2	1.74	1.97
3	1.96	1.95

The maximum concentration of Ag and Co in solution assuming that Ag and Co remain in solution was 2 mg dm^{-3}. Crystals were observed after leaving the solution to stand overnight which indicates that $Zr(HPO_4)_2$ precipitated, however the method was unsuccessful at co-precipitating AgI.

The following section shows results of eluting cation exchange resin with $NaNO_2$ to separate Ag from Co.

3.8 Ag separation with $NaNO_2$ eluant on cation resin

Table 29 shows the percentage recovery of Ag and Co in the $NaNO_2$ eluate calculated from ICP-AES results.

Table 29 Ag elution with 2% $NaNO_2$

Eluate	% Ag eluted	% Co eluted
Initial 100 cm^3 solution	0	0
2 % $NaNO_2$ (1st 10 cm^3)	0	0
2 % $NaNO_2$ (2nd 10 cm^3)	0	6
2 % $NaNO_2$ (3rd 10 cm^3)	0	0
2 % $NaNO_2$ (4th 10 cm^3)	0	0
2 % $NaNO_2$ (5th 10 cm^3)	7	0
2 % $NaNO_2$ (6th 10 cm^3)	10	0
2 % $NaNO_2$ (7th 10 cm^3)	11	0
2 % $NaNO_2$ (8th 10 cm^3)	10	0
2 % $NaNO_2$ (9th 10 cm^3)	10	0
2 % $NaNO_2$ (10th 10 cm^3)	9	0
2 % $NaNO_2$ (11th 10 cm^3)	6	0
2 % $NaNO_2$ (12th 10 cm^3)	4	1
2 % $NaNO_2$ (13th 10 cm^3)	4	1
2 % $NaNO_2$ (14th 10 cm^3)	3	1
2 % $NaNO_2$ (15th 10 cm^3)	2	1
2 % $NaNO_2$ (16th 10 cm^3)	2	1
2 % $NaNO_2$ (17th 10 cm^3)	2	1
2 % $NaNO_2$ (18th 10 cm^3)	1	1
2 % $NaNO_2$ (19th 10 cm^3)	1	1
2 % $NaNO_2$ (20th 10 cm^3)	1	1
Total % eluted	83	15

The results show a separation of > 80% Ag from > 80% Co. A small percentage of Co was eluted over 200 cm^3 of 2% $NaNO_2$, 6% of which was detected in the second 10 cm^3 fraction. The Co complex believed to be formed was $Co(NO_2)_2$. However the NO_2^- ions were shown to prefer to react with Ag forming the $[Ag(NO_2)_2]^-$ complex.

Table 30 shows results of further elution of the same resin with a higher concentration $NaNO_2$ solution.

Table 30 Co elution with 5% $NaNO_2$

5% $NaNO_2$ eluate	% Ag eluted	% Co eluted
1st 50 cm^3	7	15
2nd 50 cm^3	1	10
3rd 50 cm^3	0	7
4th 50 cm^3	0	5

The results show that when the concentration of $NaNO_2$ was increased to a 5% w/v solution, Co was eluted from the resin. However only a further 37% of the initial added Co concentration was eluted. These results suggest that because more NO_2^- ions were provided by the increased concentration of $NaNO_2$ solution, these reacted with Co^{2+} forming cobalt nitrite.

The following section shows the results of an experiment adapted to prevent the small amount of Co observed in the last experiment from being channelled through the resin by the nitrogen dioxide gas bubbles.

3.8.1 Increased contact time of $NaNO_2$ on resin

Table 31 shows the percentage recovery of Ag and Co in the $NaNO_2$ eluate calculated from ICP-AES results for an experiment with an increased initial contact time of $NaNO_2$ with the resin.

Table 31 Increased initial contact time of $NaNO_2$ with cation exchange resin

Eluate	% Ag eluted	% Co eluted
Initial 100 cm^3 solution	0	0
2 % $NaNO_2$ (1st 20 cm^3)	0	0
2 % $NaNO_2$ (2nd 20 cm^3)	0	0
2 % $NaNO_2$ (3rd 20 cm^3)	22	0
2 % $NaNO_2$ (4th 20 cm^3)	31	0
2 % $NaNO_2$ (5th 20 cm^3)	9	1
2 % $NaNO_2$ (6th 20 cm^3)	0	1
2 % $NaNO_2$ (7th 20 cm^3)	0	1
2 % $NaNO_2$ (8th 20 cm^3)	0	1
2 % $NaNO_2$ (9th 20 cm^3)	0	1
2 % $NaNO_2$ (10th 20 cm^3)	0	1
2 % $NaNO_2$ (11th 20 cm^3)	0	1
2 % $NaNO_2$ (12th 20 cm^3)	0	1
2 % $NaNO_2$ (13th 20 cm^3)	0	1
2 % $NaNO_2$ (14th 20 cm^3)	0	1
2 % $NaNO_2$ (15th 20 cm^3)	1	1
Total % eluted	63	11

The results show that by leaving the first 10 cm^3 of 2% $NaNO_2$ solution in contact with the resin for 30 minutes, the elution of a small amount of Co within the first 20 cm^3 was prevented. A total of > 60% Ag was eluted after 200 cm^3 of 2% $NaNO_2$. The results also show that no more Ag was eluted with a further 100 cm^3 of 2% $NaNO_2$ solution.

Table 32 shows results of further elution of the same resin with 5% and 8% $NaNO_2$ solutions.

Table 32 Attempted Co recovery using 5% and 8% $NaNO_2$ solutions

Eluate	% Ag eluted	% Co eluted
5 % $NaNO_2$ (1st 100 cm^3)	0	23
5 % $NaNO_2$ (2nd 100 cm^3)	0	8
5 % $NaNO_2$ (3rd 100 cm^3)	0	5
5 % $NaNO_2$ (4th 100 cm^3)	0	4
8 % $NaNO_2$ (1st 100 cm^3)	0	2
8 % $NaNO_2$ (2nd 100 cm^3)	0	0

The results show that no more Ag was eluted when the strength of $NaNO_2$ was increased. A further 40% Co was eluted after 400 cm^3 of 5% $NaNO_2$ solution, most of which was detected in the first 200 cm^3. Therefore the quantitative separation of Ag from > 90% Co was achieved within 200 cm^3 of 2% $NaNO_2$ solution. Only a further 2% Co was eluted with an increased strength of 8% $NaNO_2$ solution. Therefore > 50% of the initial concentration of Co remained adsorbed to the resin.

Figure 18 summarises the percentage recovery of Ag and Co calculated from ICP-AES results of four repeat experiments using 200 cm^3 of 2% $NaNO_2$ solutions.

Figure 18 Ag separation from Co using 2% $NaNO_2$

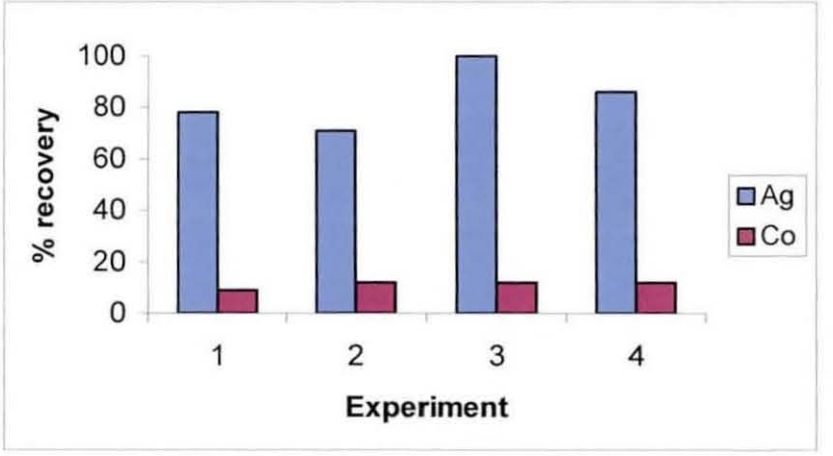

Figure 18 shows consistent elution of > 70% Ag and an average of 12% Co using an $NaNO_2$ eluant. This ion exchange method provides a good separation of Ag from Co. It was reported that 80% Ag was separated from Co after the elution of a cation exchange resin with 200 cm^3 of 2% $NaNO_2$ solution[90,91,138]. It was also reported that the same concentration of $NaNO_2$ solution resulted in the separation of 75% Pd^{2+} from Au^{3+}[138]. Therefore the results of this experiment were very similar to reported separations using the $NaNO_2$ eluant.

3.9 Separation of Ho from Co

Following the development of a suitable method for the separation of Ag from Co the next section shows results of the investigation into the separation of Ho from Co using various eluants and resins.

3.9.1 Ammonium citrate eluant

Table 33 shows the ICP-AES results for the ammonium citrate eluates of two experiments involving cation exchange resins loaded with Ag, Co and Ho.

Table 33 Ammonium citrate elution

Sample	Ag (mg dm^{-3})	Co (mg dm^{-3})	Ho (mg dm^{-3})
1	0.09	0.44	0.43
2	0.07	0.23	0.29

The maximum concentration of Ag, Co and Ho in the eluates assuming these elements were completely eluted was 2 mg dm^{-3}. The results show that between 10 and 20% of the initial concentration of Ho loaded onto the resin was eluted. It was believed that the pH of the citrate solution may have been reduced by the use of the H-form cation resin.

The ICP-AES results of two repeat experiments using the Na-form cation resin to avoid reducing the pH of solution are shown in table 34.

Table 34 Ammonium citrate elution using Na form resin

Sample	Ag (mg dm^{-3})	Co (mg dm^{-3})	Ho (mg dm^{-3})
1	0.17	1.67	1.18
2	0.28	1.76	1.51

The maximum concentration of Ag, Co and Ho in the eluates assuming these elements were completely eluted was 2 mg dm^{-3}. The results show that between 60 and 75% of the initial concentration of Ho loaded onto the resin was eluted as a holmium citrate complex. However 85% of the initial concentration of Co loaded onto the resin was also eluted. These results suggest that Co^{2+} was oxidised to Co^{3+} forming a cobalt citrate complex possibly $[Co(C_6H_5O_7)_2]^{3-}$. Therefore ammonium citrate was not a selective eluant for the separation of Ho from Co on a cation exchange resin.

The following sections show results of two eluants investigated to achieve separation of Co from Ho on a cation exchange resin.

3.9.2 Ammonium oxalate eluant

Table 35 shows ICP-AES results of the ammonium oxalate eluates of two experiments involving cation exchange resins loaded with Ag, Co and Ho.

Table 35 Ammonium oxalate elution

Sample	Ag (mg dm^{-3})	Co (mg dm^{-3})	Ho (mg dm^{-3})
1	0.10	1.55	0.80
2	0.26	1.76	1.17

The maximum concentration of Ag, Co and Ho in the eluates assuming these elements were completely eluted was 2 mg dm^{-3}. The results show that > 75% of the initial concentration of Co loaded onto the resin was eluted as a cobalt oxalate complex as expected. However between 40 and 60% of the initial concentration of Ho loaded

onto the resin was also eluted. This result suggests that a holmium oxalate complex was eluted and that Co was again oxidised to Co^{3+} possibly forming $[Co(C_2O_4)_3]^{3-}$. It was therefore shown that ammonium oxalate was not selective towards Co in the presence of Ho.

3.9.3 Nitroso-R salt eluant

Table 36 shows ICP-AES results of the nitroso-R salt eluates of two experiments involving cation exchange resins loaded with Co and Ho.

Table 36 Nitroso-R salt elution

Nitroso-R eluate	Co (mg dm^{-3})	Ho (mg dm^{-3})
1	0.86	0.31
2	0.07	0.01

The maximum concentration of Co and Ho in the eluates assuming these elements were completely eluted was 2 mg dm^{-3}. The results show that 48% Co and 16% Ho were eluted in the first 50 cm^3 of the nitroso-R salt eluate. However the remaining Co and Ag initially loaded onto the resin were not eluted with further nitroso-R salt solution. Despite the complexing salts ability to form complexes with Co, it was found not to be 100% selective towards Co in the presence of Ho.

The following results show the separation of Ho from Co using a lanthanide resin.

3.9.4 Extraction of Ho with lanthanide resin

Table 37 shows the ICP-AES results of various concentrations of HNO_3 eluate on a lanthanide resin for solutions containing Co and Ho.

Table 37 Separation of Ho from Co using lanthanide resin

Eluate	Co (mg dm^{-3})	Ho (mg dm^{-3})
0.15 mol dm^{-3} HNO_3	1.86	0.00
0.25 mol dm^{-3} HNO_3 1	0.00	0.00
0.25 mol dm^{-3} HNO_3 2	0.00	0.00
1 mol dm^{-3} HNO_3	0.00	0.92

The maximum concentration of Co and Ho in the eluates assuming these elements were completely eluted was 2 mg dm^{-3}. The results show that all of the initial concentration of Co loaded onto the resin was eluted with 0.15 mol dm^{-3} HNO_3 whilst Ho was retained by the resin. Ho was not eluted with a higher concentration of 0.25 mol dm^{-3} HNO_3 solution. However 46% of the initial concentration of Ho loaded onto the resin was eluted when the concentration of HNO_3 was increased to 1 mol dm^{-3}. Therefore 0.15 mol dm^{-3} HNO_3 was successful at separating Ho from Co on lanthanide resin.

Table 38 shows ICP-AES results for a repeat experiment without the inclusion of the 1 mol dm^{-3} HNO_3 eluate.

Table 38 Repeated separation of Ho from solution using lanthanide resin

Eluate	Co (mg dm^{-3})	Ho (mg dm^{-3})
0.15 mol dm^{-3} HNO_3	1.92	0.00
0.25 mol dm^{-3} HNO_3 1	0.00	0.00
0.25 mol dm^{-3} HNO_3 2	0.00	0.00

The maximum concentration of Co and Ho in the eluates assuming these elements were completely eluted was 2 mg dm^{-3}. Similar results were observed.

The following results show Ho separation from Co using lanthanide resin with the inclusion of Nb and Ag analytes.

3.9.4.1 Extraction of Ho and Nb from solution using lanthanide resin

Table 39 shows ICP-AES results of eluates for three experiments after solutions containing Co, Ho and Nb were passed through lanthanide resin.

Table 39 Separation of Ho and Nb from solution using lanthanide resin

Sample	Co (mg dm^{-3})	Ho (mg dm^{-3})	Nb (mg dm^{-3})
1	1.89	0.00	0.00
2	2.07	0.00	0.01
3	1.86	0.01	0.01

The maximum concentration of Co, Ho and Nb in the eluates assuming these elements completely passed through the resin was 2 mg dm^{-3}. Similar results were observed. Nb was also shown to be retained by the lanthanide resin. This result was unexpected because Nb was believed to be present as $[NbOF_5]^{2-}$ from previous results. The result was explained by the dilution of trace HF in the stock solution causing a positively charged Nb species to dominate in solution resulting in Nb retention on the resin.

Table 40 shows the ICP-AES results of eluates for three experiments after solutions containing Ag, Co, Ho and Nb were passed through lanthanide resin.

Table 40 Separation of Ho and Nb from Co and Ag using lanthanide resin

Sample	Ag (mg dm^{-3})	Co (mg dm^{-3})	Ho (mg dm^{-3})	Nb (mg dm^{-3})
1	0.81	0.78	0.00	0.01
2	0.83	0.86	0.00	0.00
3	1.00	0.95	0.00	0.00

The maximum concentration of each element in the eluates assuming these elements completely passed through the resin was 1 mg dm^{-3}. The results show that when all the analytes were passed through the resin in solution, Ag and Co were both eluted as expected whilst Ho and Nb were both retained by the resin. The lanthanide resin experiments therefore show that solutions containing Ag, Co, Ho and Nb with an acid concentration below 1 mol dm^{-3} resulted in the separation of Ho and Nb from Ag and Co.

3.9.4.2 Application of separation using Ln resin to dissolution samples

Figure 19 summarises the percentage recoveries of Ag, Co, Ho and Nb in solution calculated from ICP-AES results after four dissolution samples were passed through separate lanthanide resin columns.

Figure 19 Application of lanthanide resin to dissolution samples

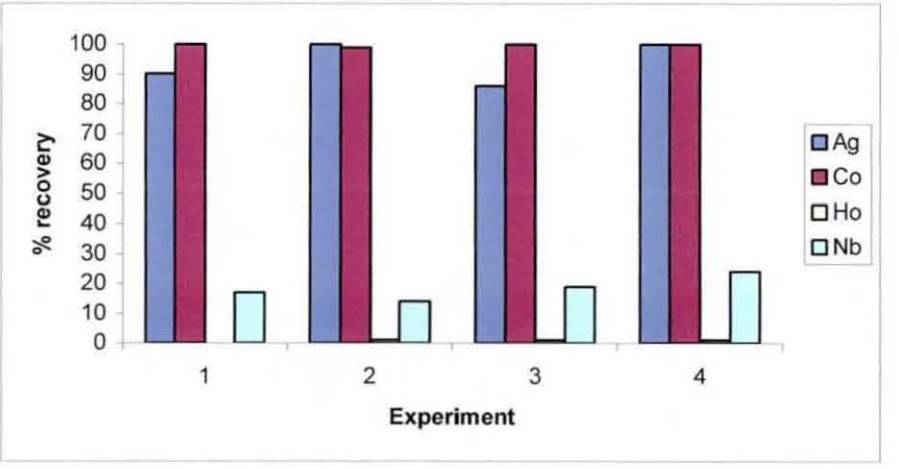

The maximum concentration of each element after dilution assuming these elements completely passed through the resin was 1 mg dm^{-3}. Therefore 100% recovery was equivalent to 1 mg dm^{-3}. The results show that > 80% Ag passed through the resin in each experiment simultaneously with 100% Co as expected. 100% Ho and > 80% Nb were retained by the resin. Therefore the method was successful at separating Ho and Nb from Ag and Co in inactive dissolved tacky swab samples.

Figure 20 shows another set of dissolution samples containing the analytes at higher concentrations after the solutions were passed through lanthanide resin.

Figure 20 Application of lanthanide resin to dissolution samples containing higher concentrations of analytes

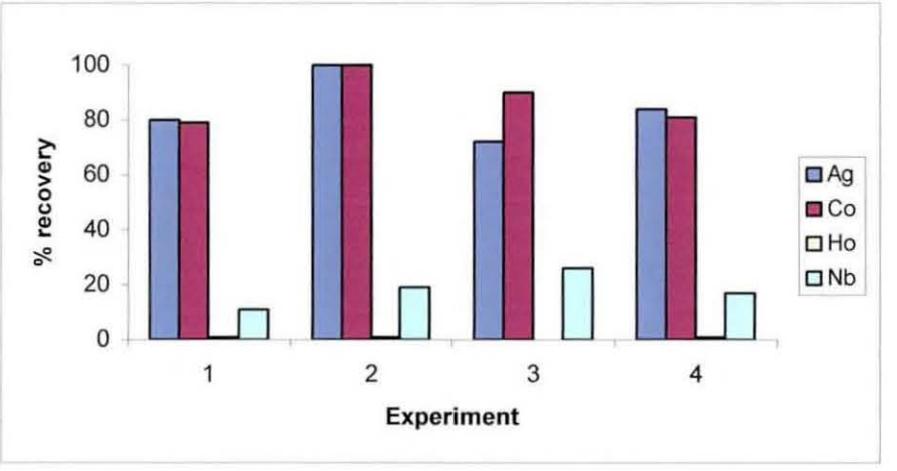

The maximum concentration of each element after dilution assuming these elements completely passed through the resin was 2 mg dm^{-3}. Therefore 100% recovery was equivalent to 2 mg dm^{-3}. Similar results were observed confirming that the method of separation was successful when applied to dissolved tacky swab samples containing Ag, Co, Ho and Nb between 1 and 2 mg dm^{-3}.

3.9.4.3 Flow rate of solution through lanthanide resin

Table 41 shows ICP-AES results of a dissolution sample containing Ag, Co, Ho and Nb after being pumped through lanthanide resin at various rates.

Table 41 Lanthanide resin flow rate

Flow rate (cm^3 min^{-1})	Ag (mg dm^{-3})	Co (mg dm^{-3})	Ho (mg dm^{-3})	Nb (mg dm^{-3})
40	1.96	1.97	0.00	0.01
70	1.98	2.00	0.00	0.01
100	2.14	1.99	0.02	0.02

The maximum concentration of each element in solution after it was pumped through the resin assuming that these elements completely passed through the resin was 2 mg dm^{-3}. The results show that the separation was not affected by the flow rate of solution. Therefore the solution could be pumped through the resin at a faster rate making the method less time consuming.

3.10 Radioactive tacky swab / filter paper ICP-AES analysis

Section 3.10.1 shows the reproducibility of the inactive tracer element behaviour at each stage of the method applied to radioactive and blank swab and filter samples by summarising the ICP-AES percentage tracer recoveries. Section 3.10.2 shows specific concentrations detected at each stage of the overall applied method for the radioactive samples.

3.10.1 Reproducibility of inactive tracer element recoveries in radioactive and blank samples

Figures 21 to 24 summarise and compare the percentage recoveries of the inactive tracer elements of the radioactive swab and filter and blank swab and filter samples at each stage of the method.

Figure 21 Reproducibility of analyte recoveries after dissolution

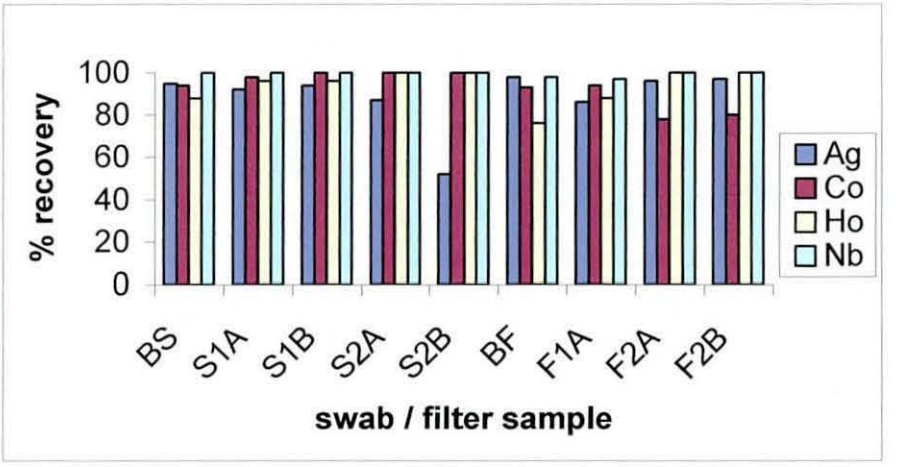

BS = Blank swab

S1A = Sample A of Swab 1

S1B = Sample B of Swab 1

S2A = Sample A of Swab 2

S2B = Sample B of Swab 2

BF = Blank filter

F1A = Sample A of Filter 1

F1B = Sample B of Filter 1

F2A = Sample A of Filter 2

F2B = Sample B of Filter 2

The recoveries were calculated as percentage yields relative to the concentration of each element that would be transferred to solution with the successful and complete transfer of each element from the solid samples to solution. The chart shows that an average of > 80% of each analyte were successfully transferred from the solid samples to solution and the dissolution stage results were reproducible for radioactive and blank samples.

Figure 22 shows a summary of the percentage recovery of Ag, Co, Ho and Nb for each sample in solution after they were passed through lanthanide resin.

Figure 22 Reproducibility of analyte recoveries after the lanthanide resin stage

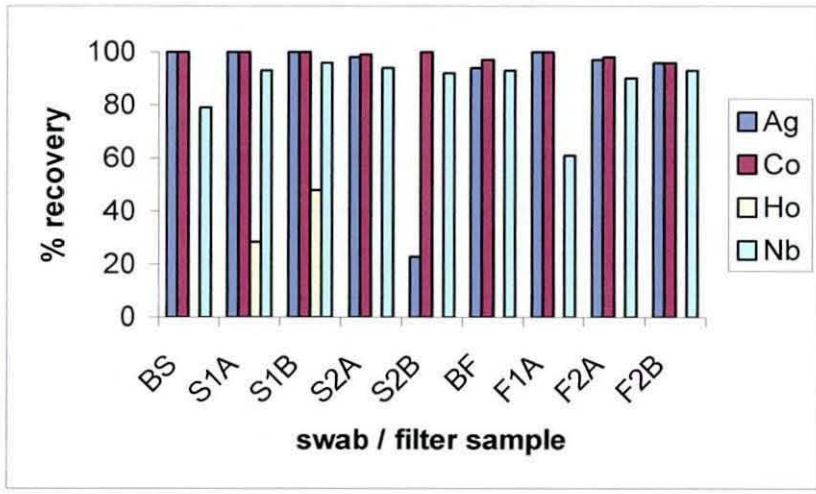

The recoveries were calculated as percentage yields relative to the initial concentration detected at the dissolution stage. The general observation was that > 80% Ag, Co, and Nb passed through the lanthanide resin whilst Ho was retained. The results were therefore reproducible at the Ho separation stage of the method for radioactive and blank samples.

Figure 23 shows a summary of the percentage recovery of Ag, Co, Ho and Nb in each sample after being passed through cation exchange resin.

Figure 23 Reproducibility of analyte recoveries after cation resin stage

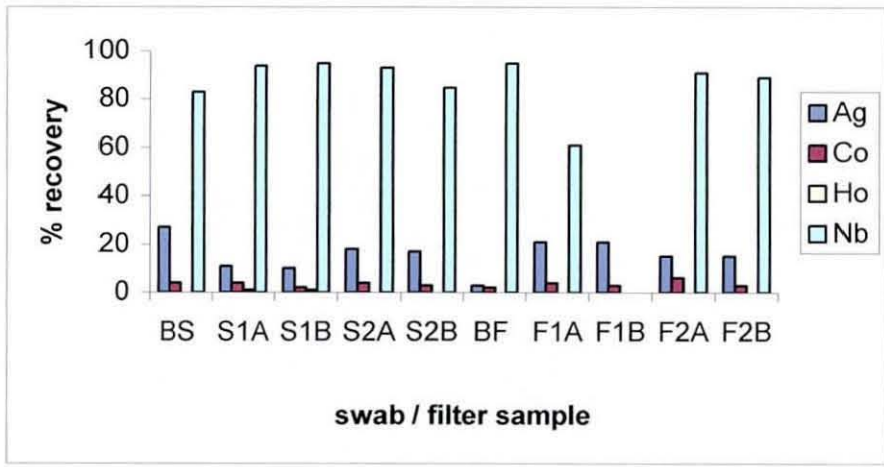

The recoveries were calculated as percentage yields relative to the initial concentrations detected. An average separation of > 80% Nb and between 10 and 20% Ag from > 95% Co was observed at this stage of the method. The percentage Nb recovery for filter sample 1B was not available because of instrument detection errors at the dissolution stage. However the results at the Nb separation stage of the method were reproducible for radioactive and blank samples.

Figure 24 shows a summary of the percentage recovery of Ag, Co, Ho and Nb in each $NaNO_2$ eluate.

Figure 24 Reproducibility of analyte recoveries in $NaNO_2$ eluates

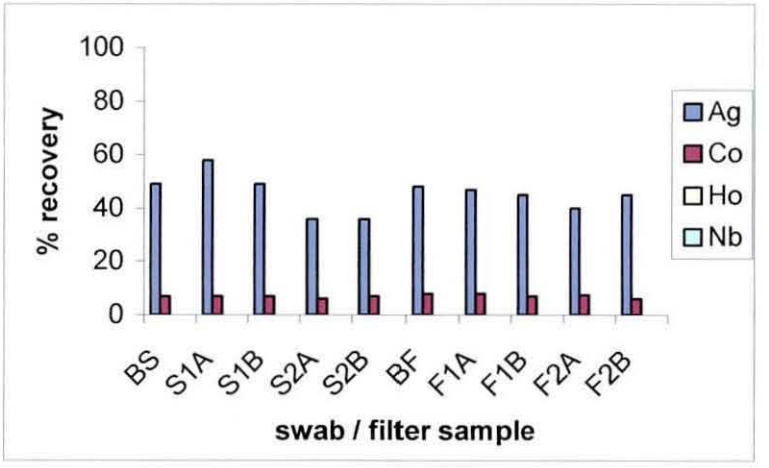

The recoveries were calculated as percentage yields relative to the initial concentrations detected. The mean average of all the radioactive samples shows that 45% Ag was separated from > 90% Co and the results were shown to be reproducible at the Ag separation stage of the method for radioactive and blank samples.

The tracer element yield summaries show consistent and reproducible results throughout the dissolution and separation stages of the method when applied to radioactive and blank samples. The behaviour of Ag, Co, Ho and Nb in both inactive samples (blank swab and blank filter samples) were shown to be similar to the behaviour in the radioactive samples. The reason why Nb behaved differently in inactive experiments performed at Loughborough University was thought to be because the amount of trace HF present in the Nb stock solution was slightly lower

than the amount present in the Nb stock solution provided by Berkeley Centre. This led to hydrated Nb oxide species[44] pre-dominating over the predicted $[NbOF_5]^{2-}$ species and explains the retention of 80% Nb to the lanthanide resin in the method development experiments. The retention was not 100% because of the Nb oxide colloidal suspension formed from hydrolytic decomposition[44]. It is known that increasing the HF concentration of a Nb solution increases the adsorption of Nb on anion exchange resins at higher than 5% concentrations[139]. This is because it is the heptafluoro anion $[NbF_7]^{2-}$[44] that dominates over the oxyfluoro anion $[NbOF_5]^{2-}$ and is more strongly adsorbed to the resin. This provides an understanding for why Nb differs in behaviour in solutions containing trace levels of HF. There was not sufficient HF in some of the samples to form oxyflouro complexes and therefore Nb did not pass through the resin.

3.10.2 Radioactive swab / filter ICP-AES analysis

The following tables show concentrations detected by ICP-AES, percentage recoveries of the concentrations and 2σ uncertainty values for Ag, Co, Ho and Nb tracer elements in the radioactive tacky swab and filter paper samples at each stage of the method. Percentage tracer recoveries were obtained by calculating the concentrations in mol dm^{-3} and comparing them to the initial concentrations detected. Uncertainty values were calculated by 2sd where sd is the standard deviation calculated by the instrument.

3.10.2.1 Swab samples

Tables 42 to 45 show the ICP-AES analysis of duplicate samples taken from swab sample 1. Concentrations were expressed in mg dm^{-3} and the maximum concentration of each element assuming that each element remains in solution at the different stages of the method (apart from in the $NaNO_2$ eluates) was 1 mg dm^{-3}.

Table 42 Swab 1 dissolution

	Sample	Ag	Co	Ho	Nb
Concentration detected	1A	0.92	0.98	0.96	1.02
($mg\ dm^{-3}$)	1B	0.94	1.00	0.96	1.03
2σ uncertainty ($mg\ dm^{-3}$)	1A	± 0.02	± 0.02	± 0.02	± 0.02
	1B	± 0.01	± 0.02	± 0.01	± 0.01

The results show that each of the analytes were successfully transferred to solution for both samples taken from swab 1.

Table 43 Swab 1 solutions after lanthanide resin

	Sample	Ag	Co	Ho	Nb
Concentration detected ($mg\ dm^{-3}$)	1A	0.92	1.00	0.27	0.95
	1B	0.95	1.02	0.46	0.99
2σ uncertainty ($mg\ dm^{-3}$)	1A	± 0.02	± 0.02	± 0.01	± 0.01
	1B	± 0.01	± 0.01	± 0.01	± 0.01
% tracer recovery	1A	100	100	28.5	93
	1B	100	100	48	96

From these results it was calculated that between 52 and 71.5% of the initial detected concentration of Ho was retained by the lanthanide resin. Some of the Ho was therefore observed to pass through the lanthanide resin. This was thought to be a result of channelling and was not consistent with other radioactive and blank sample results. This retention of less than 60% Ho was considered a freak result. Ag, Co and Nb passed through the resin as predicted.

Table 44 Swab 1 solutions after cation exchange resin

	Sample	Ag	Co	Ho	Nb
Concentration detected (mg dm^{-3})	1A	0.10	0.04	0.01	0.95
	1B	0.09	0.02	0.01	0.98
2σ uncertainty (mg dm^{-3})	1A	± 0.01	± 0.01	± 0.01	± 0.02
	1B	± 0.01	± 0.01	± 0.01	± 0.02
% tracer recovery	1A	11	4	1	94
	1B	10	2	1	95

The results show that relatively small percentages of the initial detected concentrations of Ag and Co passed through the resin. Nb was shown to pass through the cation exchange resin supporting the theory that the $[NbOF_5]^{2-}$ species was predominant in the tacky swab samples. Despite the difference in Nb behaviour to that in the method development experiments a quantitative separation of Nb from Co was observed by its isolation in solution after the samples were passed through the cation exchange resin.

Table 45 $NaNO_2$ eluates for Swab 1

	Sample	Ag	Co	Ho	Nb
Concentration detected (mg dm^{-3})	1A	5.34	0.65	0.00	0.00
	1B	4.65	0.73	0.00	0.02
2σ uncertainty (mg dm^{-3})	1A	± 0.01	± 0.01	± 0.01	± 0.01
	1B	± 0.04	± 0.01	± 0.01	± 0.01
% tracer recovery	1A	58	7	0	0
	1B	49	7	0	0

The volume of the $NaNO_2$ eluate added to the resin was smaller than the volume of the sample at previous stages of the method, therefore the concentrations detected at this stage of the method were divided by a dilution factor to calculate the percentage tracer recoveries. The results show that between 49 and 58% of the initial detected concentration of Ag was detected in swab sample 1 and was therefore separated from

> 90% of the initial detected concentration of Co. From the results of the last two stages of the method it was calculated that between 31 and 41% of the initial detected concentration of Ag and between 89 and 91% of the initial detected concentration of Co remained adsorbed to the cation exchange resin.

Tables 46 to 49 show the ICP-AES analysis for duplicate samples taken from swab sample 2. Concentrations were expressed in mg dm^{-3} and the maximum concentration of each element assuming that each element remains in solution at the different stages of the method (apart from in the $NaNO_2$ eluates) was 1 mg dm^{-3}.

Table 46 Swab 2 dissolution

	Sample	Ag	Co	Ho	Nb
Concentration detected (mg dm^{-3})	2A	0.87	1.04	1.05	1.07
	2B	0.52	1.00	1.00	1.05
2σ uncertainty (mg dm^{-3})	2A	± 0.01	± 0.02	± 0.01	± 0.02
	2B	± 0.01	± 0.01	± 0.02	± 0.01

The results show that all of the analytes were successfully transferred to solution for swab sample 2A. However only half of the expected concentration of Ag was detected for swab sample 2B. This was thought to be experimental error because both samples were taken from the same swab and the successful transfer of Ag was observed in the first sample (2A).

Table 47 Swab 2 solutions after lanthanide resin

	Sample	Ag	Co	Ho	Nb
Concentration detected (mg dm^{-3})	2A	0.85	1.02	0.00	1.01
	2B	0.12	1.00	0.00	0.96
2σ uncertainty (mg dm^{-3})	2A	± 0.01	± 0.01	± 0.01	± 0.01
	2B	± 0.01	± 0.01	± 0.01	± 0.01
% tracer recovery	2A	98	99	0	94
	2B	23	100	0	92

The results show that Ag, Co and Nb passed through the lanthanide resin and Ho was retained which was similar to the analyte behaviour observed for swab 1. However only a small percentage of the initial detected concentration of Ag was measured in sample 2B. The low Ag detection suggests that Ag was retained by the lanthanide resin which is the opposite result to other radioactive and blank samples. A loss of solution was ruled out as a possibility for the low Ag detection because > 90% Co and Nb were shown to pass through the resin.

Table 48 Swab 2 solutions after cation exchange resin

	Sample	Ag	Co	Ho	Nb
Concentration detected (mg dm^{-3})	2A	0.16	0.04	0.00	0.99
	2B	0.09	0.03	0.00	0.89
2σ uncertainty (mg dm^{-3})	2A	± 0.01	± 0.01	± 0.01	± 0.05
	2B	± 0.01	± 0.01	± 0.01	± 0.02
% tracer recovery	2A	18	4	0	93
	2B	17	3	0	85

The results show that between 17 and 18% of the initial detected concentration of Ag passed through the resin. The results also show that Nb passed through the resin and was therefore separated from > 95% of the initial detected concentration of Co.

Table 49 $NaNO_2$ eluates for Swab 2

	Sample	Ag	Co	Ho	Nb
Concentration detected (mg dm^{-3})	2A	3.15	0.66	0.02	0.01
	2B	1.86	0.73	0.00	0.02
2σ uncertainty (mg dm^{-3})	2A	± 0.06	± 0.02	± 0.01	± 0.01
	2B	± 0.02	± 0.03	± 0.01	± 0.01
% tracer recovery	2A	36	6	0	0
	2B	36	7	0	0

The volume of the $NaNO_2$ eluate added to the resin was smaller than the volume of the sample at previous stages of the method, therefore the concentrations detected at this stage of the method were divided by a dilution factor to calculate the percentage tracer recoveries. The results show that 36% of the initial detected concentration of Ag was detected in swab sample 2 and was therefore separated from > 90% of the initial detected concentration of Co. Therefore 46% of the initial detected concentration of Ag and 90% of the initial detected concentration of Co were calculated to remain adsorbed to the cation exchange resin. The yield of Ag in the $NaNO_2$ eluates were shown to be the same in both of these samples indicating that the Ag that was detected in the dissolution sample had passed through the lanthanide resin but was not detected. The same observations were made at each stage of the method when ^{108m}Ag was detected in the same sample by gamma spectrometry eliminating an instrument detection error. A possible explanation points towards the instability of Ag when samples are left in light for long periods of time.

3.10.2.2 Filter samples

Tables 50 to 53 show the ICP-AES analysis of duplicate samples taken from filter sample 1. Concentrations were expressed in mg dm^{-3} and the maximum concentration of each element assuming that each element remains in solution at the different stages of the method (apart from in the $NaNO_2$ eluates) was 1 mg dm^{-3}. The solutions after dissolution were measured before dilution to 2000 cm^3 and therefore the maximum concentration of each element assuming that each element remains in solution at this stage of the method was 4 mg dm^{-3}.

Table 50 Filter 1 dissolution

	Sample	Ag	Co	Ho	Nb
Concentration detected (mg dm^{-3})	1A	3.45	3.76	3.53	3.87
	1B	2.69	2.78	2.64	2.88
2σ uncertainty (mg dm^{-3})	1A	± 0.04	± 0.02	± 0.07	± 0.06
	1B	± 0.04	± 0.03	± 0.04	± 0.03

The results show that each of the analytes were successfully transferred to solution for the first sample taken from filter 1. However the concentrations of each element at this stage of the method for the second sample taken from filter 1 were lower than expected because of an instrument detection error. This was concluded because of the successful transfer of each analyte in sample 1A and because the detection of > 98% of the initial detected concentrations of Ag and Co were observed after the solution of sample 1B was passed through the lanthanide resin. Therefore the percentage tracer recoveries for the following stages of the method for sample 1B were calculated relative to the concentrations detected in solution after it had passed through the lanthanide resin to avoid a follow through of the errors observed after dissolution.

Table 51 Filter 1 solutions after lanthanide resin

	Sample	Ag	Co	Ho	Nb
Concentration detected (mg dm^{-3})	1A	0.94	1.00	0.00	0.59
	1B	0.98	1.03	0.00	0.68
2σ uncertainty (mg dm^{-3})	1A	± 0.01	± 0.01	± 0.01	± 0.01
	1B	± 0.01	± 0.01	± 0.01	± 0.01
% tracer recovery	1A	100	100	0	61
	1B	----	----	----	----

The results show that Ag and Co passed through the lanthanide resin and Ho was retained, similar to the behaviour of the analytes in the swab samples. However only 61% Nb passed through the resin in sample 1A whereas swab sample results showed that Nb completely passed through the resin. This suggests that a small amount of Nb was not present as an anionic species and was retained by the resin. Therefore there was not sufficient HF present in this filter sample to produce 100% of the Nb anionic fluro complex discussed previously. The Nb detection for filter sample 1B was similar to that in filter sample 1A indicating that Nb mostly passed through the resin as the anionic fluoro complex. The percentage tracer recoveries were not calculated for filter sample 1B because of the detection errors observed at the dissolution stage for this sample, however the results suggest that Ag, Co and the same percentage of Nb as in filter sample 1A passed through the resin. From these results it was shown that Ho

was not detected suggesting that it was fully retained by the resin, similar to the Ho behaviour in filter sample 1A and previous swab samples.

Table 52 Filter 1 solutions after cation exchange resin

	Sample	Ag	Co	Ho	Nb
Concentration detected (mg dm^{-3})	1A	0.18	0.04	0.00	0.59
	1B	0.20	0.04	0.00	0.65
2σ uncertainty (mg dm^{-3})	1A	± 0.01	± 0.01	± 0.01	± 0.01
	1B	± 0.01	± 0.01	± 0.01	± 0.02
% tracer recovery	1A	21	4	0	61
	1B	21	3	0	----

Similar results to each of the previously analysed swab samples were observed at this stage of the method for filter sample 1. The Nb that was detected in the solution after it had passed through the lanthanide resin was detected in solution after the cation exchange resin for both samples. The percentage tracer recovery for Nb, however was not calculated because the initial concentration of Nb transferred to solution at the dissolution stage was not known due to an instrument detection error.

Table 53 $NaNO_2$ eluates for Filter 1

	Sample	Ag	Co	Ho	Nb
Concentration detected (mg dm^{-3})	1A	4.07	0.71	0.00	0.01
	1B	4.40	0.73	0.00	0.01
2σ uncertainty (mg dm^{-3})	1A	± 0.03	± 0.01	± 0.01	± 0.01
	1B	± 0.04	± 0.01	± 0.01	± 0.01
% tracer recovery	1A	47	8	0	0
	1B	45	7	0	0

The volume of the $NaNO_2$ eluate added to the resin was smaller than the volume of the sample at previous stages of the method, therefore the concentrations detected at this stage of the method were divided by a dilution factor to calculate the percentage tracer recoveries. The results show that between 45 and 47% of the initial detected

concentration of Ag was detected in filter sample 1 and was therefore separated from > 90% of the initial detected concentration of Co. From the results of the previous two stages of the method it was calculated that between 32 and 34% of the initial detected concentration of Ag and between 88 and 90% of the initial detected concentration of Co remained adsorbed to the cation exchange resin.

Tables 54 to 57 show the ICP-AES analysis for duplicate samples taken from filter sample 2. Concentrations were expressed in mg dm^{-3} and the maximum concentration of each element assuming that each element remains in solution at the different stages of the method (apart from in the $NaNO_2$ eluates) was 1 mg dm^{-3}.

Table 54 Filter 2 dissolution

	Sample	Ag	Co	Ho	Nb
Concentration detected (mg dm^{-3})	2A	0.96	0.78	1.03	1.00
	2B	0.97	0.80	1.03	1.04
2σ uncertainty (mg dm^{-3})	2A	± 0.01	± 0.01	± 0.01	± 0.01
	2B	± 0.02	± 0.01	± 0.01	± 0.02

These results show that each of the analytes were successfully transferred to solution for both samples taken from filter sample 2.

Table 55 Filter 2 solutions after lanthanide resin

	Sample	Ag	Co	Ho	Nb
Concentration detected (mg dm^{-3})	2A	0.94	0.77	0.00	0.93
	2B	0.93	0.77	0.00	0.93
2σ uncertainty (mg dm^{-3})	2A	± 0.02	± 0.01	± 0.01	± 0.02
	2B	± 0.02	± 0.02	± 0.01	± 0.01
% tracer recovery	2A	97	98	0	93
	2B	96	97	0	90

These results show that Ag, Co and Nb passed through the lanthanide resin and Ho was retained. These results follow the same pattern observed for the first filter sample and the previous swab samples.

Table 56 Filter 2 solutions after cation exchange resin

	Sample	Ag	Co	Ho	Nb
Concentration detected (mg dm^{-3})	2A	0.15	0.05	0.00	0.91
	2B	0.14	0.03	0.00	0.92
2σ uncertainty (mg dm^{-3})	2A	± 0.02	± 0.01	± 0.01	± 0.01
	2B	± 0.01	± 0.01	± 0.01	± 0.01
% tracer recovery	2A	15	6	0	91
	2B	15	3	0	89

The results were consistent with the other radioactive samples and also show the separation of Nb from > 90% Co with a small percentage of the initial detected concentration of Ag in solution.

Table 57 $NaNO_2$ eluates of Filter 2

	Sample	Ag	Co	Ho	Nb
Concentration detected (mg dm^{-3})	2A	3.88	0.59	0.00	0.01
	2B	4.38	0.45	0.00	0.01
2σ uncertainty (mg dm^{-3})	2A	± 0.02	± 0.01	± 0.01	± 0.01
	2B	± 0.07	± 0.29	± 0.01	± 0.02
% tracer recovery	2A	40	7.5	0	0
	2B	45	6	0	0

The volume of the $NaNO_2$ eluate added to the resin was smaller than the volume of the sample at previous stages of the method, therefore the concentrations detected at this stage of the method were divided by a dilution factor to calculate the percentage tracer recoveries. The results show that between 40 and 45% of the initial detected concentration of Ag was detected in filter sample 2 and was therefore separated from

> 90% of the initial detected concentration of Co. From the results of the previous two stages of the method it was calculated that between 86 and 91% of the initial detected concentration of Co remained adsorbed to the cation exchange resin.

3.10.2.3 Blank swab sample

Tables 58 to 61 show ICP-AES results of the dissolution and separation methods applied to a blank tacky swab sample containing no activity at Berkeley Centre. Concentrations were expressed in mg dm^{-3} and the maximum concentration of each element assuming that each element remains in solution at each stage of the method (apart from after dissolution and in the $NaNO_2$ eluate) was 1 mg dm^{-3}.

Table 58 Blank swab dissolution

	Ag	Co	Ho	Nb
Concentration detected (mg dm^{-3})	3.79	3.74	3.51	4.49
2σ uncertainty (mg dm^{-3})	± 0.16	± 0.14	± 0.17	± 0.20

Table 59 Blank swab solution after lanthanide resin

	Ag	Co	Ho	Nb
Concentration detected (mg dm^{-3})	1.03	1.00	0.00	0.89
2σ uncertainty (mg dm^{-3})	± 0.01	± 0.02	± 0.01	± 0.01

Table 60 Blank swab solution after cation exchange resin

	Ag	Co	Ho	Nb
Concentration detected (mg dm^{-3})	0.26	0.04	0.00	0.93
2σ uncertainty (mg dm^{-3})	± 0.01	± 0.01	± 0.01	± 0.02

Table 61 $NaNO_2$ eluate of blank swab

	Ag	Co	Ho	Nb
Concentration detected ($mg\ dm^{-3}$)	4.68	0.67	0.00	0.02
2σ uncertainty ($mg\ dm^{-3}$)	± 0.03	± 0.01	± 0.01	± 0.01

The recoveries of Ag and Co at the Ag separation stage for the blank swab sample were 49 and 7% respectively. Similar results observed to those of the radioactive samples were observed throughout the method.

3.10.2.4.1 Blank filter sample

Tables 62 to 65 show the ICP-AES analysis of a blank filter sample containing no activity. Concentrations were expressed in $mg\ dm^{-3}$ and the maximum concentration of each element assuming that each element remains in solution at each stage of the method (apart from in the $NaNO_2$ eluate) was 1 $mg\ dm^{-3}$.

Table 62 Blank filter dissolution

	Ag	Co	Ho	Nb
Concentration detected ($mg\ dm^{-3}$)	0.98	0.93	0.76	0.98
2σ uncertainty ($mg\ dm^{-3}$)	± 0.03	± 0.01	± 0.01	± 0.02

Table 63 Blank filter solution after lanthanide resin

	Ag	Co	Ho	Nb
Concentration detected ($mg\ dm^{-3}$)	0.92	0.90	0.01	0.91
2σ uncertainty ($mg\ dm^{-3}$)	± 0.05	± 0.07	± 0.01	± 0.05

Table 64 Blank filter solution after cation exchange resin

	Ag	Co	Ho	Nb
Concentration detected ($mg\ dm^{-3}$)	0.03	0.02	0.00	0.93
2σ uncertainty ($mg\ dm^{-3}$)	± 0.01	± 0.01	± 0.01	± 0.01

Table 65 $NaNO_2$ eluate of blank filter

	Ag	Co	Ho	Nb
Concentration detected ($mg\ dm^{-3}$)	4.70	0.72	0.00	0.01
2σ uncertainty ($mg\ dm^{-3}$)	± 0.21	± 0.02	± 0.01	± 0.01

The recoveries of Ag and Co at the Ag separation stage were 48 and 8% respectively. Similar results were observed to radioactive filter samples throughout the method.

3.11 Radioactive swab / filter sample gamma spectrometry analysis

Section 3.11.1 shows the reproducibility of the gamma spectrometry results by summarising the ^{60}Co and ^{108m}Ag activity detected in the radioactive swab samples and comparing it to the activity corrected using the inactive tracer element yields. Summaries of activity measured in the filter samples were not shown because the low ^{108m}Ag in these samples prevented quantitative measurement of this radioanalyte at various stages of the method. Section 3.11.2 shows detailed analysis of detected activity, corrected activity using tracer recoveries and uncertainty values at each stage of the method for duplicate swab and filter samples.

3.11.1 Reproducibility of gamma spectrometry results for radioactive swab samples

Figures 25 to 28 summarise the ^{108m}Ag and ^{60}Co activity detected in the radioactive swab samples calculated as percentages of initial activity detected. These are compared with the activity corrected using inactive tracer element yields at various stages of the method.

Figure 25 Reproducibility of swab sample ^{108m}Ag and ^{60}Co activity detection in solution after lanthanide resin

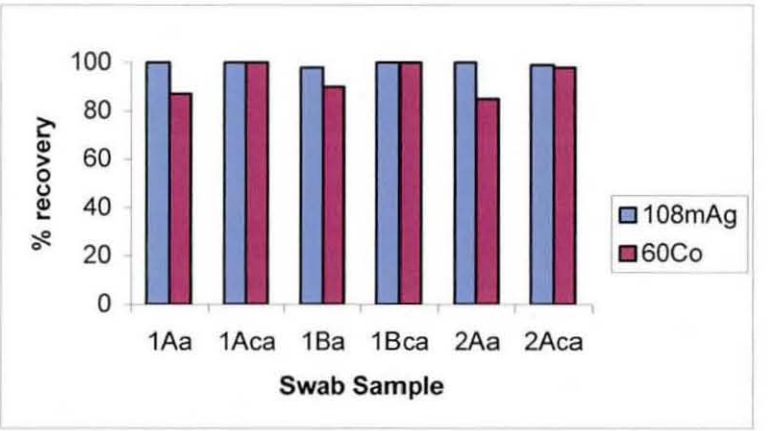

a = activity detected (shown as a percentage of initial activity detected)

ca = corrected activity using tracer yield (shown as a percentage of initial activity detected)

The results show that the activity detected for the swab samples were similar to the corrected activity showing that all of the initial detected ^{108m}Ag and ^{60}Co activity passed through the lanthanide resin. Significant amounts of ^{108m}Ag and ^{60}Co were not detected in the lanthanide resin slurry and reproducible results were observed for ^{60}Co and ^{108m}Ag in solution after it was passed through lanthanide resin.

Figure 26 Reproducibility of swab sample ^{108m}Ag and ^{60}Co activity detection in solution after cation exchange resin

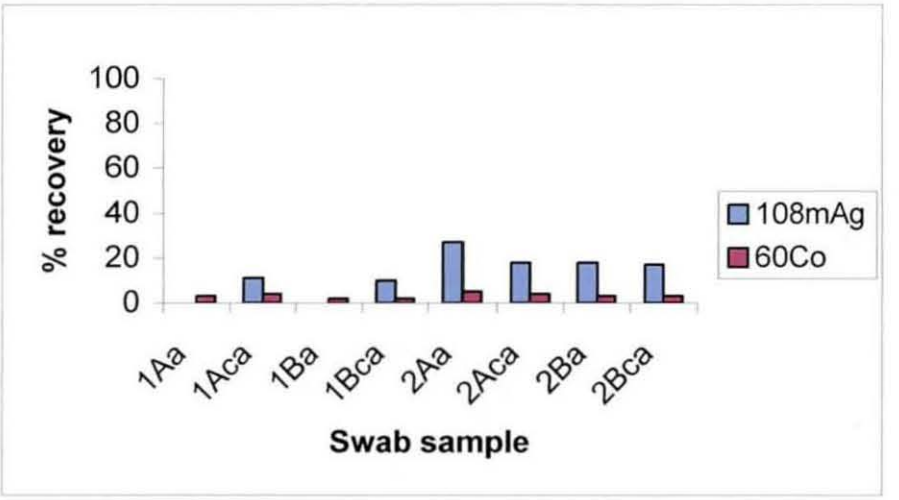

Less than values were detected for ^{108m}Ag activity in swab samples 1A and 1B because the amount of initial ^{108m}Ag activity was lower than the detection limits of the instrument. In samples such as swab samples 2A and 2B where the initial ^{108m}Ag activity was higher, the detected activity values were similar to the corrected activity indicating that ^{108m}Ag was behaving in the same way as inactive Ag at this stage of the method. The results show that the removal of ^{60}Co and ^{108m}Ag from solution was reproducible in the radioactive swab samples.

Figure 27 Reproducibility of swab sample ^{108m}Ag and ^{60}Co activity detection in $NaNO_2$ eluates

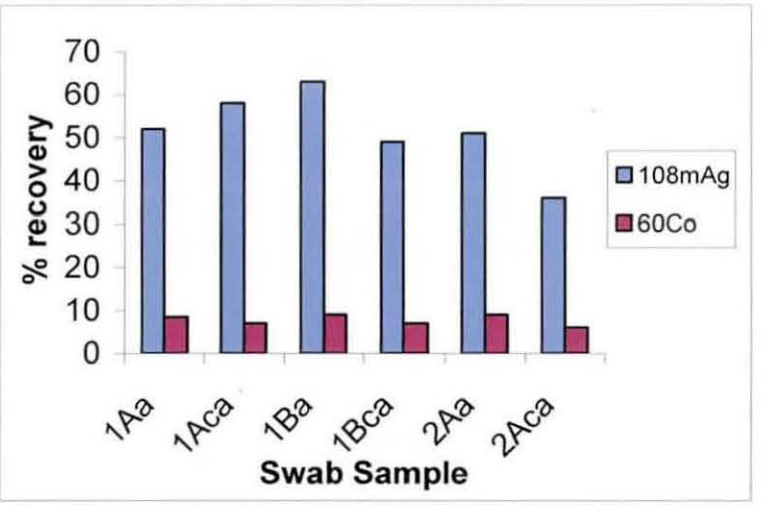

The results show that an average separation of 50% of the initial detected ^{108m}Ag was observed which was similar to the corrected activity calculated from the inactive tracer yields. However in sample 1B the detected activity was slightly higher than the corrected activity and the reason for this was shown to be because of swamping of the initial ^{108m}Ag peak by the ^{60}Co Compton edge scattering. This was confirmed because it was known that the initial ^{108m}Ag activity was swamped at the dissolution stage for swab 1A. Therefore by separating ^{108m}Ag from ^{60}Co, the initial ^{108m}Ag activity in the swab samples was either determined or confirmed using the percentage inactive tracer yield at the Ag separation stage.

The separation of ^{108m}Ag from ^{60}Co using $NaNO_2$ was successful and reproducible in the radioactive swab samples achieving better detection limits for ^{108m}Ag detection.

Figure 28 Reproducibility of swab sample ^{108m}Ag and ^{60}Co activity detection on cation exchange resin

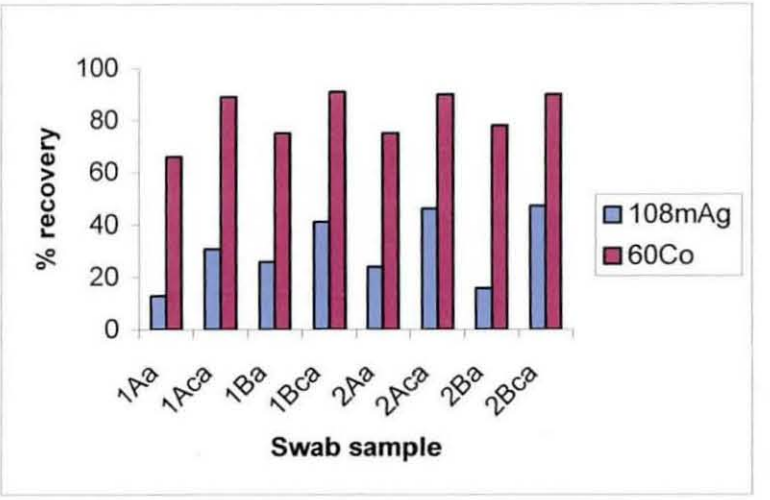

The remaining ^{108m}Ag and ^{60}Co were shown to be adsorbed to the cation exchange resin. However ^{108m}Ag was not quantitatively measured on the resin because of the large amount of ^{60}Co interference also adsorbed to the resin.

3.11.2 Gamma spectrometry analysis of swab samples

Tables 66 to 77 show the specific activity detected, uncertainty values for that activity and corrected activity values calculated from the initial activity measurements using ICP tracer yields at each stage of the method for the radioactive swab samples (shown as Bq per gram of sample).

The sample activities were not measured prior to dissolution. This was because areas of sample that contain contamination were cut from the total swab and analysed and therefore this does not give a quantitative measurement of activity relative to the whole sample but a qualitative measurement of radionuclides present. Relating the activity obtained back to the total sample would not be correct because only the contaminated part of the sample was analysed and the samples were not homogeneous. Therefore the quantitative measurements discussed in the following analysis relate to the comparison of detected activity values at various stages of the

method to the initial detected activity of the sample solution after it was dissolved providing a ratio measurement of isotopes required for radionuclide inventories[6].

Activity values for the solutions at each stage of the method are shown as total activity calculated by multiplying the measured activity in the 100 cm^3 beaker by relevant factors relating to the total volume of solution at that particular stage. These calculations account for the volume taken for ICP analysis. Where the activity values are quoted as less than values, the activity was below the instruments minimum detectable amount for that radioisotope. The corrected activity values were calculated using inactive tracer yields from previous ICP results.

Dissolution was the first stage of the method and the following table shows the gamma spectrometry analysis of swab sample 1 solution at this stage.

Table 66 Activity detected for Swab 1 dissolution

	Sample	^{108m}Ag	^{60}Co
Activity detected (Bq g^{-1})	1A	6.77	1.5×10^3
	1B	6.64	1.5×10^3
2σ uncertainty (Bq g^{-1})	1A	± 1.88	± 247
	1B	± 1.64	± 260

A large amount of ^{60}Co and a relatively small amount of ^{108m}Ag were detected in both samples of swab 1. These results show that > 6 Bq g^{-1} of ^{108m}Ag was detected in 220 times the amount of ^{60}Co activity. However the detected ^{108m}Ag activity was close to the minimum detectable amount and therefore the actual amount of ^{108m}Ag present maybe partially swamped by the ^{60}Co Compton edge scattering.

Table 67 Activity detected for Swab 1 solutions after lanthanide resin

	Sample	^{108m}Ag	^{60}Co
Activity detected (Bq g^{-1})	1A	9.08	1.3×10^3
	1B	6.51	1.4×10^3
2σ uncertainty (Bq g^{-1})	1A	± 2.92	± 216
	1B	± 1.85	± 233
Corrected activity (Bq g^{-1})	1A	9.08	1.5×10^3
	1B	6.64	1.5×10^3

A higher amount of ^{108m}Ag activity was detected at this stage of the method for sample 1A compared to the dissolution stage suggesting that the initial ^{108m}Ag gamma emission peak was partially swamped by ^{60}Co and that the actual ^{108m}Ag activity of the sample was higher than the amount initially detected. A 100% yield of Ag was observed in ICP results at this stage of the method. The measured activity of 9.08 Bq g^{-1} was therefore used as the initial amount of ^{108m}Ag present in the sample for the corrected activity calculations that follow for swab sample 1A. The activity values corrected for the inactive tracer yields for swab sample 1B were obtained by calculating the percentage of initial activity at the dissolution stage using the inactive tracer recoveries of Ag and Co that passed through the lanthanide resin (shown in table 43, section 3.10.2.1, chapter 3). The results for this sample show that the same amount of ^{108m}Ag activity was detected at this stage as in the dissolution stage. However because the ^{108m}Ag activity was close in value to the minimum detectable amount, the ^{108m}Ag activity was still partially swamped by the ^{60}Co Compton edge scattering. The theory of swamping was strengthened by the higher activity result measured at this stage of the method for swab sample 1A. The detection limits for ^{108m}Ag at the later Ag separation stage were shown to be lower than the detection limits at this stage of the method and therefore the initial ^{108m}Ag activity in swab sample 1 was determined from those results using inactive tracer recoveries.

The lanthanide resin was analysed as a slurry.

Table 68 Activity detected for Swab 1 on the lanthanide resin

	Sample	^{108m}Ag	^{60}Co
Activity detected (Bq g^{-1})	1A	< 0.08	1.71
	1B	< 0.09	1.65
2σ uncertainty (Bq g^{-1})	1A	----	± 0.36
	1B	----	± 0.31
Corrected activity (Bq g^{-1})	1A	0	0
	1B	0	0

Only a relatively small amount of ^{60}Co activity was detected on the resin (< 1% of the initial detected activity). The corrected activity for both ^{108m}Ag and ^{60}Co was zero because Ag and Co tracer elements were not retained by the lanthanide resin (calculated using the yield of tracer elements measured in solution after the solution was passed through the resin, shown in table 43, section 3.10.2.1, chapter 3).

The peak library that was used to measure the radioactive samples did not include ^{166m}Ho. Therefore it was not possible to confirm whether or not there was any ^{166m}Ho in this sample. However between 52 and 72% of inactive Ho was retained by the resin. This result suggests that if there were any ^{166m}Ho present in the sample, it would have also been retained on the lanthanide resin and removed from > 99% of the interfering ^{60}Co radioisotope.

Any ^{94}Nb that was present in the swab sample was expected to be detected by gamma spectrometry analysis of the solutions after they were passed through the cation exchange resin.

Table 69 Activity detected for Swab 1 solutions after cation exchange resin

	Sample	^{108m}Ag	^{60}Co
Activity detected (Bq g^{-1})	1A	< 2.22	51
	1B	< 1.50	33
2σ uncertainty (Bq g^{-1})	1A	----	± 9.62
	1B	----	± 6.59
Corrected activity (Bq g^{-1})	1A	1.00	60
	1B	0.66	31

The corrected activity values were calculated from the initial activity at the dissolution stage using the inactive tracer element yields (shown in table 44, section 3.10.2.1, chapter 3). In sample 1A however, the ^{108m}Ag activity was corrected using the higher activity value (thought to be the initial ^{108m}Ag activity for this sample) measured in solution after the lanthanide resin. The corrected ^{108m}Ag activity for both samples of swab 1 were very low relative to the initial ^{108m}Ag activity detected therefore it was expected that ^{108m}Ag would be measured as a less than value because the amount of activity present was lower than the minimum detectable amount of ^{108m}Ag at this stage of the method. The ^{60}Co corrected activity was very close in value to the detected activity suggesting that this radioisotope was behaving similarly to inactive Co. A value of < 0.22 Bq of ^{94}Nb was also measured indicating that ^{94}Nb was present in the sample but was not quantitatively measured because the activity was lower than the minimum detectable amount for this radioisotope. Between 94 and 95% of inactive Nb was detected at this stage of the method and > 95% of the interfering ^{60}Co radioisotope was removed from solution by the cation exchange resin therefore these results suggest that there was no detectable amount of ^{94}Nb in this swab sample.

Table 70 Activity detected for Swab 1 $NaNO_2$ eluates

	Sample	^{108m}Ag	^{60}Co
Activity detected (Bq g^{-1})	1A	4.76	128
	1B	4.19	145
2σ uncertainty (Bq g^{-1})	1A	± 1.09	± 21
	1B	± 0.98	± 24
Corrected activity (Bq g^{-1})	1A	5.27	105
	1B	3.25	109

The corrected activity values were calculated from the initial activity at the dissolution stage using the inactive tracer element yields (shown in table 45, section 3.10.2.1, chapter 3). In sample 1A however, the ^{108m}Ag activity was corrected using the higher activity value (thought to be the initial ^{108m}Ag activity for this sample) measured in solution after the lanthanide resin. The ^{60}Co interference was greatly reduced at this stage of the method allowing 52% of the initial ^{108m}Ag activity in sample 1A to be detected which was very close in value to the corrected ^{108m}Ag activity. Therefore the results for sample 1A show successful separation of 52% ^{108m}Ag from > 90% ^{60}Co. The detection limits were improved at this stage of the method compared to the earlier stages because of the reduction in ^{60}Co interference. This result also supports the previous result which suggested that the initial ^{108m}Ag activity was partially swamped by the interference and that 9.08 Bq g^{-1} was the initial amount of ^{108m}Ag activity in this sample. The corrected activity for ^{108m}Ag for sample 1B was lower than the detected activity suggesting that the initial ^{108m}Ag activity in this sample was swamped by ^{60}Co interference and was actually higher than 6.64 Bq g^{-1}. The improved detection limits at this stage together with the knowledge that 52% of ^{108m}Ag activity was detected in swab 1A strengthen the theory of signal swamping. Therefore it initially appears that 63% ^{108m}Ag was separated, however by using the tracer yield results and observing the ^{108m}Ag behaviour from the previous sample, the unexpectedly high ^{108m}Ag separation was explained. Using the tracer yield value of 49% for Ag and assuming that ^{108m}Ag behaves similarly, the initial ^{108m}Ag activity was calculated to be 8.55 Bq g^{-1} for sample 1B (4.19 Bq g^{-1} was assumed to be 49% of the initial activity).

Table 71 Activity detected for Swab 1 on the cation exchange resin

	Sample	^{108m}Ag	^{60}Co
Activity detected (Bq g^{-1})	1A	1.20	990
	1B	1.74	1.2×10^3
2σ uncertainty (Bq g^{-1})	1A	± 0.66	± 162
	1B	± 0.56	± 192
Corrected activity (Bq g^{-1})	1A	2.82	1.3×10^3
	1B	2.72	1.4×10^3

The corrected activity values were calculated from the initial activity using inactive tracer element yields (the amount of each tracer remaining adsorbed to the cation resin were calculated from the recoveries in solution shown in tables 44 and 45, section 3.10.2.1, chapter 3). < 20% of the initial detected ^{108m}Ag activity was detected on the cation exchange resin indicating that the remaining ^{108m}Ag that was not eluted remained adsorbed to the resin. However it was not possible to quantitatively measure ^{108m}Ag on the resin because of the large excess of ^{60}Co also adsorbed to the resin.

Successful separation of ^{108m}Ag from ^{60}Co was observed for swab sample 1, however the initial amount of ^{108m}Ag activity detected at the dissolution stages were close in value to the minimum detectable amount for the ^{108m}Ag radionuclide. This was confirmed by calculating the initial amount of ^{108m}Ag using the activity detected in the $NaNO_2$ eluate and the tracer element yield. Lower detection limits were observed in the $NaNO_2$ eluates than at the dissolution stages and therefore lower ^{108m}Ag activity was detected because of the reduction in ^{60}Co interference.

The gamma spectrometry analysis of duplicate samples of swab sample 2 at each stage of the method is shown in the following tables.

Table 72 Activity detected for Swab 2 dissolution

	Sample	^{108m}Ag	^{60}Co
Activity detected (Bq g^{-1})	2A	23.39	5.2×10^3
	2B	19.95	5.4×10^3
2σ uncertainty (Bq g^{-1})	2A	± 0.66	± 860
	2B	± 6.19	± 887

There was approximately two thirds more ^{108m}Ag detected in swab 2 than in swab 1. However the ratio of ^{108m}Ag to ^{60}Co remained the same as in swab 1 which meant that signal swamping may still be a problem and the detected values were close to the minimum detectable amount of ^{108m}Ag.

Table 73 Activity detected for Swab 2 solutions after lanthanide resin

	Sample	^{108m}Ag	^{60}Co
Activity detected (Bq g^{-1})	2A	23.92	4.5×10^3
	2B	< 11.25	4.7×10^3
2σ uncertainty (Bq g^{-1})	2A	± 6.49	± 735
	2B	----	± 771
Corrected activity (Bq g^{-1})	2A	23.16	5.1×10^3
	2B	4.59	5.4×10^3

The activity values were corrected by calculating the percentage of initial activity from the dissolution stage using the inactive tracer recoveries of Ag and Co that passed through the lanthanide resin (shown in table 47, section 3.10.2.1, chapter 3). The results show that the same amount of ^{108m}Ag activity was detected at this stage as at the dissolution stage for swab sample 2A. Therefore all of the detected ^{108m}Ag for this sample was shown to have passed through the resin and was behaving the same as the inactive tracer element. However for an unknown reason only 23% Ag was detected in solution after the lanthanide resin for swab sample 2B (shown in table 47, section 3.10.2.1, chapter 3) and a less than value was detected for ^{108m}Ag. The results show no significant reduction in ^{60}Co which suggests there was no loss of solution to

cause this strange result. A detector problem was also eliminated because of the loss of inactive Ag observed by ICP-AES at this stage with no loss of inactive Co.

The lanthanide resin was analysed as a slurry.

Table 74 Activity detected for Swab 2 on lanthanide resin

	Sample	^{108m}Ag	^{60}Co
Activity detected (Bq g^{-1})	2A	< 0.19	4.86
	2B	3.34	8.49
2σ uncertainty (Bq g^{-1})	2A	----	± 0.85
	2B	± 0.76	± 1.48
Corrected activity (Bq g^{-1})	2A	0	0
	2B	0	0

Only a relatively small amount of ^{60}Co activity was detected on the resin for both samples (< 1% of the initial activity detected). For sample 2B, 17% of the ^{108m}Ag activity that was expected to be detected in the solution after the lanthanide resin was detected on the lanthanide resin. Ag was not expected to be retained by the lanthanide resin and this result is the opposite to other radioactive samples, therefore this was a freak experimental error at this stage of the method for sample 2B. The remaining ^{108m}Ag that was detected at the dissolution stage of the method was not observed in either the resin slurry or the solution after it was passed through the lanthanide resin.

The peak library that was used to measure the radioactive samples did not include ^{166m}Ho. Therefore it was not possible to confirm whether or not there was any ^{166m}Ho in this sample. However 100% of inactive Ho was retained by the resin. This result suggests that if there were any ^{166m}Ho present in the sample, it would have also been retained on the lanthanide resin and removed from > 99% of the interfering ^{60}Co radioisotope.

Any ^{94}Nb that was present in the swab sample was expected to be detected by gamma spectrometry analysis of the solutions after they were passed through the cation exchange resin.

Table 75 Activity detected for Swab 2 solutions after cation exchange resin

	Sample	^{108m}Ag	^{60}Co
Activity detected (Bq g^{-1})	2A	6.33	211
	2B	3.58	155
2σ uncertainty (Bq g^{-1})	2A	± 1.92	± 37
	2B	± 1.03	± 26
Corrected activity (Bq g^{-1})	2A	4.21	209
	2B	3.39	162

The corrected activity values were calculated from the initial activity at the dissolution stage using the inactive tracer element yields in solution after they had passed through the cation exchange resin (shown in table 48, section 3.10.2.1, chapter 3). The initial ^{108m}Ag activity in swab sample 2 was much higher than in swab sample 1 and therefore the small amount of ^{108m}Ag activity that passed through the resin was detected. The corrected activity values were shown to be similar to the detected activity indicating that only a small amount of each isotope passed through the resin as expected despite previous results showing that ^{108m}Ag was not present in solution for sample 2B. The results for sample 2B together with ICP results suggest that Ag and ^{108m}Ag were present in the sample but were for an unknown reason not detected. A value of < 0.24 Bq of ^{94}Nb was also detected in solution at this stage indicating that ^{94}Nb was present in the sample but was not quantitatively measured because the activity was lower than the minimum detectable amount for this radioisotope. Between 89 and 93% of inactive Nb was detected at this stage of the method and > 95% of the interfering ^{60}Co radioisotope was removed from solution by the cation exchange resin. Therefore these results suggest that there was no detectable amount of ^{94}Nb in this swab sample.

Table 76 Activity detected for Swab 2 $NaNO_2$ eluates

	Sample	^{108m}Ag	^{60}Co
Activity detected (Bq g^{-1})	2A	11.92	460
	2B	5.02	500
2σ uncertainty (Bq g^{-1})	2A	± 2.68	± 76
	2B	± 1.24	± 82
Corrected activity (Bq g^{-1})	2A	8.42	314
	2B	7.18	378

The corrected activity values were calculated from the initial activity at the dissolution stage using the inactive tracer element yields in the $NaNO_2$ eluate (shown in table 49, section 3.10.2.1, chapter 3). These results show that 51% of the initial detected ^{108m}Ag activity was measured after the removal of > 90% ^{60}Co for sample 2A. The corrected ^{108m}Ag activity appears lower than the detected activity for sample 2A, however this is explained by uncertainty in the ICP-AES detection of inactive Ag tracer. ^{108m}Ag detection in sample 2B was measured as only 25% of the initial detected ^{108m}Ag activity and was not expected to be a successful separation because of the unexplainable loss of ^{108m}Ag in solution after the lanthanide resin.

Table 77 Activity detected for Swab 2 on the cation exchange resin

	Sample	^{108m}Ag	^{60}Co
Activity detected (Bq g^{-1})	2A	5.53	3.9×10^3
	2B	3.15	4.2×10^3
2σ uncertainty (Bq g^{-1})	2A	± 1.32	± 644
	2B	± 1.10	± 676
Corrected activity (Bq g^{-1})	2A	10.76	4.2×10^3
	2B	9.38	4.8×10^3

The corrected activity values were calculated from the detected activity at the dissolution stage using inactive tracer element yields (the amount of each tracer remaining adsorbed to the cation resin were calculated from the recoveries in solution,

shown in tables 48 and 49, section 3.10.2.1, chapter 3). It was not possible to quantitatively measure ^{108m}Ag on the resin because of the large excess of ^{60}Co also adsorbed to the resin.

The behaviour of the analytes in swab sample 2B followed the same pattern as in swab sample 2A despite Ag not being detected at certain stages where it was known to be present and despite the separation of ^{108m}Ag being unsuccessful.

3.11.3 MDA calculations

The minimum detectable amount of ^{108m}Ag in samples containing various concentrations of ^{60}Co activity was calculated using an equation based on Currie's equation:

$$\mathbf{MDA\ (Bq\ dm^{-3})} = \frac{\mathbf{K\ D\sqrt{N_o}}}{\mathbf{tE_cV_s}} \qquad \text{Equation 15[140]}$$

K = volume correction factor (1000), N_o = Number of counts in background count time (counts), t = sample count time (s), E_c = counting efficiency, V_s = volume of sample (cm^3), D = decay factor shown in equation 16.

$$\mathbf{D = exp\text{-}[(ln2 / t_{1/2}) \times t]} \qquad \text{Equation 16}$$

The MDA values were calculated by the vision 1 gamma spectrometry software were multiplied by a factor of three and plotted against ^{60}Co activity detected in each of the dissolution samples. The MDA values were multiplied by a factor of three to account for the ^{60}Co Compton edge interference therefore producing a graph of estimated MDA values that would be detected above the level of interference at the region of interest. A factor of 3 was chosen based on equation 17.

$$\mathbf{MDA \approx 3\sqrt{\sigma}} \qquad \text{Equation 17}$$

Figure 29 ^{108m}Ag MDA in dissolution samples

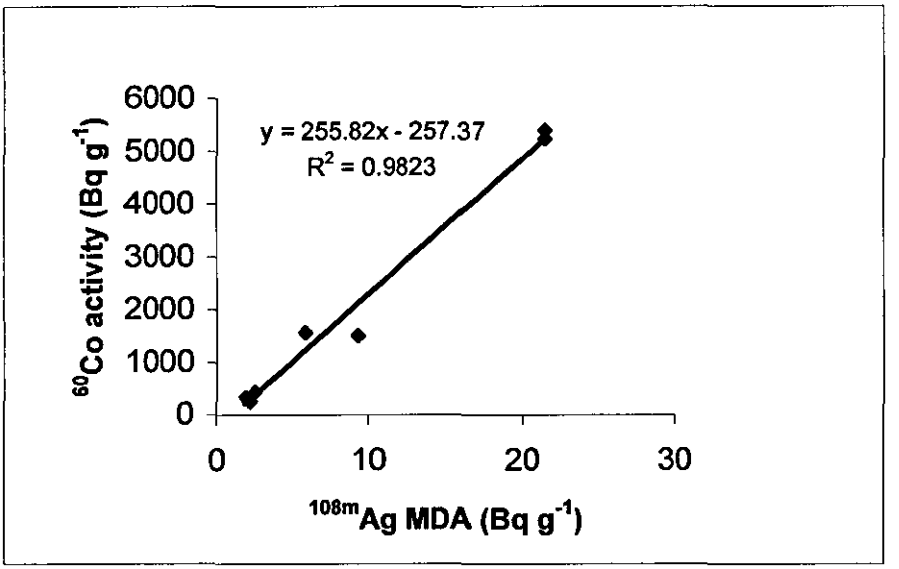

Figure 29 helps to understand why the ^{108m}Ag activity in some of the radioactive dissolution samples was partially swamped by ^{60}Co interference. The initial amount of ^{108m}Ag was close to the minimum detectable amount in each sample because the ratio of ^{108m}Ag and ^{60}Co remained the same even when the concentration of ^{108m}Ag was relatively high. For example the initial amount of ^{108m}Ag activity in swab sample 1 was 9 Bq g^{-1} which was detected in the presence of 1300 Bq g^{-1} ^{60}Co. However only 6.7 Bq g^{-1} of ^{108m}Ag was detected initially because the presence of ^{60}Co was higher (1400 Bq g^{-1}). This increase in ^{60}Co interference resulted in the detected value being closer to the minimum detectable amount and therefore appeared lower than the actual value because of the interference.

Lower detection limits were obtained in the $NaNO_2$ eluates of the radioactive samples from which the ^{108m}Ag yield was used to calculate the initial concentration of ^{108m}Ag in the samples.

Figure 30 ^{108m}Ag MDA in $NaNO_2$ eluates

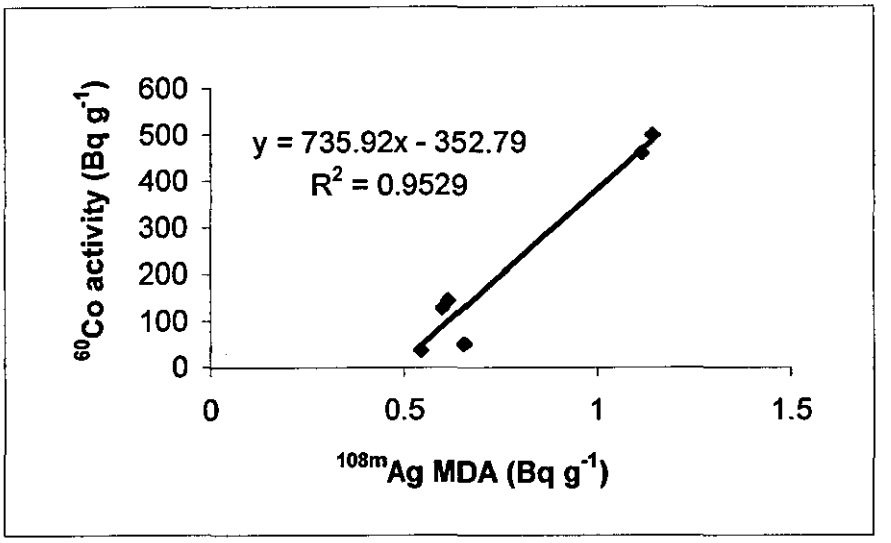

The ^{60}Co concentration was reduced to such a low level at this separation stage that the minimum detectable amount of ^{108m}Ag was as low as 0.6 Bq g^{-1}.

3.11.4 Gamma spectrometry analysis of filter samples

Tables 78 to 79 show the specific activity detected, uncertainty values for that activity and corrected activity values calculated from the initial activity measurements using the ICP inactive tracer yields at each stage of the method for the filter samples (shown as Bq per gram of sample).

Activity values for the solutions at each stage of the method are shown as the total activity calculated by multiplying the measured activity in the 100 cm^3 beakers by relevant factors relating to the total volume of solution of that particular stage. These calculations account for the volume taken for ICP analysis. Where the activity values are quoted as less than values, the activity was below the instruments minimum detectable amount for that radioisotope.

Dissolution was the first stage of the method and the following table shows the gamma spectrometry analysis of filter sample 1 at this stage of the method.

Table 78 Activity detected for Filter 1 dissolution

	Sample	^{108m}Ag	^{60}Co
Activity detected (Bq g^{-1})	1A	1.86	430
	1B	1.53	338
2σ uncertainty (Bq g^{-1})	1A	± 0.50	± 69
	1B	± 0.42	± 57

The activity values detected for this filter sample were much less than those detected in the swab samples. The results show that between 1.53 and 1.86 Bq g^{-1} of ^{108m}Ag was detected in > 230 times the amount of ^{60}Co activity. Therefore the ratio of ^{60}Co to ^{108m}Ag activity remained the same and the MDA graphs shown in the previous section also apply to the filter samples.

Table 79 Activity detected for Filter 1 solutions after lanthanide resin

	Sample	^{108m}Ag	^{60}Co
Activity detected (Bq g^{-1})	1A	< 11.38	436
	1B	< 0.31	602
2σ uncertainty (Bq g^{-1})	1A	----	± 77
	1B	----	± 99
Corrected activity (Bq g^{-1})	1A	1.86	430
	1B	1.51	338

The activity values corrected for the inactive tracer yields were obtained by calculating the percentage of initial activity at the dissolution stage using the inactive tracer element yields of Ag and Co that passed through the lanthanide resin (shown in table 51, section 3.10.2.2, chapter 3). The results show that ^{108m}Ag was below the minimum detectable amount for both samples and was therefore measured as less than values. The detected activity for ^{60}Co in filter sample 1B was slightly higher than the amount detected at the dissolution stage and this value was therefore used as the initial amount of ^{60}Co in this sample. The ^{60}Co activity varied slightly because of the relatively high uncertainty values measured for this radioisotope.

The lanthanide resin was analysed as a slurry.

Table 80 Activity detected for Filter 1 on the lanthanide resin

	Sample	^{108m}Ag	^{60}Co
Activity detected (Bq g^{-1})	1A	< 0.09	0.72
	1B	< 0.10	1.04
2σ uncertainty (Bq g^{-1})	1A	----	± 0.19
	1B	----	± 0.26
Corrected activity (Bq g^{-1})	1A	0	0
	1B	0	0

Only a relatively small amount of ^{60}Co activity was detected on the resin for both samples (< 1% of the initial activity detected). The corrected activity for both ^{108m}Ag and ^{60}Co was zero because there was no inactive Ag or Co tracer elements retained by the lanthanide resin (calculated using the yield of tracer elements found in solution after it was passed through the resin, shown in table 51, section 3.10.2.2, chapter 3).

The peak library that was used to measure the radioactive samples did not include ^{166m}Ho. Therefore it was not possible to confirm whether or not there was any ^{166m}Ho in this sample. However 100% of inactive Ho was retained by the resin. This result suggests that if there were any ^{166m}Ho present in the sample, it would have also been retained on the lanthanide resin and removed from > 99% of the interfering ^{60}Co radioisotope.

Any ^{94}Nb that was present was expected to be detected by gamma spectrometry analysis of the solutions after they were passed through the cation exchange resin.

Table 81 Activity detected for Filter 1 solutions after cation exchange resin

	Sample	^{108m}Ag	^{60}Co
Activity detected (Bq g^{-1})	1A	< 2.74	21
	1B	< 0.14	23
2σ uncertainty (Bq g^{-1})	1A	----	± 9.21
	1B	----	± 7
Corrected activity (Bq g^{-1})	1A	0.39	17
	1B	0.31	24

The corrected activity values were calculated from the initial activity at the dissolution stage using the inactive tracer element yields after the solution had passed through the cation exchange resin (shown in table 52, section 3.10.2.2, chapter 3). The corrected ^{108m}Ag activity was very low relative to the initial ^{108m}Ag activity detected at the dissolution stage. Therefore it was expected that ^{108m}Ag would be detected as a less than value because the amount of activity present was much lower than the minimum detectable amount. The ^{60}Co corrected activity was very close in value to the actual detected activity suggesting that this radioisotope was behaving similarly to inactive Co. A value of < 0.21 Bq of ^{94}Nb was also detected in solution indicating that ^{94}Nb was present in the sample but was not quantitatively measured because the activity was lower than the minimum detectable amount for this radioisotope. > 60% of inactive Nb was detected at this stage of the method and > 95% of the interfering ^{60}Co radioisotope was removed from solution by the cation exchange resin therefore these results suggest that there was no detectable amount of ^{94}Nb in this filter sample.

Table 82 Activity detected for Filter 1 $NaNO_2$ eluates

	Sample	^{108m}Ag	^{60}Co
Activity detected (Bq g^{-1})	1A	1.09	37
	1B	1.39	51
2σ uncertainty (Bq g^{-1})	1A	± 0.35	± 6.32
	1B	± 0.43	± 8.81
Corrected activity (Bq g^{-1})	1A	0.87	34
	1B	1.22	84

The corrected activity values were calculated from the initial activity at the dissolution stage using the inactive tracer element yields in the $NaNO_2$ eluates (shown in table 53, section 3.10.2.2, chapter 3). These results show that 59% ^{108m}Ag was separated from ^{60}Co in filter sample 1A. However by using the tracer element yield at this stage of the method to correct the activity it was shown that a lower ^{108m}Ag activity would have expected to have been detected. Therefore from these results it was determined that ^{108m}Ag was partially swamped by ^{60}Co at the dissolution stage of the method. By taking 1.09 Bq g^{-1} of ^{108m}Ag detected as being the same percentage yield of Ag tracer (47%), the initial amount of ^{108m}Ag present in the filter sample was calculated to be 2.32 Bq g^{-1} in sample 1A. The results for sample 1B were similar. If the initial amount detected for this sample was the total amount present in the sample then 91% ^{108m}Ag activity was separated. It was however more probable that the initial activity was swamped by the ^{60}Co interference. This theory was strengthened by the low corrected activity result and the knowledge that the initial activity in sample 1A was also swamped by ^{60}Co interference. Therefore the initial activity was predicted to be approximately 3.09 Bq g^{-1} for sample 1B by assuming that 1.39 Bq g^{-1} detected at this stage was 45% of the initial amount of ^{108m}Ag activity (45% was the inactive tracer yield at this stage of the method).

Table 83 Activity detected for Filter 1 on the cation exchange resin

	Sample	^{108m}Ag	^{60}Co
Activity detected (Bq g^{-1})	1A	1.03	353
	1B	< 0.57	437
2σ uncertainty (Bq g^{-1})	1A	± 0.39	± 57
	1B	----	± 70
Corrected activity (Bq g^{-1})	1A	0.59	349
	1B	0	494

The corrected activity values were calculated from the initial detected activity at the dissolution stage using inactive tracer element yields (the amounts of each tracer remaining adsorbed to the resin were calculated from the recoveries in solution, shown in tables 52 and 53, section 3.10.2.2, chapter 3). It was not possible to quantitatively measure the remaining ^{108m}Ag on the cation exchange resin for either sample even though a small amount of ^{108m}Ag was detected for sample 1A. This was because of the large excess of ^{60}Co interference also adsorbed to the resin.

The activity analysis for filter sample 1 showed that the minimum detectable amount of ^{108m}Ag in the $NaNO_2$ eluate was lower than in the initial filter sample and therefore the detection limits were improved. The results at that stage of the method determined the true initial ^{108m}Ag activity present which was partially swamped by the large excess of ^{60}Co interference using ICP tracer yields.

The following tables show activity results for filter sample 2 at each stage of the method beginning with the dissolution stage.

Table 84 Activity detected for Filter 2 dissolution

	Sample	^{108m}Ag	^{60}Co
Activity detected (Bq g^{-1})	2A	0.94	250
	2B	< 0.05	232
2σ uncertainty (Bq g^{-1})	2A	± 0.5	± 40
	2B	----	± 38

The ^{108m}Ag activity detected in sample 2A was less than that of filter 1 and was measured at a value lower than the minimum detectable amount in sample 2B.

Table 85 Activity detected for Filter 2 solutions after lanthanide resin

	Sample	^{108m}Ag	^{60}Co
Activity detected (Bq g^{-1})	2A	< 2.53	215
	2B	< 0.24	195
2σ uncertainty (Bq g^{-1})	2A	----	± 36
	2B	----	± 33
Corrected activity (Bq g^{-1})	2A	0.91	246
	2B	0	223

The activity values corrected for the inactive tracer yields were obtained by calculating the percentage of initial activity at the dissolution stage using the inactive tracer recoveries of Ag and Co that passed through the lanthanide resin (shown in table 55, section 3.10.2.2, chapter 3). Similar results to filter sample 1 were observed and no ^{108m}Ag activity was detected.

The lanthanide resin was analysed as a slurry.

Table 86 Activity detected for Filter 2 on lanthanide resin

	Sample	^{108m}Ag	^{60}Co
Activity detected (Bq g^{-1})	2A	< 0.05	2.26
	2B	< 0.09	1.51
2σ uncertainty (Bq g^{-1})	2A	----	± 0.40
	2B	----	± 0.13
Corrected activity (Bq g^{-1})	2A	0	0
	2B	0	0

Only a relatively small amount of ^{60}Co activity was detected on the resin (< 1% of the initial activity detected) and less than values were recorded for ^{108m}Ag as expected. The corrected activity for both ^{108m}Ag and ^{60}Co was zero because there were no tracer elements retained by the lanthanide resin (calculated from the yield of tracer elements found in solution after it was passed through the resin, shown in table 55, section 3.10.2.2, chapter 3).

The peak library that was used to measure the radioactive samples did not include ^{166m}Ho. Therefore it was not possible to confirm whether or not there was any ^{166m}Ho in this sample. However 100% of inactive Ho was retained by the resin. This result suggests that if there were any ^{166m}Ho present in the sample, it would have also been retained on the lanthanide resin and removed from > 99% of the interfering ^{60}Co radioisotope.

Any ^{94}Nb that was present in the filter sample was expected to be detected by gamma spectrometry analysis of the solutions after they were passed through the cation exchange resin.

Table 87 Activity detected for Filter 2 solutions after cation exchange resin

	Sample	^{108m}Ag	^{60}Co
Activity detected (Bq g^{-1})	2A	< 0.24	18
	2B	< 0.14	10
2σ uncertainty (Bq g^{-1})	2A	----	± 3.93
	2B	----	± 2.70
Corrected activity (Bq g^{-1})	2A	0.14	15
	2B	0	9

The corrected activity value of ^{108m}Ag and ^{60}Co for sample 2A were calculated as a percentage relative to the dissolution stage using the inactive tracer yields detected after the solution had passed through the cation exchange resin (shown in table 56, section 3.10.2.2, chapter 3). The corrected activity values for sample 2B were also calculated from the initial activity at the dissolution stage using the inactive tracer element yields detected after the solution had passed through the cation exchange resin (shown in table 56, section 3.10.2.2, chapter 3). The corrected ^{108m}Ag activity was very low relative to the initial ^{108m}Ag activity detected therefore it was expected that ^{108m}Ag would be detected as a less than value because the amount of activity present was lower than the minimum detectable amount. A value of < 0.13 Bq of ^{94}Nb was also detected in solution indicating that ^{94}Nb was present in the sample but was not quantitatively measured because the activity was lower than the minimum detectable amount for this radioisotope. Between 89 and 91% of inactive Nb was detected at this stage of the method and > 95% of the interfering ^{60}Co radioisotope was removed from solution by the cation exchange resin. Therefore these results suggest that there was no detectable amount of ^{94}Nb in this filter sample.

Table 88 Activity detected for Filter 2 $NaNO_2$ eluates

	Sample	^{108m}Ag	^{60}Co
Activity detected (Bq g^{-1})	2A	< 0.27	21
	2B	< 0.29	19
2σ uncertainty (Bq g^{-1})	2A	----	± 3.51
	2B	----	± 3.23
Corrected activity (Bq g^{-1})	2A	0.37	19
	2B	0	25

^{108m}Ag activity was not detected at this stage of the method and the separation of ^{108m}Ag from ^{60}Co was not observed for this filter sample. The initial ^{108m}Ag activity was lower than 1 Bq g^{-1} and therefore the amount separated at this stage of the method was predicted to be < 0.6 Bq g^{-1} which was too low for detection despite most of the ^{60}Co having been removed.

Table 89 Activity detected for Filter 2 on the cation exchange resin

	Sample	^{108m}Ag	^{60}Co
Activity detected (Bq g^{-1})	2A	< 0.24	155
	2B	< 0.45	139
2σ uncertainty (Bq g^{-1})	2A	----	± 25
	2B	----	± 22
Corrected activity (Bq g^{-1})	2A	0.42	217
	2B	0	197

The measurement of ^{108m}Ag at this stage of the method in samples containing much higher initial amounts of ^{108m}Ag activity have shown no detection of ^{108m}Ag therefore it was not surprising that ^{108m}Ag was not detected in these samples containing a much lower initial ^{108m}Ag activity.

Filter sample 2 contained ^{108m}Ag activity at such low concentrations that the Ag separation stage did not determine the initial ^{108m}Ag activity.

3.12 Steel sample analysis

The following sections show the results of dissolution and separation methods performed on four common types of steel found in Decommissioning Waste.

3.12.1 Stainless steel dissolution

Table 90 shows the ICP-AES results for a stainless steel dissolution sample dissolved in HCl / HNO_3 / HF.

Table 90 Stainless steel control sample

	Ag	Co	Ho	Nb
Conc. (mg dm^{-3})	0.12	1.91	0.03	0.21

This stainless steel control sample shows that small amounts of Ag, Co and Nb were present in the steel.

Table 91 shows the ICP-AES results for two doped stainless steel sample dissolutions using only HNO_3 / HF.

Table 91 Doped stainless steel samples

Experiment	Ag (mg dm^{-3})	Co (mg dm^{-3})	Ho (mg dm^{-3})	Nb (mg dm^{-3})
1	0.01	0.00	0.00	0.51
2	0.00	0.00	0.00	0.01

The maximum concentration of each element after dissolution assuming that each element was successfully transferred from the stainless steel samples to solution was 2 mg dm^{-3}. Not all of the steel sample dissolved because HCl was not added and therefore the samples were heated for a longer time to obtain a more complete dissolution. It was not possible to fully dissolve the stainless steel samples without HCl. The results of the dissolved steel solutions show that the analytes were not

detected after dissolution. Fe and Cr are known to interfere with analyte detection on ICP-AES and many peaks were observed in the spectra. Only 25% of the initial amount of Nb added was detected in one of the samples. Therefore the transfer of analytes to solution in doped stainless steel samples was unsuccessful.

The following section gives the results of the investigation into the separation of Nb from Co in the dissolved steel samples.

3.12.2 Separation of Nb from Co in stainless steel

Table 92 shows ICP-AES results of the two previous sample solutions after they were passed through cation exchange resin to remove the cationic interferences.

Table 92 Solutions after cation exchange resins

Experiment	Ag (mg dm^{-3})	Co (mg dm^{-3})	Ho (mg dm^{-3})	Nb (mg dm^{-3})
1	0.03	0.42	0.03	2.20
2	0.07	0.32	0.02	2.15

The maximum concentration of each element in solution assuming that each element passed through the resin and remained in solution was 2 mg dm^{-3}. The results show that Nb passed through the resin as expected. The detected concentration for Nb was slightly higher than the concentration added because the control experiment showed that 0.2 mg dm^{-3} Nb was already present in the steel before any Nb was added. Therefore the HF used in the dissolution process promoted the anionic Nb fluoro complex that formed in previous tacky swab experiments. Although Nb was separated from most of the initial concentration of Co that was added, between 15 and 20% of Co passed through the resin. Therefore the resin removed most but not 100% of the cationic interferences.

$NaNO_2$ was used to elute the cation exchange resins in an attempt to separate Ag from Co.

3.12.3 Separation of Ag from Co in stainless steel

The ICP-AES results of the $NaNO_2$ eluates that were passed through the cation exchange resins of the last two experiments are shown in table 93.

Table 93 $NaNO_2$ eluates for stainless steel

Experiment	Ag (mg dm^{-3})	Co (mg dm^{-3})	Ho (mg dm^{-3})	Nb (mg dm^{-3})
1	0.04	1.60	0.03	0.05
2	0.15	1.53	0.01	0.05

The maximum concentration of each element in solution assuming that each element was eluted from the resin was 2 mg dm^{-3}. The results show that $NaNO_2$ was not successful at removing Ag from the resin like it was in the tacky swab samples. Instead $NaNO_2$ favoured complexation with Co, and the remaining Co that did not pass straight through the resin was detected in the eluates. Therefore a separation of Ag from Co was achieved. However Ag remained on the resin with excess Fe^{3+} and it was not possible to confirm that the Ag that was added was successfully transferred to solution in the dissolution stage due to the interference when the samples were measured after dissolution. Some Co may also remain adsorbed to the resin because Co was found to be present in the stainless steel control sample. Therefore it cannot be concluded that Ag was completely separated from Co because the results were not quantitative. The change in behaviour of the eluant towards the analytes in steel samples compared to swab samples was explained by the non-selective adsorption characteristics of the cation exchange resin complicating Ag desorption because of the high loading of metal cations[121].

It was not possible to detect the analytes after the dissolution of stainless steel samples because of the large amount of interference from elements such as Fe and Cr. The samples were very difficult to dissolve because of the high chromium and titanium content. Nb was however separated from Co in the stainless steel samples by using a cation exchange resin and a separation of Ag from Co was observed in the $NaNO_2$

eluate from the detection of Co in solution however these results were not quantitative because of the unsuccessful detection of Ag and Co in the partially dissolved samples.

The following section focuses on the analysis of mild steel which was found to be much simpler to dissolve than stainless steel.

3.12.4 Mild steel dissolution

Table 94 shows ICP-AES results of two mild steel control dissolution samples.

Table 94 Mild steel control samples

Control sample	Ag (mg dm^{-3})	Co (mg dm^{-3})	Ho (mg dm^{-3})	Nb (mg dm^{-3})
1	0.05	0.92	0.04	0.06
2	0.04	0.76	0.08	0.05

Between 0.76 and 0.92 mg dm^{-3} Co was detected in the mild steel samples.

Table 95 shows ICP-AES results of two doped mild steel dissolution samples.

Table 95 Doped mild steel samples

Doped sample	Ag (mg dm^{-3})	Co (mg dm^{-3})	Ho (mg dm^{-3})	Nb (mg dm^{-3})
1	1.71	3.83	1.96	1.86
2	1.65	2.67	1.50	1.54

The maximum concentration of each element in solution assuming that each element was successfully transferred from the mild steel to solution was 2 mg dm^{-3}. The results show that > 75% of each analyte were successfully transferred to solution. Between 0.6 and 1.8 mg dm^{-3} excess Co was also detected which was previously found in the mild steel. Therefore the amount of Co initially present in the mild steel samples varies slightly.

The successful cation exchange resin method of separating Nb from stainless steel was performed on mild steel samples and the results are shown below.

3.12.5 Separation of Nb from Co in mild steel

Table 96 shows ICP-AES results of four dissolved doped mild steel samples after they were passed through cation exchange resin.

Table 96 Separation of Nb from Co in mild steel samples

Experiment	Ag (mg dm^{-3})	Co (mg dm^{-3})	Ho (mg dm^{-3})	Nb (mg dm^{-3})
1	0.33	0.02	0.01	0.76
2	0.12	0.02	0.01	0.67
3	0.21	0.09	0.00	1.25
4	0.09	0.09	0.00	0.76

The maximum concentration of each element in solution assuming that each element passed through the resin and remained in solution was 1 mg dm^{-3}. The results show that > 67% Nb passed through the resin for each sample. A small amount of Ag also passed through the resin. Co however was not detected in solution and therefore remained adsorbed to the resin. All of the cationic interferences were removed by the larger amount of resin used.

Table 97 shows ICP-AES results for two further mild steel dissolution samples after they were passed through cation exchange resin following the addition of 2 cm^3 and 3 cm^3 concentrated HF respectively.

Table 97 Affect on retention of analytes with increased HF concentration

Sample	Ag (mg dm^{-3})	Co (mg dm^{-3})	Ho (mg dm^{-3})	Nb (mg dm^{-3})
1	0.33	0.97	0.41	2.10
2	0.92	0.77	0.37	1.78

The maximum concentration of each element in solution assuming that each element passed through the resin and remained in solution was 2 mg dm^{-3}. The results show that Nb completely passed through the resin as expected. A higher concentration of Ag also passed through the resin and the increased HF concentration was therefore successful at eluting a higher concentration of Ag from the resin. However the increased HF concentration eluted 50% of the initial added concentration of Co and a small amount of Ho. The experiments were not successful at separating both Nb and Ag from Co in one step.

The results of an experiment using a safer alternative reagent than HF are shown in the following section.

3.12.5.1 Separation of Nb from Co using NaF

Table 98 shows ICP-AES results for two doped mild steel dissolutions after the addition of NaF followed by passage through cation exchange resin.

Table 98 NaF experiments

Sample	Ag (mg dm^{-3})	Co (mg dm^{-3})	Ho (mg dm^{-3})	Nb (mg dm^{-3})
1	0.04	0.18	0.12	1.50
2	0.26	0.33	0.03	1.79

The maximum concentration of each element in solution assuming that each element passed through the resin and remained in solution was 2 mg dm^{-3}. The successful separation of Nb from Co was observed using NaF as a substitute for HF. Therefore an alternative reagent to HF was found to be successful that was safer to handle.

3.12.6 Separation of Ag from Co in mild steel

The following sections show the results of various methods performed on mild steel samples to separate Ag from Co.

3.12.6.1 Attempted separation using co-precipitation on Pd

The formation of a black solution when Ag was attempted to be co-precipitated with Pd suggests that the ascorbic acid was reducing the Pd. However the solution was observed to turn colourless after a few minutes indicating that Pd was oxidised back to Pd^{2+}. Nitric acid is known to be a strong oxidising agent and it was stated in the original method that HNO_3 impedes the reduction reaction[129]. This together with the observations confirmed that the reduction of Pd was unsuccessful in this experiment.

The observations for experiments performed using steps to overcome the oxidation of Pd are discussed below.

3.12.6.1.1 Steel doped with Ag and dissolved with lower HNO_3 concentration

The yield of Pd precipitate by ascorbic acid decreases with an increase in HNO_3 concentration[141]. Therefore the use of a lower concentrations of HNO_3 and HCl were used for dissolution. HCl was used because lowering the HNO_3 concentration required a stronger acid for dissolution. The use of HCl was supported by reports that trace elements precipitate as chlorides from copper salt matrices with ascorbic acid[127]. The high concentrations of Ag, Co, Ho and Nb added in the previous experiment may have had an affect on the reduction of Pd by competition of the reaction with ascorbic acid. Therefore Ag was added to the sample without Co, Ho and Nb. The small amount of precipitate formed in the experiment was believed to be undissolved ascorbic acid because nitrogen dioxide gas was produced when HNO_3 was added which was the same observation as when the ascorbic acid was initially added to the acidic solution in the flask. Ag was not detected by ICP-AES analysis of the dissolved precipitate which strengthens the theory that the precipitate consisted of undissolved ascorbic acid. The solution still did not remain black despite the steps taken to prevent the oxidation of Pd. It was not surprising that Ag was not detected in the dissolved precipitate because Pd was not successfully reduced.

The observations of an experiment involving the addition of three times the original amount of ascorbic acid are discussed below.

3.12.6.1.2 Addition of more ascorbic acid

The solution turned black when a higher concentration of ascorbic acid was added to a repeat experiment. Ag was not detected in the precipitate by ICP-AES analysis and the filtrate remained black. These observations suggest that Pd remained in solution.

The following results confirm that Pd was not precipitated.

3.12.6.1.3 Determination of Pd

Table 99 shows results of the analysis of Pd in the filtrate and filter of a dissolved mild steel sample after the procedure of the reductive co-precipitation method was performed.

Table 99 Determination of Pd

	Pd (mg dm^{-3})
Filtrate	5.91
Filter	0.01

The maximum concentration of Pd in solution assuming that Pd remained in the filtrate was 6 mg dm^{-3}. The results show that all the Pd was detected in the black filtrate and not in the dissolved filter paper. Therefore it was concluded that Pd remained in solution as a colloidal species and was not successfully precipitated by this method despite steps taken to prevent Pd from re-oxidising. This result explains why Ag was not co-precipitating in this method.

The following section shows results of Fe precipitation experiments and the affect on Ag, Co, Ho and Nb.

3.12.6.2 Precipitation of Fe using NaOH

Table 100 shows ICP-AES results of eleven experiments adjusted to various pH values with NaOH.

Table 100 Analyte concentrations detected in mild steel dissolution samples adjusted to various pH values with NaOH

pH	Ag (mg dm^{-3})	Co (mg dm^{-3})	Ho (mg dm^{-3})	Nb (mg dm^{-3})	Max. conc. (mg dm^{-3})
2	0.23	4.06	2.40	2.34	2.50
3	1.76	2.84	1.14	0.32	1.87
4	1.65	3.13	1.53	0.02	1.82
5	1.00	2.95	0.31	0.02	2.00
6	0.67	1.49	0.02	0.01	1.79
7	1.39	0.08	0.01	0.00	2.00
8	0.84	0.26	0.01	0.00	1.75
9	0.18	0.01	0.01	0.02	1.79
10	0.21	0.00	0.00	0.00	1.77
11	0.18	0.00	0.00	0.00	1.86
12	0.58	0.00	0.00	0.00	1.56

The maximum concentrations of each element for each sample at the various pH values assuming that each element remained soluble are shown in the last column of the table. These concentrations differ because of the varying volume of NaOH added to achieve the desired pH. Varying volumes of NaOH were required because the amount of HNO_3 that evaporated during heating varied in each sample. The results show that Co began to precipitate at pH 6. The concentrations detected at pH values below 6 were all higher than the maximum expected concentration because of the extra 0.9 to 1.5 mg dm^{-3} Co present in the mild steel samples before they were doped (determined from previous control experiments). The precipitation of Co began at a higher pH than pH 4 predicted by the JCHESS speciation programme[33]. Ag was also observed to behave differently to the speciation prediction because it precipitated

at pH 2 and showed partial precipitation above pH 3. Ho and Nb also began to precipitate above pH 3. Fe was observed to precipitate between pH 2 and 3 because the colour of solution changed from brown / orange to clear when solutions were adjusted to > pH 3

Figure 31 shows a summary of the concentration of Ag, Co, Ho and Nb detected plotted against pH.

Figure 31 Summary of detected analyte concentration using NaOH at pH 2 to 12 for experiment set 1

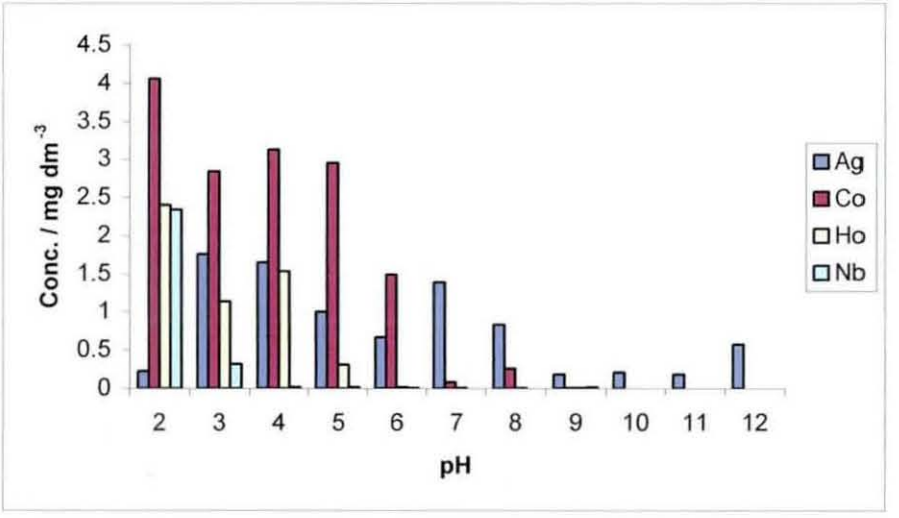

The chart shows a pattern of decreasing concentration for Nb, Co and Ho as the pH increased. However the decrease in concentration was shown to occur at different pH values than those predicted by JCHESS[33].

Figure 32 summarises the ICP-AES results of a repeat set of experiments between pH 2 and 12.

Figure 32 Summary of detected analyte concentration using NaOH at pH 2 to 12 for experiment set 2

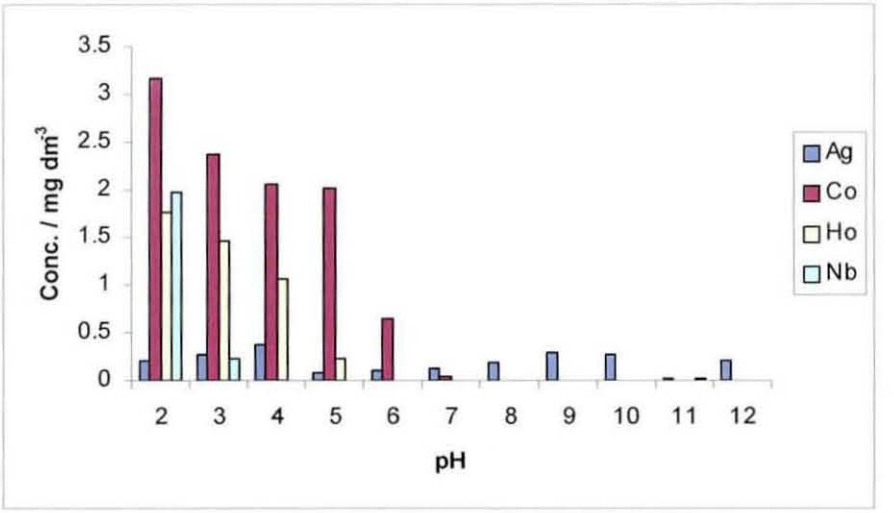

The second set of results showed similar trends to the first. Ag was precipitated over the whole range of pH values which was opposite to the JCHESS prediction. One possible explanation for this could be that the steel matrix was having a co-precipitation affect on the analytes and as Fe began to precipitate it co-precipitated Ag. This may also explain the result that Ho was precipitated at a lower pH than predicted. The co-precipitation theory was strengthened by reports that the metals Pb, Bi and Po were found to co-precipitate on $Fe(OH)_3$[135].

The theory of co-precipitation was then confirmed. Figure 33 shows a summary of analyte concentrations plotted against pH for solutions containing the same initial concentrations of analytes with no steel present.

Figure 33 Summary of detected analyte concentration using NaOH at pH 2 to 12 without steel present

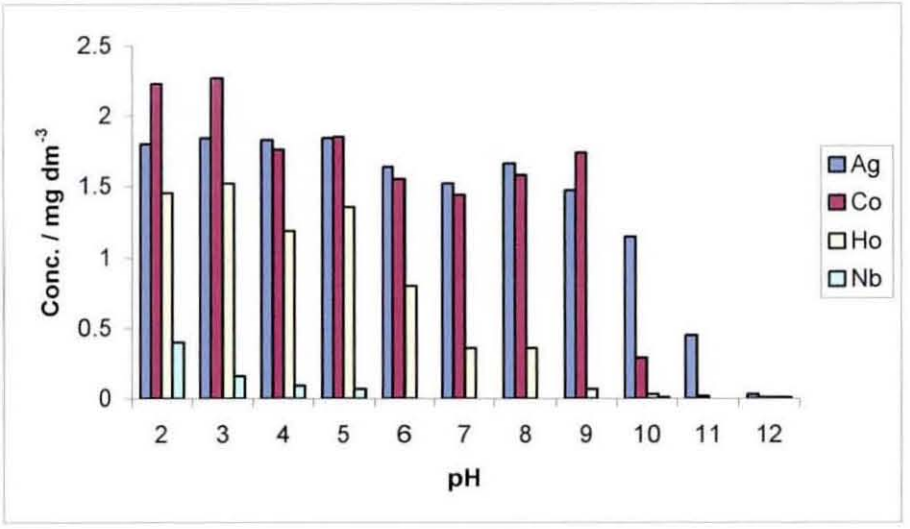

These results show similar patterns of analyte behaviour to those predicted. Ag began to precipitate above pH 10 which was similar to the JCHESS[33] prediction. Ho was also shown to precipitate between pH 6 and 8. This suggests that the precipitation of Fe in steel was causing the co-precipitation of these two analytes. Co however was shown to precipitate between pH 9 and 11 which was a higher pH than predicted. The results for Nb remained the same as those with steel present and this analyte precipitated > pH 2.

The results show that Fe precipitation of mild steel samples was not successful at separating the analytes from Fe and Co because the analytes did not form highly soluble complexes.

The following section shows results of the investigation into Fe precipitation using ammonia solution to form soluble ammine complexes.

3.12.6.3 Precipitation of Fe using NH_4OH solution

Table 101 shows ICP-AES results of nine experiments adjusted to various pH values with NH_4OH.

Table 101 Analyte concentrations detected in mild steel dissolution samples adjusted to various pH values with NH_4OH

pH	Ag (mg dm^{-3})	Co (mg dm^{-3})	Ho (mg dm^{-3})	Nb (mg dm^{-3})	Max. conc. (mg dm^{-3})
2	2.42	3.93	1.96	1.95	2.02
3	1.54	3.37	1.70	0.41	1.63
4	1.14	3.37	1.46	0.14	1.77
5	1.56	3.41	0.27	0.15	1.83
6	1.66	0.03	0.04	0.14	1.71
7	1.46	0.08	0.05	0.16	1.59
8	1.64	0.03	0.04	0.17	1.49
9	1.75	0.00	0.00	0.00	1.64
10	0.69	0.01	0.00	0.00	0.71

The maximum concentrations of each element assuming that each element remained soluble are shown in the last column of the table. These differ because of the varying volume of NH_4OH added to achieve the desired pH. The results show that the separation of Ag from Co was successful because Ag remained in solution as a soluble ammine complex while Co precipitated above pH 6. In addition to the initial Co concentration added an extra 1.5 to 2 mg dm^{-3} of Co was detected in solution before it was precipitated. This was the amount of Co in the steel prior to it being doped. The pH of solution began to increase very gradually after pH 10 therefore the dilution necessary to reach higher pH values was too high for ICP-AES detection of the analytes.

Figure 34 shows a summary of the ICP-AES analyte concentrations detected plotted against pH.

Figure 34 Summary of detected analyte concentration using NH_4OH between pH 2 to 10

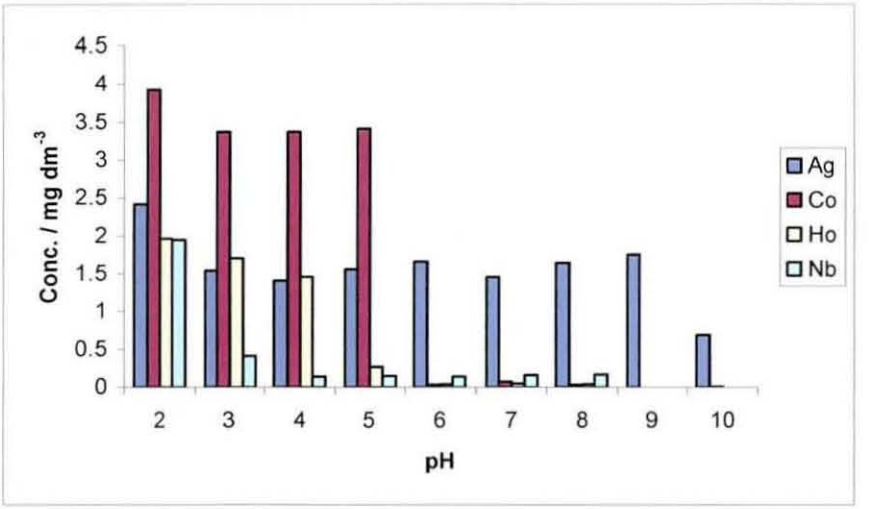

The summary shows a pattern of precipitation that was similar to the prediction made by the JCHESS speciation programme[33]. Co was shown to precipitate above pH 5 whereas Ag remained in solution and was therefore separated from Fe and Co. It is known that large formation constants are only observed for AgL^+ and AgL_2^+ complexes (L = ligand)[40]. This is because of the preference for linear co-ordination $[H_3N—Ag—NH_3]^+$ observed crystallographically[41].

Figure 35 shows a summary of ICP-AES results for a repeat set of experiments using NH_4OH.

Figure 35 Summary of detected analyte concentration using NH_4OH between pH 2 to 10 for repeat set of experiments

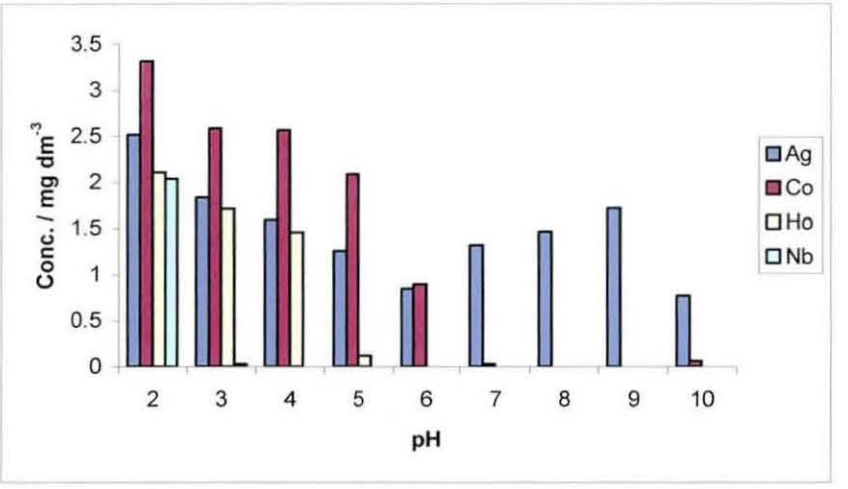

A repeat set of experiments shows similar results and the separation of Ag from Co was successful. Ho was the lesser important analyte because Ag and Nb radioisotopes are more abundant in steel waste samples. A separation method for Ho from Fe and Co was still desirable although not as desirable as a method of separation for Ag and Nb from Fe and Co. The results show the successful separation of Fe from Ho between pH 3 and 4. However Ho precipitated in the same pH range as Co and the method does not therefore separate Ho from Co. It was also reported that rare earth elements were determined in Fe minerals and quartz using iron hydroxide precipitation[142] and the separation of rare earth elements from Fe was achieved in pure iron and low alloy steels using chromatographic separation techniques[143,144]. The radioactive Co interference remained a problem for radioactive Ho determination.

A summary of the analyte precipitation reactions that occurred in the precipitation experiments using NH_4OH is shown below.

pH 2-3:

$$\mathbf{Fe^{3+} + 3OH^- \rightarrow Fe(OH)_3\downarrow \text{ (red / brown colour)}} \qquad \text{Equation 18[145,134]}$$

pH 4-6:

$$\mathbf{Ho^{3+} + 3OH^- \rightarrow Ho(OH)_3\downarrow} \qquad \text{Equation 19[146]}$$

$$\mathbf{Co^{2+} + 2OH^- \rightarrow Co(OH)_2\downarrow} \qquad \text{Equation 20[134]}$$

pH 5-7:

$$\mathbf{2Ag^+ + 2OH^- \leftrightarrow 2[AgOH] \leftrightarrow Ag_2O\downarrow + H_2O} \qquad \text{Equation 21[32]}$$

At first, Ag formed soluble hydroxide complexes which began to precipitate as Ag_2O. However at the same pH, the following reaction rapidly occurred forming the soluble ammine complexes.

>pH 5:

$$\mathbf{Ag_2O + 4NH_3 + H_2O \leftrightarrow 2[Ag(NH_3)_2]^+ + 2OH^-} \qquad \text{Equation 22[32]}$$

Nb also precipitated at a low pH with Fe, however no quantitative stoichiometric reactions producing hydroxide precipitates of definite composition are known[44]. One possibility is that the $Nb(OH)_5$ precipitate formed.

The following section shows dissolution, Nb separation and Ag separation results for boron containing steel.

3.12.7 Dissolution of boron containing steel

Table 102 shows ICP-AES results for two boron containing steel control samples.

Table 102 Control boron containing steel samples

Control sample	Ag (mg dm^{-3})	Co (mg dm^{-3})	Ho (mg dm^{-3})	Nb (mg dm^{-3})
1	0.06	1.68	0.04	0.26
2	0.06	1.79	0.04	0.27

The results show that between 1.68 and 1.79 mg dm^{-3} Co and 0.27 mg dm^{-3} Nb were present in the boron containing steel samples prior to the samples being doped.

Table 103 shows ICP-AES results for two boron containing steel samples doped with Ag, Co, Ho and Nb.

Table 103 Doped boron containing steel samples

Doped Sample	Ag (mg dm^{-3})	Co (mg dm^{-3})	Ho (mg dm^{-3})	Nb (mg dm^{-3})
1	1.46	3.04	1.38	1.78
2	2.25	4.51	1.64	2.50

The maximum concentration of each element assuming that each element was successfully transferred from the steel to solution was 2 mg dm^{-3}. The results show that > 70% of each element was successfully transferred to solution for sample 1 and > 80% of each element was successfully transferred to solution for sample 2 after the subtraction of concentrations detected in control samples prior to the samples being doped. An extra 1 to 2.5 mg dm^{-3} Co was detected in addition to the concentrations added because of the Co initially present in the steel prior to the samples being doped (determined in control experiments).

3.12.8 Separation of Nb from Co in boron containing steel

Table 104 shows ICP-AES results for two boron containing steel sample solutions doped with Ag, Co, Ho and Nb after they were passed through cation exchange resin.

Table 104 Separation of Nb from Co in boron containing steel

Solution	Ag (mg dm^{-3})	Co (mg dm^{-3})	Ho (mg dm^{-3})	Nb (mg dm^{-3})
1	0.44	1.06	0.24	1.94
2	0.25	1.00	0.14	2.30

The maximum concentration of each element assuming that each element passed through the resin was 2 mg dm^{-3}. The results show that Nb passed through the resin. However 50% of the initial concentration of Co added was also shown to have passed through the resin with small amounts of Ag and Ho. Therefore the separation of Nb from Co was only partial. It was thought that the relatively highly charged B^{3+} ion together with Fe^{3+} and Ni^{2+} provided a large amount of competition for adsorption sites on the resin, which resulted in the partial elution of each analyte because the sites that were previously available in stainless and mild steel sample analysis were occupied by these competing cations.

3.12.9 Separation of Ag from Co in boron containing steel

Table 105 shows ICP-AES results of two boron containing steel samples adjusted to pH 9 for Ag separation.

Table 105 Separation of Ag from Co in boron containing steel

Filtrate	Ag (mg dm^{-3})	Co (mg dm^{-3})	Ho (mg dm^{-3})	Nb (mg dm^{-3})	Max. conc. (mg dm^{-3})
1	1.12	0.05	0.00	0.00	1.29
2	1.15	0.06	0.00	0.00	1.17

The maximum concentrations for each element assuming that each element remains in solution are shown in the last column. These values differ because a slightly higher volume of NH_4OH was added in filtrate 1 to achieve pH 9. The results show that Ag remained in solution after filtration and was successfully separated from Fe and Co in these samples.

The following section shows results of dissolution, Nb separation and Ag separation methods performed on low alloy steel samples.

3.12.10 Dissolution of low alloy steel

Table 106 shows ICP-AES results for two control low alloy steel samples.

Table 106 Low alloy steel control samples

Control sample	Ag (mg dm^{-3})	Co (mg dm^{-3})	Ho (mg dm^{-3})	Nb (mg dm^{-3})
1	0.08	1.25	0.05	0.17
2	0.07	1.25	0.04	0.15

The results show that 1.25 mg dm^{-3} Co and 0.16 mg dm^{-3} Nb were present in the low alloy steel samples prior to them being doped.

Table 107 shows ICP-AES results of two low alloy steel sample dissolutions doped with Ag, Co, Ho and Nb.

Table 107 Low alloy steel doped samples

Doped sample	Ag (mg dm^{-3})	Co (mg dm^{-3})	Ho (mg dm^{-3})	Nb (mg dm^{-3})
1	1.94	3.09	1.80	1.96
2	1.86	2.85	1.68	1.88

The maximum concentration of each element assuming that each element was successfully transferred from the steel to solution was 2 mg dm^{-3}. The results show

that > 80% of each element were successfully transferred to solution. An extra 0.85 to 1 mg dm^{-3} Co was detected in addition to the concentration added because of the Co initially present in the steel prior to the samples being doped (determined in control experiments).

3.12.11 Separation of Nb from Co in low alloy steel

Table 108 shows ICP-AES results for two low alloy steel sample solutions doped with Ag, Co, Ho and Nb after they were passed through cation exchange resin.

Table 108 Separation of Nb from Co in low alloy steel

Solution	Ag (mg dm^{-3})	Co (mg dm^{-3})	Ho (mg dm^{-3})	Nb (mg dm^{-3})
1	0.10	0.31	0.04	1.65
2	0.14	0.32	0.03	1.62

The maximum concentration of each element assuming that each element passed through the resin was 2 mg dm^{-3}. The results show the successful separation of Nb from most of the initial concentration of Co added. A small amount of Co (approximately 10% of total Co in the sample after doping) was however determined in solution after it was passed through the resin.

3.12.12 Separation of Ag from Co in low alloy steel

Table 109 shows ICP-AES results of two low alloy steel samples adjusted to pH 9 for Ag separation.

Table 109 Separation of Ag from Co in low alloy steel

Filtrate	Ag (mg dm^{-3})	Co (mg dm^{-3})	Ho (mg dm^{-3})	Nb (mg dm^{-3})	Max. conc. (mg dm^{-3})
1	1.08	0.12	0.00	0.00	1.24
2	0.74	0.01	0.00	0.00	1.11 .

The maximum concentrations for each element assuming that each element remains soluble are shown in the last column. These values differ because a slightly higher volume of NH_4OH was added in the second filtrate to achieve pH 9. The results show that Ag remained in solution after filtration and was successfully separated from Fe and Co.

Successful dissolution of each of the different types of steel apart from stainless steel resulted in the successful transfer of Ag, Co, Ho and Nb to solution after the subtraction of Co and Nb concentrations detected in control samples prior to the samples being doped. The control samples showed that < 2 mg dm^{-3} of Co was initially present in each steel sample. A small amount of Nb (< 0.3 mg dm^{-3}) was detected in each steel apart from mild steel. Nb was successfully separated from Co in the steel samples by passing dissolved samples spiked with HF through cation exchange resin. The separation of Nb from Co was less successful for boron containing steels. The elution of Ag from cation exchange resins with $NaNO_2$ was successful for the separation from Co in previous tacky swab samples but was not suitable for steel samples because the elution resulted in both Ag and Co nitrite complexes. The separation of Ag from Co for steel samples was successfully achieved by adjusting dissolved samples to pH 9 with ammonia solution so that Co, Fe, Nb and Ho were precipitated leaving the soluble $[Ag(NH_3)_2]^+$ complex in solution. When the method of Ag separation was applied to stainless steel samples, the results showed that Co was not fully precipitated at pH 9 or pH 10.

The following section shows results of dissolution and separation methods performed sequentially.

3.12.13 Combination of successful dissolution and separation methods for mild steel

Table 110 shows ICP-AES results at each stage of the combined dissolution and separation methods performed on inactive mild steel samples.

Table 110 Ag, Co, Ho and Nb recoveries at each stage of the combined methods

Stage	Sample	Ag (mg dm^{-3})	Co (mg dm^{-3})	Ho (mg dm^{-3})	Nb (mg dm^{-3})	Max. conc. (mg dm^{-3})
Dissolution	S1	0.69	1.12	0.63	0.60	0.67
	S2	0.72	1.12	0.65	0.60	0.67
Nb separation	S1	0.01	0.07	0.02	0.57	0.67
	S2	0.00	0.23	0.00	0.42	0.67
Ag separation	S1	0.37	0.00	0.00	0.00	0.62
	S2	0.47	0.00	0.00	0.00	0.62

The results show the detected concentrations for each of the analytes for two mild steel samples, sample 1 and sample 2 (S1 and S2 in table 110). The maximum concentrations at each stage of the combined method calculated from the initial concentration of elements added to the samples taking into account any dilutions are shown in the last column of the table. The slightly higher concentration of Co detected after dissolution was because Co was present in the steel samples prior to the samples being doped. The two samples show the successful transfer of each analyte to solution. In sample 1, 95% of the initial detected concentration of Nb was separated from Co and in sample 2, 70% of the initial concentration of Nb was separated from Co. However in the second sample, 20% of the initial detected concentration of Co also passed through the resin. Between 55 and 70% Ag was successfully separated from Co at the Ag separation stage.

The successful combined method process of dissolution and analyte separation was then applied to radioactive mild steel samples.

3.12.14 Radioactive mild steel analysis

Table 111 shows the initial ^{60}Co, ^{55}Fe and ^{63}Ni activity estimated in six solid mild steel samples.

Table 111 Radioactive mild steel samples before dissolution

Sample	Mass (g)	^{60}Co estimated (Bq g^{-1})	^{55}Fe estimated (Bq g^{-1})	^{63}Ni estimated (Bq g^{-1})
1	0.79	3.9×10^4	7.8×10^4	3.0×10^3
2	0.95	3.1×10^4	6.3×10^4	2.4×10^3
3	0.65	4.4×10^4	8.7×10^4	3.3×10^3
4	0.44	7.5×10^4	1.5×10^5	5.7×10^3
5	0.34	1.1×10^5	2.3×10^5	8.7×10^3
6	0.52	5.8×10^4	1.2×10^5	4.4×10^3

The table shows a relatively high Co interference, ^{55}Fe and ^{63}Ni in each of the mild steel samples. ^{108m}Ag and ^{94}Nb were not directly measured because of the large excess of ^{60}Co interference. The separation methods for Ag and Nb determination were required to analyse the samples for these radioisotopes.

The following section shows ICP-AES results at each stage of the combined methods for each of the six radioactive samples analysed.

3.12.14.1 ICP-AES analysis of radioactive mild steel samples

Tables 112 to 114 show ICP-AES detected concentrations, 2σ uncertainty values and percentage tracer yields at each stage of the method. The set of standard solutions used in the calibration of these samples contained 2000 mg dm^{-3} Fe to match the sample solution matrix.

Table 112 Mild steel sample dissolution ICP-AES analysis

	Sample	Ag	Co	Ho	Nb
Concentration detected ($mg\ dm^{-3}$)	1	0.19	1.01	0.70	0.72
	2	0.18	1.12	0.71	0.70
	3	0.23	0.90	0.68	0.40
	4	0.20	0.85	0.68	0.27
	5	0.24	0.80	0.68	0.25
	6	0.19	0.88	0.68	0.38
2σ uncertainty ($mg\ dm^{-3}$)	1	± 0.03	± 0.01	± 0.01	± 0.04
	2	± 0.01	± 0.01	± 0.01	± 0.01
	3	± 0.01	± 0.01	± 0.01	± 0.01
	4	± 0.01	± 0.01	± 0.01	± 0.01
	5	± 0.08	± 0.01	± 0.02	± 0.01
	6	± 0.01	± 0.02	± 0.01	± 0.01

The expected concentration of each tracer element in the active mild steel dissolution samples assuming that each element was successfully transferred from the steel to solution was 0.667 mg dm^{-3}. The samples were known to contain 0.015% Co impurity and this explains the slightly higher than expected concentrations of Co detected. The samples were not analysed immediately after preparation because of ICP instrument unavailability and several months of the solutions having been left standing was thought to be responsible for Ag and Nb instabilities. The first two samples shown in the table were the largest samples by weight and required HF for their dissolution. The results show that only those two samples contained the expected concentration of Nb and was explained by the stability of Nb in solution with HF.

The steel solutions were then analysed after they were passed through cation exchange resin using standard solutions also containing Fe even though some of the Fe was removed from solution by the resin. A few drops of HF were added to the samples before analysis because of the instability of Nb observed after dissolution.

Table 113 Mild steel Nb separation stage ICP-AES analysis

	Sample	Ag	Co	Ho	Nb
Concentration detected ($mg\ dm^{-3}$)	1	0.01	0.00	0.00	0.40
	2	0.00	0.00	0.00	0.53
	3	0.01	0.00	0.00	0.54
	4	0.03	0.00	0.00	0.54
	5	0.04	0.00	0.00	0.67
	6	0.01	0.00	0.00	0.50
2σ uncertainty ($mg\ dm^{-3}$)	1	± 0.03	± 0.01	± 0.01	---
	2	± 0.02	± 0.01	± 0.02	---
	3	± 0.05	± 0.01	± 0.01	---
	4	± 0.05	± 0.01	± 0.01	---
	5	± 0.03	± 0.01	± 0.01	---
	6	± 0.03	± 0.01	± 0.01	---
% tracer yield	1	5	0	0	60
	2	0	0	0	79
	3	4	0	0	80
	4	15	0	0	81
	5	17	0	0	100
	6	5	0	0	75

A relatively high concentration of Na present in solution after the samples were passed through cation exchange resin compromised the Nb tracer yield. This was concluded from the observation of a decrease in analyte concentrations in the standard solutions measured before and after measurement of the samples. The following results were therefore adjusted to account for this. The increased Na content resulted from ion exchange with a large amount of cations, particularly Fe^{3+} and therefore the ICP-AES data for these solutions was subject to a high degree of uncertainty due to nebuliser problems. This finding also explains why 100% Nb was not detected in method development experiments despite the formation of the highly soluble Nb anionic fluoro complex. The tracer yield for Ag was calculated relative to the initial detected concentration of Ag after dissolution and shows that most of the Ag adsorbs

to the resin. The tracer yield for Nb was calculated relative to the expected concentration of Nb used to dope the samples. The sample yields would ideally have been calculated relative to the concentrations detected after dissolution, however this was not possible because samples 3 to 6 showed instability of Nb. The results show that a separation of Nb from Co and Ho was achieved at this stage of the method in active mild steel samples despite the increased uncertainty due to nebuliser problems.

The solutions obtained at the Ag separation stage were measured against standard solutions containing no Fe because all of the Fe precipitated from the sample solutions.

Table 114 Mild steel Ag separation stage ICP-AES analysis

	Sample	Ag	Co	Ho	Nb
Concentration detected ($mg\ dm^{-3}$)	1	0.19	0.00	0.00	0.02
	2	0.14	0.00	0.00	0.04
	3	0.11	0.00	0.00	0.01
	4	0.17	0.00	0.00	0.01
	5	0.13	0.00	0.00	0.00
	6	0.15	0.00	0.00	0.01
2σ uncertainty ($mg\ dm^{-3}$)	1	± 0.02	± 0.01	± 0.01	± 0.02
	2	± 0.02	± 0.01	± 0.02	± 0.01
	3	± 0.02	± 0.01	± 0.02	± 0.02
	4	± 0.07	± 0.01	± 0.01	± 0.02
	5	± 0.05	± 0.01	± 0.01	± 0.01
	6	± 0.05	± 0.01	± 0.02	± 0.01
% tracer yield	1	100	0	0	3
	2	78	0	0	6
	3	48	0	0	2
	4	85	0	0	2
	5	54	0	0	0
	6	79	0	0	2

The percentage tracer yield of Ag was calculated relative to the amount detected after dissolution because the same degree of Ag instability in solution was observed at both stages of the method due to the samples being left standing in light for a long period of time. However the separation of the remaining Ag in solution was shown to be successful and no trace of Co was detected.

3.12.14.2 Gamma spectrometry analysis of radioactive mild steel samples

Tables 115 to 119 show ^{108m}Ag, ^{94}Nb and ^{60}Co measured at each stage of the method for the six radioactive mild steel samples.

Table 115 Radionuclides detected after dissolution of mild steel samples

	Sample	^{108m}Ag	^{94}Nb	^{60}Co
Activity detected ($Bq\ g^{-1}$)	1	< 6.12	< 5.11	1.4×10^4
	2	< 4.72	< 3.99	1.5×10^4
	3	< 7.24	< 7.85	1.6×10^4
	4	< 16.99	< 18.97	3.0×10^4
	5	< 18.48	< 24.42	3.8×10^4
	6	< 17.57	< 18.98	1.9×10^4

^{60}Co activity was detected in each of the steel samples with 10% uncertainty. Neither ^{108m}Ag or ^{94}Nb were detected above the minimum detectable amount for those radionuclides. The less than values in table 115 are the minimum detectable amounts of ^{108m}Ag and ^{94}Nb.

Figure 36 shows a graph of MDA values for ^{108m}Ag and ^{94}Nb in the mild steel dissolution samples.

Figure 36 **^{108m}Ag and ^{94}Nb MDA values in mild steel dissolution samples**

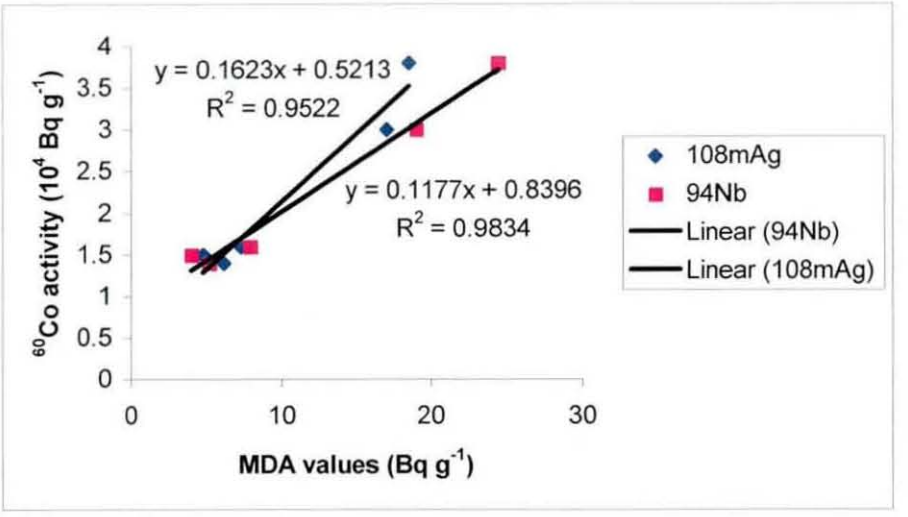

The MDA values for ^{108m}Ag and ^{94}Nb in sample 6 were not included in the graph because of the short count time (5000 seconds) of the sample compared with the other five samples which resulted from limited availability of the gamma spectrometer.

Table 116 **Radionuclides detected in mild steel samples at the Nb separation stage**

	Sample	^{108m}Ag	^{94}Nb	^{60}Co
Activity detected (Bq g^{-1})	1	< 0.36	< 0.36	36.56
	2	< 0.16	< 0.11	29.67
	3	< 0.31	< 0.25	10.51
	4	< 0.52	< 0.60	40.62
	5	< 0.66	< 0.61	60.29
	6	< 0.67	< 0.44	75.64

^{60}Co activity was detected in each of the steel samples with 10% uncertainty. However the amount detected was below 1% of the initial ^{60}Co detected after dissolution. Therefore because most of the ^{60}Co interference was removed from solution and the ICP tracer results show a significant yield of Nb, it was concluded that there was no positively identifiable ^{94}Nb in these mild steel samples.

Figure 37 shows a graph of ^{94}Nb MDA values after the solutions were passed through cation exchange resin.

Figure 37 ^{94}Nb MDA values in mild steel after Nb separation

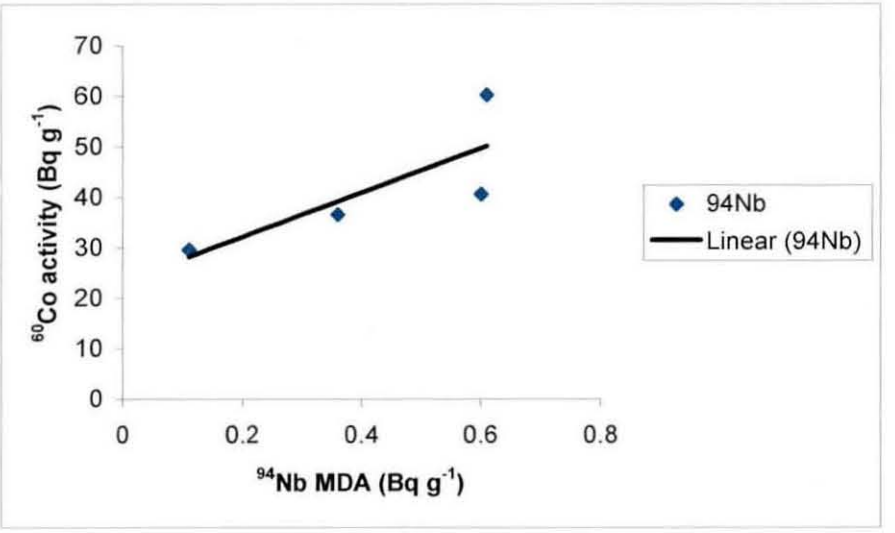

The graph shows that much lower detection limits were achieved after Nb was separated from Co strengthening the suitability of the separation method for mild steel despite ^{94}Nb not being positively identified.

Table 117 Radionuclides detected on the cation resin for mild steel samples

	Sample	^{108m}Ag	^{94}Nb	^{60}Co
Activity detected (Bq g^{-1})	1	< 7.63	< 5.21	1.2×10^4
	2	< 6.90	< 6.94	1.1×10^4
	3	< 12.34	< 5.75	1.4×10^4
	4	< 16.66	< 12.32	2.7×10^4
	5	< 21.40	< 23.88	3.8×10^4
	6	< 14.90	< 14.81	1.9×10^4

^{60}Co activity was detected in each of the steel samples with 10% uncertainty. The results show that ^{60}Co was adsorbed to the resin and therefore removed from solution. The ^{108m}Ag and ^{94}Nb MDA values were larger than those measured in solution because of the high background caused by ^{60}Co.

Table 118 Radionuclides detected in mild steel samples at the Ag separation stage

	Sample	^{108m}Ag	^{94}Nb	^{60}Co
Activity detected (Bq g^{-1})	1	< 0.17	< 0.11	9.80
	2	< 0.12	< 0.04	6.66
	3	< 0.23	< 0.30	8.25
	4	< 0.56	< 0.46	40.25
	5	< 0.81	< 0.53	64.33
	6	< 0.34	< 0.41	18.78

^{60}Co activity was detected in each of the steel samples with 10% uncertainty. However the amount detected was below 1% of the initial ^{60}Co detected after dissolution. Therefore because most of the ^{60}Co interference was precipitated from solution and the ICP tracer results show a significant yield of Ag compared to the amount detected after dissolution, it was concluded that there was no positively identifiable ^{108m}Ag in these mild steel samples.

Figure 38 shows a graph of MDA values for ^{108m}Ag after precipitation of ^{55}Fe and ^{60}Co.

Figure 38 ^{108m}Ag MDA values in mild steel after Ag separation

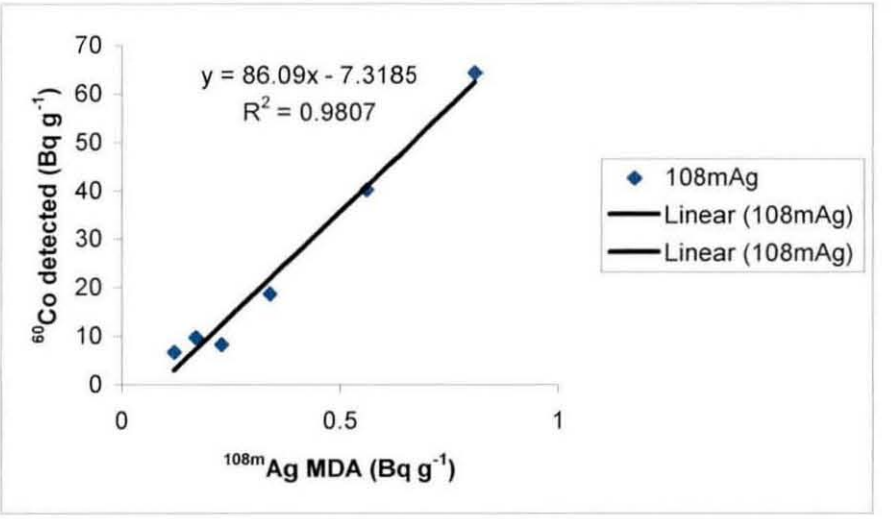

The graph shows that much lower detection limits were achieved after Ag was separated from Co strengthening the suitability of the separation method for mild steel despite ^{108m}Ag not being positively identified.

Table 119 shows activity results for the filter paper containing the ^{60}Co precipitate.

Table 119 Radionuclides detected on the filter for mild steel samples

	Sample	^{108m}Ag	^{94}Nb	^{60}Co
Activity detected (Bq g^{-1})	1	< 6.51	< 9.13	1.1×10^4
	2	< 7.09	< 6.35	1.0×10^4
	3	< 10.05	< 8.94	1.3×10^4
	4	< 12.77	< 16.77	2.3×10^4
	5	< 19.24	< 10.38	3.3×10^4
	6	< 11.81	< 13.28	1.5×10^4

^{60}Co activity was detected in each of the steel samples with 10% uncertainty. The results show that ^{60}Co was precipitated by addition of ammonia solution. The ^{108m}Ag and ^{94}Nb MDA values were larger than those measured in solution because of the high background caused by ^{60}Co.

Chapter 4

Conclusion and Future Work

4.0 Conclusion and Future Work

4.1 Tacky swab and filter paper samples

A method was developed which successfully dissolves radioactive tacky swab and filter paper samples. Ag, Ho and Nb were then separated from Co and the tracer yields were used to determine ^{108m}Ag and ^{94}Nb activities.

4.1.1 Nb separation

Nb was separated from Co using a strong cation exchange resin. The anionic fluoro species $[NbOF_5]^{2-}$ was pre-dominant and did not adsorb to the resin. Co was removed from solution by adsorption to the resin. The behaviour of Nb was observed to differ in method development experiments performed at Loughborough University and experiments performed at Berkeley Centre. Method development experiments showed that 80% Nb was retained by lanthanide resin at the Ho separation stage of the method whereas the inactive control experiments at Berkeley showed that Nb was not retained by lanthanide resin. Work throughout the project concluded that the separation of Nb was dependent on the concentration of HF in solution and the difference in results was explained by the varying concentration of HF due to the dilution of samples. To promote the formation of anionic Nb fluoro complexes, additional HF was required.

^{94}Nb was detected in the tacky swab and filter paper samples but not measured above the minimum detectable amount for the ^{94}Nb radionuclide. The removal of > 99% ^{60}Co from solution together with the high Nb tracer yield resulted in the conclusion that there was no measurable ^{94}Nb activity in any of the radioactive samples. However the separation method was shown to be successful at separating Nb from Co in radioactive tacky swab and filter paper samples so that ^{94}Nb can be determined in solution.

4.1.2 Ho separation

Ho was separated from Co using lanthanide resin. Ho was selectively retained by the resin while Co remained in solution. The peak library that was used in gamma spectrometry to measure the radioactive samples did not include ^{166m}Ho and therefore it was not possible to conclude whether or not there was any significant amount of ^{166m}Ho in the samples. The results however suggest that if there were any ^{166m}Ho present in the samples, it would have been retained on the lanthanide resin and removed from > 99% of the interfering ^{60}Co radioisotope providing a suitable separation method.

4.1.3 Ag separation

Ag was separated from Co using a $NaNO_2$ eluant on a strong cation exchange resin. The mean average of all the radioactive samples showed that 45% Ag was separated from > 90% Co. ^{108m}Ag was the only radionuclide detected above its minimum detectable amount and was separated from the interfering ^{60}Co Compton interference in the $NaNO_2$ eluate. The swab samples were shown to contain a higher amount of ^{108m}Ag and ^{60}Co activity than the filter paper samples. The ^{108m}Ag MDA values show that the initial ^{108m}Ag activity detected after dissolution was close to the minimum detectable amount of ^{108m}Ag. Therefore partial swamping of the ^{108m}Ag gamma emission signal by ^{60}Co Compton interference in most of the radioactive samples was observed and confirmed because the percentage of the initial ^{108m}Ag that was detected in the $NaNO_2$ eluates was significantly higher than the Ag tracer yield detected by ICP-AES. The improved detection limits in the $NaNO_2$ eluates enabled the determination of the initial ^{108m}Ag activity that was partially swamped. This was achieved by correcting the ^{108m}Ag activity detected in the $NaNO_2$ eluates using the Ag tracer yield. The initial ratio of ^{108m}Ag to ^{60}Co was therefore estimated, providing supporting data to verify the inventory calculated for the reactor core and the bioshield.

The Berkeley Centre Power Station from which the radioactive samples were taken was shutdown in 1989 and the samples were taken in 1999. Therefore the supporting

data suggests that after a few more decades, ^{108m}Ag will be the dominating radionuclide in these samples because of its long half-life compared to that of ^{60}Co and the ^{108m}Ag activity can be estimated using the data. It was not possible to estimate the ^{108m}Ag to ^{60}Co ratio in filter paper samples containing < 1 Bq g^{-1} of ^{108m}Ag activity because the ^{108m}Ag activity in the $NaNO_2$ eluate was below the lower detection limit of the gamma spectrometer.

4.2 Steel samples

From the four types of steel analysed, stainless steel was the most difficult to dissolve because of its high Cr and Ti content and was not successfully dissolved without the addition of HCl which caused problems for the recovery of Ag when the samples were doped with Ag, Co, Ho and Nb. Boron containing and low alloy steel were successfully dissolved using HNO_3 and HF. Mild steel was the simplest of the four types of steel to dissolve and was successfully dissolved in 5 cm^3 concentrated HNO_3. The tracer elements Ag, Co, Ho and Nb were successfully measured in solution after the dissolution of boron containing, low alloy and mild steel samples doped with those elements. Ag and Nb were separated from Co and the tracer yields were used to determine ^{108m}Ag and ^{94}Nb in radioactive mild steel samples.

4.2.1 Nb separation

Nb was separated from > 90% of the total Co concentration in inactive low alloy and mild steel dissolution samples and > 70% of the total Co concentration in inactive boron containing steel dissolution samples that were doped with Nb and Co. This was achieved by passing the solutions through a strong cation exchange resin. The principals behind the separation were the same as the Nb separation for tacky swab and filter paper samples.

The use of NaF was also successful for the separation of Nb from steel solutions on a cation exchange resin which provides a safer alternative reagent to HF.

Nb was successfully separated from Co in radioactive mild steel samples but ^{94}Nb was not measured above its minimum detectable amount. The separation method removed > 99% ^{60}Co and achieved lower detection limits for ^{94}Nb than those observed in solution after dissolution, therefore the method was shown to be suitable for the determination of ^{94}Nb in radioactive steel samples despite ^{94}Nb not being positively identified.

4.2.2 Ag separation

Ag was successfully separated from Co and Fe in inactive boron containing, low alloy and mild steel dissolution samples by adjusting the solutions to pH 9 with ammonia solution. Fe and Co were removed from solution by the precipitation of $Fe(OH)_3$ and $Co(OH)_2$ providing a solution containing the Ag diammine complex $[Ag(NH_3)_2]^+$.

Ag was successfully separated from Co in radioactive mild steel samples but ^{108m}Ag was not measured above its minimum detectable amount. The separation method removed > 99% ^{60}Co and achieved lower detection limits for ^{108m}Ag than those observed in solution after dissolution, therefore the method was shown to be suitable for the determination of ^{108m}Ag in radioactive steel samples despite ^{108m}Ag not being positively identified. The Ag separation method also requires the storage of samples in the dark before analysis to prevent the destabilisation of Ag in solution.

The Ag and Nb separation methods applied to radioactive mild steel show that no measurable amount of ^{108m}Ag or ^{94}Nb were present in the samples that were analysed. As the radiological consequences of a nuclide entering the environment are proportional to the quantity of nuclide, the use of MDA values in the absence of better data will lead to an overestimate of the radiological impact of ^{108m}Ag and ^{94}Nb. This additional data will therefore not eliminate the uncertainties contained in the inventory of mild steel.

4.3 Future Work

This section discusses some suitable experimental work that would be appropriate for a continuation of the project.

The active mild steel analysis showed the basis of a suitable method, however this clearly needs refinement. ICP nebuliser congestion caused by high Na content after Nb separation needs to be overcome in order to obtain quantitative analysis. Method development work showed that this problem was drastically reduced in steel samples below 0.5 g. Therefore a reduction in steel sample size would overcome the problem. Furthermore it would also be useful to perform experiments with varying known concentrations of Na and the affect it has on analyte recovery. Alternatively a cation exchange resin in the H^+ or NH_4^+ form could be investigated in the separation of Nb from Co in mild steel samples.

The successful Ag separation method for steel samples was believed to be suitable for Ag separation from Co in tacky swab and filter paper samples. The method of sample analysis would however have to be altered slightly. Once dissolved, the samples would be divided into two equal volumes. The Ho and Nb separation methods would be applied to one half of the solution in the usual way and Ag separation via the precipitation method would be applied to the other half of the solution. Co is expected to precipitate at pH 9 leaving Ag in solution as the diammine complex for analysis. The precipitation method could not be used sequentially with the Ho and Nb separation methods because Nb is required to remain in solution for its separation using a cation exchange resin and this would not be possible because it is known to precipitate at low pH values. If the application of this separation method to tacky swab and filter paper samples was successful, a better Ag separation would be achieved than the existing $NaNO_2$ method of separation and it may then be possible to quantitatively determine ^{108m}Ag in very low radioactive samples such as the second radioactive filter paper sample analysed at Berkeley Centre.

Although separation methods were developed for the more abundant ^{108m}Ag and ^{94}Nb radionuclides in steel samples a separation method for ^{166m}Ho would be desirable. An investigation into the separation of Ho from Co in steel samples would be the next

logical step. The suggested path to achieving this follows the method development for the separation of Ag and Nb and therefore methods would be developed using mild steel, the simplest to dissolve of the four steels. The use of lanthanide resin was considered because of the selectiveness of the resin towards Ho in tacky swab and filter paper samples. However there are excess Fe^{3+} cations in steel samples and these may compete for retention on the resin. The retention of similar charged cations was illustrated in tacky swab method development experiments. It is therefore strongly suggested that Fe is removed from solution before Ho separation is attempted. This could probably be achieved by precipitating Fe with ammonia solution at pH 3. This pH was suggested because previous experiments have shown that most of the Fe in mild steel samples precipitates between pH 2 and 3 whereas Ho precipitates between pH 4 and 5 with ammonia solution. Ho could then be either measured on in the lanthanide resin slurry or eluted from the resin with a suitable eluant such as citrate or oxalate. Another possibility for the investigation into the separation of Ho from steel was by elution of a cation exchange resin with HCl and HNO_3. The method was reported in the literature using 2 mol dm^{-3} HCl to elute Fe and Co from the resin followed by 8 mol dm^{-3} HNO_3 to elute the rare earth element[147].

Following the application of the successful dissolution and separation methods to mild steel it would be appropriate to apply these methods to radioactive low alloy and boron containing steel samples to obtain additional data for the ^{108m}Ag and ^{94}Nb radionuclide inventory for these waste samples.

The analysis of stainless steel dissolution samples was not successful and a different method of dissolution was required. The samples were very difficult to dissolve without the addition of HCl which was unsuitable for the method development of Ag separation. The investigation of digesting stainless steel samples at very high temperatures using microwave digestion techniques is a possibility.

Further investigations into Decommissioning Waste samples would involve analysing Ag, Co, Ho and Nb in two other common types of waste material, concrete and graphite. A leaching method is available for concrete samples[107] and this could be performed to leach concrete samples doped with Ag, Co, Ho and Nb. Graphite mostly

consists of carbon and therefore cannot be fully dissolved, therefore graphite samples would also have to be leached.

Ultimately the more data that is collected on ^{108m}Ag, ^{94}Nb and ^{166m}Ho activity levels in various waste samples leads to better estimations of the levels of these long-lived radionuclides remaining in the waste material many years after final shutdown of nuclear reactors.

References

[1] Department of the Environment, *Review of Radioactive Waste Management Policy:* Final Conclusion Cm 2919 1995, ISBN 0 10 1291922

[2] M. Bacon, *HSE Policy on Decommissioning and Radioactive Waste Management at Licensed Nuclear Sites*, Nuclear Energy 1997, **36-1**, 13-19

[3] W.A. Westall, *AGR Decommissioning*, Nuclear Electric / Berkeley Centre internal document ED/AGR/REP/0203/95, **Issue 1**, March 1996

[4] R.C. Koch, *Activation Analysis Handbook*, 1960, 76

[5] Magnox Electric Plc, Quinquennial Review of Decommissioning and Waste Management Strategies, April 2000

[6] P.B. Woolam and I.G. Pugh, *The Radioactive Inventory of a Decommissioned Magnox Power Station Structure:* A Summary of Neutron Induced Activation, Waste Disposal and Dose Equivalent Rates for the Reactor Island Structure, CEGB Report, RD/B/R4350, October 1978

[7] P.B. Woolam, *The Radioactive Inventory of a Decommissioned Magnox Power Station Structure:* A Re-assessment of Long Term Dose Rates Based on Further Measurements of Silver and Niobium in Mild Steel, CEGB Report, TPRD/B/0220/N83, February 1983

[8] E.J. Henley and E.R. Johnson, *The Chemistry and Physics of High Energy Reactions*, 1969, 10

[9] J.W.T. Spinks and R.J. Woods, *An Introduction to Radiochemistry*, 1964, 11

[10] L. Ashton, *Determination of ^{36}Cl and Other Long-Lived Radionuclides in Decommissioning Concrete Wastes*, Doctoral Thesis, Oct. 2000, 43

[11] M. Bickel, L. Holmes, C. Janzon, G. Koulouris, R. Pilvio, B. Slowikowski and C. Hill, *Applied Radiation and Isotopes*, 2000, **53**, 5-11

[12] R. Anderson, *Sample Pre-treatment*, 1987, 36-41

[13] R. Goguel, *Fresenius Journal of Analytical Chemistry*,1992, **344**, 326-333

[14] V. Sandroni, C.M.M. Smith and A. Donovan, *Talanta*, 2003, **60(4)**, 715-723

[15] J. Marrero, S. Farias and P. Smichowski, *Quimica Analitica*, 2001, **20**, 13-19

[16] M.G. Del Monte Tamba, R. Falciani, T.D. Lopez and A.G. Coedo, *The Analyst*, 1994, **119**, 2081-2085

[17] N.M.F. Avrillon, *Low Level Waste Sample Dissolution*, BNFL Magnox Work Instruction M/TE/FCR/WI/O455 Internal Document, **Issue 2**, June 2001

[18] R. Anderson, *Sample Pre-treatment*, 1987, 175-179

[19] J.H. Kaye, R.S. Strebin and A.E. Nevissi, *Journal of Radiochemical and Nuclear Chemistry Articles*, 1994, **180 (2)**, 197-200

[20] B.K. Esser, A. Volpe, J.M. Kenneally and D.K. Smith, *Pre-concentration and Purification of REE Elements in Natural Waters....*, Technical Information Department Lawrence Livermore National Laboratory University of California, 1993, 1-16

[21] S. Cerjanstefanovic, F. Briski and M. Kastelanmacan, *Fresenius Journal of Analytical Chemistry*, 1991, **339**, 636-639

[22] O. Axner, N. Chekalin, P. Ljunberg and Y. Malmsten, *International Journal of Environmental Analytaical Chemistry*, 1993, **53**, 185-193

[23] R. Pilvio, J.J. LaRosa, D. Mouchel, R. Wordel, M. Bickel and T. Altzitzoglou, *Journal of Environmental Radioactivity*, 1999, **43**, 343-356

[24] B. Skwarzec, E. Holm and D.I. Struminska, *Chemia Analityczna*, 2001, **46**, 23-30

[25] I.I.L. Cunha and R.M. de Oliveira, *Journal of Radiochemical and Nuclear Chemistry Letters*, 1996, **213 3**, 185-192

[26] S.S. Patil, and A.D. Sawant, *Indian Journal of Chemical Technology*, 2001, **8**, 88-91

[27] A.I. Vogel, *Quantitative Inorganic Analysis*, 1st edition, 717-718

[28] http://www.dti.gov.uk/energy/nuclear/technology/reactors.shtml

[29] O. Navratil, J. Hala, R. Kopunec, F. Macasek, V. Mikulaj and L. Leseticky, *Nuclear Chemistry*, 1992, 201-205

[30] G. Choppin, J.O. liljenzin and J. Rydberg, *Radiochemistry and Nuclear Chemistry*, 2nd Edition, 1995, 246

[31] A.K. Das, R. Chakraborty, M.L. Cervera and M. de la Guardia, *Talanta*, 1995, **42**, 1007-1030

[32] C.E. Housecroft and A.G. Sharpe, Inorganic Chemistry, 2001, 535

[33] J. Van der Lee, *JCHESS Speciation Program, Armines Centre d'informatique Geologique*, **Version 1.0**, May 2000

[34] D.L. Parkhurst and C.A.J. Appelo, *Users Guide to PHREEQC – A Computer Program for Speciation, Batch Reaction, One Dimentional Transport and Inverse Geochemical Calculations:* US Geological Survey Water Resources Investigations Report, 1999, **99-4259**, 310

[35] K. Chiba, I. Inamoto and M.Saeki, *Journal of Analalytical Atomic Spectrometry*, 1992, **7**, 115-119

[36] M. Rehkamper and A.N. Halliday, *Talanta*, 1997, **44**, 663-672

[37] R.P. Singh and E.R. Pambid, *Analyst*, 1990, **115**, 301-304

[38] Y. Israel, A.P. Krushevska, H. Foner, L.J. Martines and R.M. Barnes, *Journal of Analytical Atomic Spectrometry*, 1993, **8(3)**, 467-474

[39] P. Anderson, C.M. Davidson, D. Littlejohn, M.A. Ure, C.A. Shand and M.V. Cheshire, *Analitica Chimica Acta*, 1996, **327(1)**, 53-60

[40] R.K. Winge, V.A. Fassel, V.J. Peterson and M.A. Floyd, *Inductively Coupled Plasma-Atomic Emission Spectroscopy*, **Appendix B-1**, 262-275

[41] F.A. Cotton and G. Wilkinson, *Advanced Inorganic Chemistry*, 5th edition, 1988, 459 and 942

[42] P.C.L. Thorne and E.R. Roberts, *Inorganic Chemistry*, 5th edition, 1948, 702

[43] D.J. Pietrzyk and C.W. Frank, *Analytical Chemistry*, 2nd edition, 1979, 72

[44] F. Fairbrother, *Chemistry of Niobium & Tantalum*, 1967, 232-229

[45] R. Caletka, and V. Krivan, *Tantala*, 1983, **30**, 465-470

[46] G.L. Miessler and D.A. Tarr, *Inorganic Chemistry*, 2nd edition, 1999, 171-172

[47] G.F. Liptrot, *Modern Inorganic Chemistry* 4th edition, 1983, 416-417

[48] T. Moller, *Inorganic Chemistry an Advanced Textbook*, 1961, 875

[49] J.D. Lee, *Concise Inorganic Chemistry*, 4th edition, 1991, 504-505 and 792

[50] I.M. Kolthoff and E.B. Sandell, *Textbook of Quantitative Inorganic Analysis*, 1950, 82

[51] A.I. Vogel, *Quantitative Inorganic Analysis*, 1st edition, 529-530

[52] C.J. Pratt, *The Analysis of Intermediate Level Waste Dissolution Liquor for Gamma Emmiting Radionuclides*, BNFL Magnox Standard Operating Procedure TE/ECZ/SOP/401 Internal Document, **Issue 4**, June 2000

[53] R. Kellner, J-M. Mermet, M. Otto and H.M. Widmer, *Analytical Chemistry*, 1988, 152

[54] L. Dongling, H. Xiaoyan and W. Haizhou, *Analytica Chimica Acta*, 2001, **449**, 237-241

[55] C.J. Eskell and M.E. Pick, *Analitica Chimica Acta*, 1980, **117**, 275-283

[56] L. Bing, Y. Zhang and M. Yin, *Analyst*, 1997, **122**, 543-547

[57] M.I. Gromova and A.N. Gonik, *Journal of Analytical Chemistry – USSR*, 1984, **39**, 241-244

[58] H.W. Roesky, M. Zimmer, H.G. Schmidt and M. Noltemeyer, *Zeitschrift Fur Naturforschung Section B-A Journal of Chemical Sciences*, 1988, **43**, 1490-1494

[59] P.F. Kelly, Ã.M.Z. Slawin and K.W. Waring, *Inorganic chemistry communications*, 1998, **1 (7)**, 249-250

[60] J.E. Hicks, *Analytica Chimica Acta*, 1969, **45**, 101-108

[61] N.M.F. Avrillon, *The Analysis of Iron and Nickel Isotopes in Low Level Waste Samples*, BNFL Magnox Work Instruction M/TE/FCR/WI/0407 Internal Document, **Issue 2**, June 2001

[62] G.K. Schweitzer and L.H. Howe, *Analytica Chimica Acta*, 1967, **37**, 316-324

[63] I.M. Kolthoff, E.B. Sandell, E.J. Meehan and S. Bruckenstein, Quantitative Chemical Analysis, 4th edition, 1969, 351-352

[64] J.A. Dean, Chemical Separation Methods, 1969, 87

[65] C. Vandecasteele, and C.B. Black, *Modern Methods for Trace Element Determination*, 1997, 47

[66] S.M. Park, J.K. Park, J.B. Kim and M.J. Song, *Journal of Environmental Science and health Part A-Toxic/Hazardous Substances & Environmental Engineering*, 1999, **34**, 767-793

[67] J. Etoubleau, P. Cambon, h. Bougault and J.L. Joron, *Geostandards Newsletter-the Journal of Geostandards and Geoanalysis*, 1999, **23**, 187-195

[68] M. Rehkamper, *Chemical Geology*, 1994, **113**, 61-69

[69] R. Caletka and V. Krivan, *Talanta*, 1983, **30 7**, 543-545

[70] D. Schumann, S. Fischer, R. Dressler, St. Taut and H. Nitsche, *Radiochimica Acta*, 1996, **72**, 137-142

[71] P.R. Haddad and P.E. Jackson, *Ion Chromatography Principles and Applications (Journal of Chromatography Library)*, 1990, **46**, 79-95

[72] F.A. Cotton, G. Wilkinson and P.L. Gaus, *Basic Inorganic Chemistry*, 3rd edition, 1995, 185

[73] R.J. Cassella, V.A. Salim, L.S. Jesuino, R.E. Santelli, S.L.C. Fereira and M.S. de Carvalho, *Talanta*, 2001, **54**, 61-67

[74] R. Caletka, R. Hausbeck and V. Krivan, *Analytica Chimica Acta*, 1990, **229**, 127-138

[75] F.W. Fifield and D. Kealey, *Principles and Practice of Analytical Chemistry*, 1995, 199

[76] D. Skoog and D. West, *Fundamrntals of Analytical Chemistry*, 7th edition, 1997, 275

[77] R. Pribil, *Analytical Applications of EDTA and Related Compounds*, 1972, **52**, 137

[78] K. Robards, P.R. Haddad and P.E. Jackson, *Principles and Practice of Modern Chromatographic Methods*, 1994, 356

[79] U.D. Neue, *HPLC Columns Theory Technology and Practice*, 1997, 229

[80] P.J. Durrant and B. Durrant, *Introduction to Advanced Inorganic Chemistry*, 1962, 690

[81] D. Van Nostrand Company Inc., International Encyclopaedia of Chemical Science, 1964, 1054

[82] C.P. Gomes, M.F. Almeida and J.M. Loureiro, *Separation and Purification Technology*, 2001, **24**, 35-57

[83] G.C. Lukey, J.S.J. van Deventer and D.C. Shallcross, *Separation Science and Technology*, 2000, **35 (15)**, 2393-2413

[84] A. Tunceli and A.R. Turker, *Talanta*, 2000, **51 (5)**, 889-894

[85] P.C.L. Thorne and E.R. Roberts, *Inorganic Chemistry*, 5th edition, 1948, 254

[86] N. Genova, V. Caramella Crespi, S. Meloni, *Radiochem. Radioanal. Letters*, 1983, **58**, 271-284

[87] N.R. Das and H.P. Maity, *Journal of Radioanalytical Nuclear Chemistry Letters*, 1993, **176**, 45-53

[88] E.B. Barnett and C.L. Wilson, *Inorganic Chemistry A Textbook for Advanced Students*, 2nd edition, 1958, 431

[89] S. Komarneni and R. Roy, *Nature*, 1982, **299**, 707-708

[90] R.P. Bhatnager and R.P. Shukla, *Analytical Chemistry Journal*, 1960, **32**, 777-778

[91] J.T. Stewart and D.M. Lotti, *Analytical Chimica Acta*, 1970, **53**, 390-393

[92] W.F. Hillebrand, G.E.F. Lundell, H.A. Bight and J.I. Hoffman, *Applied Inorganic Analysis*, 2nd edition, 1953, 557-558

[93] A.I. Vogel, *Quantitative Inorganic Analysis*, 7th edition, 1996, 239

[94] F. Helfferich, *Ion Exchange*, 1995, 443

[95] A.I. Vogel, *Textbook of Quantitative Inorganic Analysis*, 3rd edition, 1964, 795

[96] O.P. Kalyakina, O.N. Kononova, S.V. Kachin and A.G. Kholmogorov, *Acta Hydrochimica Et Hydrobiologica*, 2000, **28**, 272-276

[97] C.L. Luke, *Analytical Chemistry*, 1960, **32**, 836-837

[98] M. Langer, *Radiochemical Characterisation of Radioactive wastes Dissertation*, 1999, 45-51

[99] H. Hubicka and D. Drobek, *Hydrometallurgy*, 1997, **47**, 127-136

[100] http://www.eichrom.com/products/extraction.cfm

[101] D. Nayak, S. Lahiri, A. Ramaswami and S.B. Manohor, *Indian Journal of Chemistry*, 2000, **39A**, 1061-1065

[102] J.P. Martin, *The Determination of Promethium-147 and Samarium-151 Using Extraction Chromatography*. Environmental Radiochemical Analysis. Royal Society of Chemistry Publications, Edited by G.W.A. Newton, 1999, 201-213

[103] R.C. Weast and G.L. Tuve, *Handbook of Chemistry and Physics (The Chemical Rubber Company)*, 49th edition, 1969, B4-B59

[104] A.G. Sharpe, Inorganic Chemistry, 3rd edition, 1991, 589

[105] B. Chen, Q. Zhang, H. Minami and S. Inoue, *Journal of Chromatographic Science*, 1999, **37**, 306-311

[106] Cobalt determination, *British Standard*, **6200-3.40.4**, 1997

[107] L. Ashton, P. Warwick and D. Giddings, *The Analyst*, 1999, **124**, 627

[108] P. Warwick, *Analytical Communications*, 1998, **35**, 157

[109] J.A. Richardson, *Chemical Analysis of Steel by ICP-OES*, BNFL Magnox Work Instruction M/TE/FCP/WI/0802 Internal Document, **Issue 1**, June 1999

[110] Analysis of Iron, *British Standard*, **6200-3.11.2**, 1991

[111] I. Hazan and J. Korkisch, *Analytica Chimica Acta*, 1965, **32**, 46-51

[112] S. Inoue, O. Mishima, Q. Zhang, H. Minami and M. Uto, *Analytical Letters*, 2001, **34(14)**, 2465-2475

[113] Determination of Nb, *British Standard*, **6200-3.21.1**, 1986

[114] K.T. Wang, X.G. Cheng, X.L. Liu and Z.D. Hu, *Bulletin Des Societes Chimiques Belges*, 1996, **105 (4)**, 163-168

[115] D.L. Li, X.Y. Hu and H.Z. Wang, *Analytica Chimica Acta*, 2001, **449 (1-2)**, 237-241

[116] A.G. Coedo, T.D. Lopez, F. Alguacil, *Analytica Chimica Acta*, 1995, **315**, 331-338

[117] K. Yamada, O. Kujirai and R Hasegawa, *Anal. Sci.*, 1993, **9(3)**, 385-390

[118] Z. Zhuang, X. Wang, P. Yang and B. Huang, *Journal of Analytical Atomic Spectrometry*, 1994, **9(7)**, 779-784

[119] L. Ebdon, A.S. Fisher and P.J. Worfold, *Journal of Analytical Atomic Spectrometry*, 1994, **9(5)**, 611-614

[120] C.W. McLeod, I.G. Cook, P.J. Worsfold, J.E. Davis and J.Queay, *Spectrochimica Acta*, 1985, **40B**, 57-62

[121] M. Stofkova and M. Stofko, *Metalurgija*, 2002, **41**, 33-36

[122] A.I. Vogel, *Textbook of Quantitative Inorganic Analysis*, 3rd Edition, 1939, 110-111

[123] W. Zmijewska, H. Polkowskamotrenko and H. Stokowska, *Journal of Radioanalytical and Nuclear Chemistry*, 1984, **2**, 320-327

[124] H. Sakurai and K. Hirokawa, *Bunseki Kagaku*, 1996, **45**, 795-798

[125] E.H. Kim, J.H. Yoo and C.S. Choi, *Radiochimica Acta*, 1998, **80**, 53-57

[126] S.H. Lee, C.H. Jung, J.S. Shon and H.S. Chung, *Separation Science and Technology*, 2000, **35**, 411-420

[127] S. Arpadjan, E. Vassileva, S. Momchilova, *The Analyst*, 1992, **117**, 1933-1937

[128] T. Ashino, K. Takada, T. Itagaki, S. Ito, K. Wagatsuma and K. Abiko, *Materials Transactions*, 2002, **43**, 111-115

[129] T. Itagaki, T. Ashino and K. Takada, *Fresenius Journal of Analytical Chemistry*, 2000, **368**, 344-349

[130] T. Watanabe, M. Hoshino, K. Uchino, Y. Nakazato and S. Nishimura, *Cim Bulletin*, 1986, **79:891**, 108

[131] J.F. Duncan and G.B. Cook, *Isotopes In Chemistry*, 1968, 203

[132] F.A. Cotton, G. Wilkinson, C.A. Murillo, M. Bochmann, Advanced Inorganic chemistry, 6th Edition, 1999, 1088-1089

[133] O.D. Sant'Ana, A.L.R. Wagner, R.E. Santelli, R.J. Cassella, M. Gallego and M. Valcarcel, *Talanta*, 2002, **56 (4)**, 673-680

[134] E.J. Margolis, *Quantitative Anion-cation Analysis*, 1962, 104-105

[135] T.M. Church, N. Hussain and T.G. Fredelman, *Talanta*, 1994, **41:2**, 243-249

[136] K.A. Gschneider Jr and L. Eyring, *Hanbook on the Physics and Chemistry of Rare Earths*, 1991, **15**, 418

[137] M. Soylak, L. Elci, I. Narin and M. Dogan, *Trace Elements and Electrolytes*, 2001, **18**, 26-29

[138] J.M. Sanchez, M. Hidalgo and V. Salvado, *Reactive and Functional Polymers*, 2001, **49**, 215-224

[139] W.G. Faix, R. Caletka and V. Krivan, *Analytical Chemistry*, 1981, **53**, 1719-1721

[140] L.A. Currie, Limits for qualitative detection and quantitative determination. Application to radiochemistry, *Analytical Chemistry*, **40** (1968) 586-593

[141] S.H. Lee, K.R. Kim, J.S. Shon, J.H. Yoo and H. Chung, *Korean Journal of Chemical Engineering*, 1999, **16 (2)**, 166-169

[142] M. Bau, P. Dulski, *European Journal of Mineralogy*, 1992, **4 (6)**, 1429-1433

[143] V.K. Karandashev, A.N. Turanov, H.M. Kuβ, I Kumpmann, L.V. Zadnepruk and V.E. Baulin, *Mikrochimica Acta*, 1998, **130**, 47-54

[144] R. Saraswati, N.R. Desikan and T.H. Rao, *Mikrochimica Acta*, 1992, **109 (5-6)**, 253-260

[145] A. Kong and R.J. Lagomarsino, *Environmental Measurements laboratory, US Department of Energy*, 1997, **Section 4.5.4 Vol. 1**, 1-10

[146] P.C.L. Thorne and E.R. Roberts, *Inorganic Chemistry*, 5th Edition, 1948, 440-442

[147] K.S. Park, N.B. Kim, H.J. Woo, K.Y. Lee, W. Hong and S.K. Chun, *Journal of Radioanalytiacal and Nuclear Chemistry-Articles*, 1992, **160 (2)**, 529-538

Appendix 1

BERKELEY CENTRE - METHOD STATEMENT	Form: BCF/DCC/8
Sheet 1 of 3	Issue: 1 Date: November 1998

Reference No.	Issue No.	Date of Issue	Period of Validity	QA Class	QA Grade
MST/LU/002	1	30/07/02			

TITLE:	Investigation of a method for separation of Ag, Ho, Co and Nb radionuclides.			
APPROVAL	**Post / Role**	**Name**	**Signature**	**Date**
Reviewed/ Validated	Reviewer/ Validator	K.Verrall		
Endorsed (QA Grades 1 and 2)	Site QA Engineer			
Approved	Group Head/ Team Leader	C.Harvey		

Purpose and Scope:
A study of the effectiveness of separation of Ag, Ho, Co and Nb radionuclides. This will be achieved by the addition of inactive carriers of Ag, Co, Ho and Nb to low activity paper and tacky swab samples followed by sample dissolution, ion exchange separation and analysis of resulting solutions by ICP-OES and gamma spectrometry.

Step	Task Description	Responsibility:
	Stage 1	
1	Weigh 2 g of tacky swab / filter paper sample	
2	Place sample into a 250 cm^3 conical flask carefully with tweezers	
3	Add 2 cm^3 of 1000 mg dm^{-3} Ag, Co, Ho and Nb stock solutions to the sample	
4	Add 2 cm^3 of Fe carrier solution (2 cm^3 of 3.7 g Fe (III) nitrate in water with 5 cm^3 6 mol dm^{-3} HNO_3 diluted to 100 cm^3 stock solution)	
5	Add 15 cm^3 fuming HNO_3 (risk assessment referenced in BC/GEN1)	
6	Cover flask with a watch glass and leave to stand overnight	
7	Add a magnetic stirrer and heat between 80 and 90°C for 1 hour with stirring using a hotplate	
8	Allow the solution to cool	
9	Dilute with distilled water (150 cm^3)	
10	Filter solution through a 47 mm diameter 0.1 μm pore membrane filter using Buchner filtration apparatus	
11	Transfer the filter to a lidded zirconium crucible	
12	Place crucible into a muffle furnace making sure the a small gap is left between the lid and the crucible to allow vapours to escape	
13	Heat to 500°C for 30 min	
14	Allow crucible to cool to room temperature	
15	Add 1 g of Na_2O_2 to the black residue and place back in the muffle furnace	
16	Heat to 600°C for 30 min	

17	Allow to cool to room temperature	
18	Suspend the residue in 40 cm^3 distilled H_2O / 10 cm^3 6 M HNO_3	
19	Filter the suspension through a 47 mm diameter 0.1 μm pore membrane filter using Buchner filtration apparatus	
20	Combine the filtrate from step 19 with the filtrate from step 10	
21	Dilute to 2000 cm^3 with distilled water and store in a polypropylene bottle	
22	Pipette a small volume of solution (10-20 cm^3) to a small vial and analyse by ICP-OES for added carriers Ag, Co, Ho and Nb using Ag, Co, Ho and Nb stock solutions to produce standards containing each of these elements at concentrations of 0.5, 1 and 3 mg dm^{-3}. Take note of volume used for analysis	
23	Analyse solution by gamma spectrometry using a 500 cm^3 marinelli beaker (count for at least 20000 seconds)	
	Stage 2	
24	Prepare lanthanide resin column by weighing 1.65 g lanthanide resin and placing in a small plastic column fitted with a base frit	
25	Wash the resin with 100 cm^3 of 0.15 mol dm^{-3} HNO_3 and allow resin to settle	
26	Pump the 2000 cm^3 solution through the resin using a peristaltic pump at a rate of approx. 40 cm^3 min^{-1}	
27	Collect solution in a clean polypropylene bottle	
28	Pipette a small volume of solution (10-20 cm^3) to a small vial and analyse by ICP-OES for added carriers Ag, Co, Ho and Nb using Ag, Co, Ho and Nb stock solutions to produce standards containing each of these elements at concentrations of 0.5, 1 and 3 mg dm^{-3}. Take note of volume used for analysis	
29	Analyse solution by gamma spectrometry using a 500 cm^3 marinelli beaker (count solution for at least 20000 seconds)	
30	Transfer the lanthanide resin to a 150 cm^3 top pot and analyse by gamma spectrometry (count for at least 20000 seconds)	
	Stage 3	
31	Weigh 10 g of Amberlite IR-120 cation exchange resin and place in a small plastic column fitted with a base frit	
32	Wash the column with 100 cm^3 distilled water and allow the resin to settle	
33	Pass the solution from step 27 through the resin	
34	Collect the resulting solution in a clean 2000 cm^3 polypropylene bottle	
35	Pipette a small volume of solution (10-20 cm^3) to a small vial and analyse by ICP-OES for added carriers Ag, Co, Ho and Nb using Ag, Co, Ho and Nb stock solutions to produce standards containing each of these elements at concentrations of 0.5, 1 and	

	3 mg dm^{-3}. Take note of volume used for analysis	
36	Analyse solution by gamma spectrometry using a 500 cm^3 marinelli beaker (count for at least 20000 seconds)	
37	Pipette 10 cm^3 of a 2% w/v solution of $NaNO_2$ onto the resin and leave in contact with the resin for 30 min	
38	Elute the resin with a further 190 cm^3 2% $NaNO_2$	
39	Collect 200 cm^3 eluate for analysis	
40	Pipette a small volume of solution (10-20 cm^3) to a small vial and analyse by ICP-OES for added carriers Ag, Co, Ho and Nb using Ag, Co, Ho and Nb stock solutions to produce standards containing each of these elements at concentrations of 0.5, 1, 3 and 6 mg dm^{-3}. Take note of volume used for analysis	
41	Analyse solution by gamma spectrometry using a 500 cm^3 marinelli beaker	
42	Transfer the cation exchange resin to a 150 cm^3 top pot and analyse by gamma spectrometry (count for at least 20000 seconds)	

Appendix 2

BERKELEY CENTRE - METHOD STATEMENT	Form: BCF/DCC/8
Sheet 1 of 3	Issue: 1 Date: November 1998

Reference No.	Issue No.	Date of Issue	Period of Validity	QA Class	QA Grade
MST/LU/003	1	01/07/03			

TITLE:	Investigation of a method for separation of Ag, Ho, Co and Nb radionuclides.			
APPROVAL	**Post / Role**	**Name**	**Signature**	**Date**
Reviewed/ Validated	Reviewer/ Validator			
Endorsed (QA Grades 1 and 2)	Site QA Engineer			
Approved	Group Head/ Team Leader			

Purpose and Scope:
A study of the effectiveness of separation of Ag, Co and Nb radionuclides in activated mild steel samples. This will be achieved by the addition of inactive carriers of Ag, Co and Nb to low activity mild steel samples followed by sample dissolution, ion exchange separation and iron hydroxide precipitation. Analysis of resulting solutions performed by ICP-OES and gamma spectrometry.

Step	Task Description	Responsibility:
1	Weigh between 0.4 and 1 g mild steel sample into a conical flask	
2	Add 0.2 cm^3 of 1000 mg dm^{-3} Ag, Ho, Co and Nb stock solutions	
3	Add 5 cm^3 concentrated HNO_3	
4	Heat at 80-90°C for 1 hour using a hotplate for dissolution	
5	Allow to cool and pipette the solution into a plastic vial. Note the volume taken	
6	Add distilled water to the flask and pipette this to the same vial until 15 cm^3 total volume of solution is obtained (to ensure no sample loss) PART 1	
7	Transfer 5 cm^3 of solution from the vial to a 100 cm^3 volumetric flask	
8	Add 1 cm^3 concentrated HF to the flask and dilute to the mark with distilled water	
9	Pass the 100 cm^3 solution through 25 g of pre-washed Amberlite IR-120 cation exchange resin (resin washed with 100 cm^3 distilled water) in a glass column	
10	Transfer the solution to a plastic bottle for gamma spectrometry analysis followed by ICP-OES analysis (Use Ag, Co, Ho and Nb stock solutions to produce standards in the range 0.5 to 6 mg dm^{-3} each containing 5 cm^3 conc. HNO_3)	
11	Transfer the resin slurry to a top pot for gamma spectrometry analysis	

Reference No.	Issue No.	Date of Issue	Period of Validity	QA Class	QA Grade
MST/LU/003	1	01/07/03			

	PART 2	
12	Transfer another 5 cm^3 of sample solution from the vial in step 6 to a beaker containing a magnetic stirrer	
13	Dilute the sample to 50 cm^3 with distilled water	
14	Add 1 mol dm^{-3} NH_3 solution with stirring to adjust the sample to pH 9 (between 20 and 25 cm^3)	
15	Filter the solution through a 0.1 μm pore membrane filter	
16	Transfer the filtrate to a plastic bottle for gamma analysis. Add 1.5 cm^3 concentrated HNO_3 to acidify the sample for ICP-OES analysis and dilute the filtrate to 100 cm^3	
17	Transfer the filter paper to a top pot for analysis PART 3	
18	Dilute the final 5 cm^3 of sample to 100 cm^3 with distilled water	
19	Transfer the solution to a plastic bottle for gamma spectrometry analysis followed by ICP-OES analysis	